arXiv:1512.03897v2 [cs.CG] 8 Apr 2016

When Convexity meets Parallelism - A Novel Geometric Structure and Its Application in an Optimization Problem*

Kai Jin†

Abstract

We consider the following geometric optimization problem: given a convex polygon P, compute the parallelograms in P with maximal area. To solve it, we invent a novel geometric structure, called $Nest(P)$, which is induced by P and is an arrangement of $\Theta(n^2)$ segments, each of which is parallel to an edge of P, where n represents the number of edges in P. We prove several nontrivial properties of $Nest(P)$, which incorporate two fundamental properties in geometry, namely, convexity and parallelism, and are of independent interests in convex and discrete geometry. We show that the structure $Nest(P)$ captures the essential nature of the maximal area parallelograms, and the original optimization problem can be reduced to answering $O(n)$ location queries on $Nest(P)$. Finally, by solving these queries efficiently, we design nearly linear time algorithm for the original problem.

We emphasize that the efficiency of our algorithm is outstanding compared with several related works in computational geometry, and the techniques develop in this paper may be useful for solving other related problems. In addition, we believe that the novel structure $Nest(P)$ with its wonderful properties may find more applications in other disciplines.

Keywords: Discrete and Convex Geometry, Geometric Optimization, Algorithm.

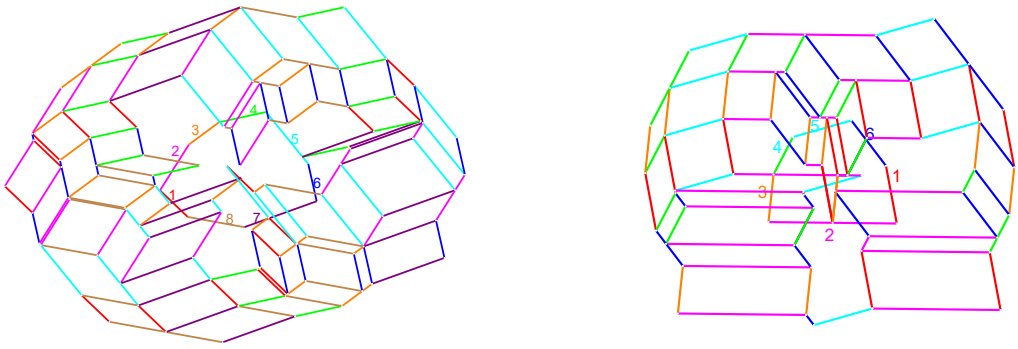

Figure 1: Examples of $Nest(P)$. The labeled edges indicate the given polygon P.

1 Introduction

Geometric optimization has always been an important topic in computational geometry, and in this paper we study a classic geometric optimization problem as follows. Given a convex polygon with n vertices, compute the parallelograms in P with local maximal area.

We design an $O(n \log^2 n)$ time algorithm for solving this problem, whose efficiency is outstanding compared with most known algorithms for solving the related problems, e.g. the

*Supported by the National Basic Research Program of China Grant 2007CB807900, 2007CB807901, and the National Natural Science Foundation of China Grant 61033001, 61061130540, 61073174.

†Institute for Interdisciplinary Information Sciences, Tsinghua University, Beijing 100084, China. E-mail: **cscjjk@gmail.com**

quadratic one for finding the maximum equilateral triangle and square ([22]), the cubic one for the largest rectangle ([8]), the $O(n^2 \log n)$ time one for the maximum similar copy of a triangle ([26]), and the quadratic one for the maximum ellipse ([23]). We also note that our algorithm computes all the local maximal parallelograms, not solely the maximum one.

To design our algorithm, we invent a new geometric structure, called $Nest(P)$, which is associated with the convex polygon P as shown in Figure 1. This structure has several interesting properties and captures the essential nature of the local maximal area parallelograms (LMAPs). We reduce the optimization problem of computing the LMAPs to answering $O(n)$ location queries on $Nest(P)$. Moreover, without building $Nest(P)$ explicitly (which would take $\Theta(n^2)$ time), we solve each of these queries in $O(\log^2 n)$ time and thus obtain the nearly linear time algorithm. As a corollary, we also prove that there are in total $O(n)$ LMAPs.

Our paper consists of two major parts. One part is dedicated to learn the properties of LMAPs and design the algorithm for computing the LMAPs, and the other to learn and prove the properties of $Nest(P)$. We think that the discovery of the novel structure $Nest(P)$ as well as its nontrivial properties is the major contribution of this paper; while the algorithm for computing the LMAPs is a perfect application of this structure.

Essentially, the properties of $Nest(P)$ are properties of the convex polygons since $Nest(P)$ is induced by P. We point out that these properties incorporate two fundamental geometric properties: parallelism and convexity, and are of independent interests in convex geometry.

Related works. Our problem belongs to the polygon inclusion problems, the classic problems that ask extremal figures with special properties inside a polygonal domain. Several such problems have been studied and applied in the area of geometric optimization, e.g., the "potato peeling" problem, which concerns of finding the largest convex polygon in a given simple polygon ([10, 15, 9]); the problem of finding the maximum area / perimeter k-gons in a convex polygon ([7, 2, 3]); the problem of finding the largest homothetic / similar copy of a convex polygon in a convex polygon or polygonal domain ([11, 26, 1]); the problem of finding the largest equilateral triangle, square, or rectangles inscribed on a convex polygon ([22, 18]); the problem of finding the largest area (axis-parallel) rectangle inside a convex or simple polygon ([8, 4, 12]).

The maximum volume parallelepiped in convex bodies has been studied in the area of convex geometry. Assume that C is a convex body in $\mathcal{R}^d$ and Q is the maximum volume parallelepiped in C. Lessek [19] proved that the concentric expanding of Q by factor $2d-1$ covers C; and Gordon et. al. [14] proved that there exists one expanding of Q by factor d which covers C.

Motivations and Applications. A motivation of our research is to solve the well-known problem in discrete geometry called the Heilbronn Triangle Problem. This is a minimax problem which concerns of placing m points in a convex region, in order to avoid triangles of small area. Several polynomial algorithms were given for finding considerable good placements ([6, 20, 21, 5, 25]). On finding the optimal placement, Jin et. al.[16] showed that the simplest case, namely $m = 4$, reduces to finding the maximum area parallelogram (MAP) in the given region.

Computing the MAPs has applications in shape recognition and shape approximation. By finding the MAP in a convex region C, we can find an affine transformation σ in special linear group $SL(2)$, so that the area of the largest square in $\sigma(C)$ is the maximized. Therefore, we can bring the body into a "good position" by an affine transformation, to avoid almost degenerate, i.e., needle-like or fat bodies. In addition, since the parallelograms are the simplest polygons that are centrally symmetric, it is natural to approximate complicated central symmetric polygons by parallelograms, and the MAP serves as a $2/\pi$-approximation for the largest centrally symmetric body inside a convex polygon (see the discussions in [16, 13, 24]).

Technique overview for computing the LMAPs. Above all, we state that the LMAPs must be inscribed on P, i.e. all of its corners must lie on the boundary of P.

First, we prove the following properties of the LMAPs. Roughly, if we restrict a pair of opposite corners of the LMAP on two given edges, or two given vertices, or an edge and a

vertex, then we can define a region related to the given edges or vertices, which is a boundary portion of P, and prove that this region contains one of the other two corners of the LMAP. These properties are corner stones of our research and are referred to as the *premier properties*.

The premier properties are not applicable for computing the LMAPs. However, from them we can deduce many other properties of the LMAPs. To this end, we first change a viewpoint and interpret the premier properties as a complete relationship between three consecutive corners of the LMAPs. This relationship is totally captured by a set of tuples of three points T that is well-defined on P. Next, we consider a "trivial property" of the LMAPs (and of all the parallelograms), which says that the midpoint of the two diagonals coincide each other. We introduce a simple geometric function f which is defined on any tuple of three points. Specifically, $f(X_1, X_2, X_3)$ is defined as the unique point X so that $XX_1X_2X_3$ forms a parallelogram. By combining the "trivial property" with the relationship between three corners implied in the premier property, we deduce the *transformed premier properties* of the LMAPs. Roughly, they state that a corner of the LMAP lies in $f(\mathsf{T})$. Moreover, it lies in some well-defined subregion of $f(\mathsf{T})$ if its neighboring corners are fixed on certain edges or vertices; and it lies in some well-defined subregion of $f(\mathsf{T})$ if its opposite corner is fixed on a certain edge or vertex.

The subregions employed in the transformed premier properties are called *blocks* and *sectors*, and notice that the blocks constitute a natural partition of $f(\mathsf{T})$, and so do all the sectors. To our surprise, the blocks and sectors are well structured. We discover six structural properties of $f(\mathsf{T})$, which are stated succinctly in Theorem 2.10. For example, the blocks can only intersect in the interior of P. Moreover, if we denote T^* the subset of T that is mapped to the boundary of P under f, then f is a bijection between T^* and $f(\mathsf{T}^*)$. Note that T^* can be regarded as a refinement of T; and it is the key information given by the premier properties. Furthermore, the sector partition has an interesting monotone property. Non-surprisingly, the proofs of these properties are nontrivial and involved; however, they are highly constructive and modularized.

In the next, we prove *advanced properties* of the LMAPs by deducing the premier ones and applying the structural properties of $f(\mathsf{T})$. Finally, these advanced properties are applicable in computing the LMAPs; once a corner of the LMAP is fixed, the other corners can be computed efficiently due to the advanced properties. However, some information should be preprocessed to apply the advanced properties; specifically, we should compute "which block and sector does V lie in for each vertex V and "which vertex and edges does region $sector(V)$ intersect for each vertex V" beforehand. Computing these information reduces to solving $O(n)$ point location or intersection location queries on a special structure $Nest(P)$, where $Nest(P)$ is defined as the union of the boundaries of the blocks and sectors and is illustrated in the front page.

Note that $Nest(P)$ is of size $\Theta(n^2)$. Without constructing $Nest(P)$ explicitly, we solve each location queries in $O(\log^2 n)$ time by using interesting algorithmic tricks.

2 Extended Abstract

Denote the boundary of P by ∂P. Let $e_1, \ldots, e_n$ be a clockwise enumeration of the edges of P. Denote the vertices of P by $v_1, \ldots, v_n$ such that $e_i = (v_i, v_{i+1})$ (where $v_{n+1} = v_1$).

We say that a parallelogram lies in P, if all its corners lie in P's interior or P's boundary. We say that a parallelogram is *inscribed* on P, if all its corners lie on P's boundary. We say that a corner of an inscribed parallelogram is *anchored*, if it lies on a vertex of P.

A parallelogram is *degenerated*, if it has two corners lying in the same edge of P.

Note that we regard all edges of P as **open** segments; so, they do not contain their endpoints. To be more clear, whence we say that some point (like a corner of a parallelogram) lies on an edge, we assume that this point does not lie on the endpoints of that edge. So, if one corner lies on some edge while another lies on its endpoint, these two corners are **not** in the same edge.

Suppose $Q = A_1A_2A_3A_4$ is a parallelogram that lies in P. We say that Q is *global maximum*, if has the largest area among all parallelograms that lie in P; and Q is *local maximal*, if it has

a larger or equal area than its "nearby" parallelograms that lie in P; formally, if

$$\forall \epsilon > 0, \exists 0 < \delta < \epsilon \text{ such that } \forall Q' \in N_\delta(Q), Area(Q) \geq Area(Q'),$$

where

$$N_\delta(A_1A_2A_3A_4) = \{B_1B_2B_3B_4 \text{ is a parallelogram in } P \mid \forall 1 \leq i \leq 4, |A_i - B_i| < \delta\}.$$

Fact 1 Jin and Matulef [16] proved that, "local maximal in P" implies "inscribed on P".

Fact 2 When a parallelogram is inscribed on P but is degenerated, we can find another inscribed parallelogram with the same area but is not degenerated. To do this, we only need to shift the corners on the same edge to the side of the edge.

A parallelogram is an *MAP* (Maximum Area Parallelogram) if it is global maximum and not degenerated; and is an *LMAP* (Local Maximal Area Parallelogram) if it is local maximal and not degenerated. (We exclude the degenerated ones safely according to Fact 2.)

Definition 2.1 (The relationship "*ahead of*" between the edges)**.** For two distinct edges, e.g. e_i and e_j, we say that e_i is *ahead of* e_j, denoted by $e_i \prec e_j$, if $o_j \in (o_i, o_i + \pi)$, where o_i and o_j denote the orientation of vector $\overrightarrow{v_i, v_{i+1}}$ and $\overrightarrow{v_j, v_{j+1}}$ respectively. See Figure 2.

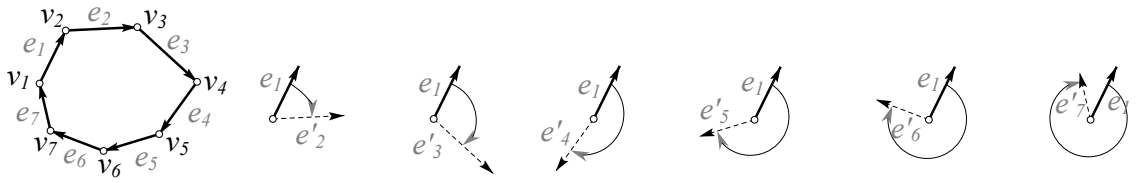

Figure 2: Illustration of the relationship "ahead of" between edges. In this example, edge e_1 is ahead of e_2 and e_3, whereas edges e_4, e_5, e_6, e_7 are ahead of e_1.

In this paper, we always assume that the edges of P are **pairwise nonparallel**. Therefore, for any pair of edges, one of them must be ahead of the other.

Definition 2.2. By a "*boundary-portion*" of P, we refer to a continuous portion of the boundary of P. For any boundary-portion, we consider it *directed* and its direction conforms with the clockwise order of ∂P; moreover, we refer to its two endpoints as the *starting point* and *terminal point* in the standard way (that conforms with the clockwise order). Note that each edge of P is a boundary-portion of P and so it is directed: the direction of e_i is from v_i to v_{i+1}.

For two points X, X' on the boundary of P, if we travel along the boundary of P in clockwise from X to X', we pass through a boundary-portion of P; the endpoints-inclusive version of this portion is denoted by $[X \circlearrowright X']$; and the endpoints-exclusive version of this portion is denoted by $(X \circlearrowright X')$. Note that $[X \circlearrowright X']$ contains a unique point X when $X = X'$.

2.1 The premier properties of the LMAPs

We first state the premier properties in Lemma 2.4, which are easy to understand but a little verbose. Then, we introduce some notations and restate them in a simpler form in Lemma 2.6.

Definition 2.3. Consider any pair of edges e_i, e_j such that $e_i \prec e_j$. Let l, l' denote the extended line of e_i, e_j respectively. The distance from a point X to (l, l'), denoted by $dist_{l,l'}(X)$, is defined as the product of the distance from X to l and the distance from X to l'. We can prove that in domain P, function $dist_{l,l}()$ achieves the maximum value at a unique point (proved in Lemma A.3), and we denote this point by $Z_{e_i}^{e_j}$ or Z_i^j.

For convenience, we call the points in set $\{Z_i^j \mid e_i \prec e_j\}$ the *Z-points*.

Lemma 2.4. *(*Premier properties of the LMAPs*) Suppose $A_0A_1A_2A_3$ is an LMAP and its corners A_0, A_1, A_2, A_3 lie in clockwise order. Consider an arbitrary corner A_i of this LMAP.*

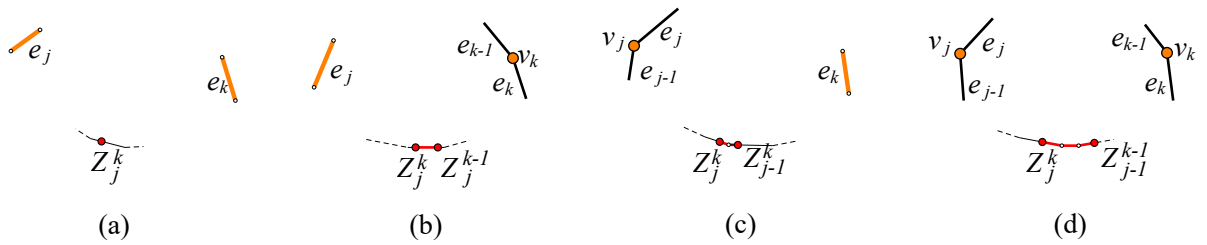

Figure 3: Premier properties of the LMAPs

1. *See Figure 3 (a). This corner must be coincided with Z_j^k if*

$$A_{i+1}, A_{i-1} \text{ lie on edges } e_j, e_k \text{ respectively and } e_j \prec e_k.$$

2. *See Figure 3 (b). This corner must lie in boundary-portion $[Z_j^{k-1} \circlearrowright Z_j^k]$ if*

$$A_{i+1}, A_{i-1} \text{ lie on } e_j, v_k \text{ respectively and } e_j \prec e_k.$$

3. *See Figure 3 (c). This corner must lie in boundary-portion $[Z_{j-1}^k \circlearrowright Z_j^k]$ if*

$$A_{i+1}, A_{i-1} \text{ lie on } v_j, e_k \text{ respectively and } e_{j-1} \prec e_k.$$

4. *See Figure 3 (d). This corner must lie in boundary-portion $[Z_{j-1}^{k-1} \circlearrowright Z_j^k]$ if*

$$A_{i+1}, A_{i-1} \text{ lie on } v_j, v_k \text{ respectively and } e_{j-1} \prec e_{k-1} \text{ and } e_j \prec e_k.$$

Note again: The edges are regarded as **open** segments; if we say that some point (like A_{i-1}, A_{i+1} above) lies on some edge, we think that it does *not* lie on the endpoints of the edge.

In what follows we describe the preceding properties in a simpler and united form. To this end, we shall introduce an important notion called *units*. In addition, we define the forward and backward edges of each unit and introduce the relationship "ahead of" between the units.

Definition 2.5. We call each edge and each vertex of P a "*unit*" of P.

For each vertex v_i, we define its *backward edge* and *forward edge* to be e_{i-1} and e_i, respectively. For each edge e_i, we define its *backward edge* and *forward edge* to be e_i itself. For each unit u, we denote its backward and forward edge by $back(u)$ and $forw(u)$ respectively.

We say that a unit u is ahead of a unit u' if

$$back(u) \prec back(u') \text{ and } forw(u) \prec forw(u').$$

When unit u is ahead of unit u', we define a boundary-portion

$$\zeta(u, u') = [Z_{back(u)}^{back(u')} \circlearrowright Z_{forw(u)}^{forw(u')}]. \tag{1}$$

Lemma 2.6 (Restatement of premier properties)**.** *Suppose that $A_0A_1A_2A_3$ is an LMAP and its corners A_0, A_1, A_2, A_3 lie in clockwise order. Consider an arbitrary corner A_i of this LMAP. Assume that A_{i+1}, A_{i-1} lie on unit u, u' respectively. We claim that A_i must lie in $\zeta(u, u')$ if*

$$u \text{ is ahead of } u'.$$

2.2 The transformed premier properties of the LMAPs

Here, we combine the premier properties of the LMAPs with the trivial property of the LMAPs (and of all the parallelograms) that says *the mid points of the two pairs of opposite corners coincide with each other*. As a result, we obtain *transformed premier properties* of the LMAPs.

First, we should interpret the premier properties from a different angle. We know the premier properties offer bounds for a corner A_i when the units u, u' containing A_i's neighboring corners are fixed. There are $\Theta(n^2)$ such bounds, since (u, u') have $\Theta(n^2)$ possibilities. These bounds together describe the following *relationship* between three consecutive corners of an LMAP.

Definition 2.7. Recall that the edges do not contain their endpoints. Therefore, each point X on ∂P belongs to a unique unit, denoted by $\mathbf{u}(X)$. Let ∂P^3 denotes $(\partial P, \partial P, \partial P)$. We define

$$\mathsf{T}^P := \{(X_1, X_2, X_3) \in \partial P^3 \mid \mathbf{u}(X_3) \text{ is ahead of } \mathbf{u}(X_1), X_2 \in \zeta(\mathbf{u}(X_3), \mathbf{u}(X_1))\}. \tag{2}$$

Lemma 2.8. *Suppose that $A_0A_1A_2A_3$ is an LMAP and A_0, A_1, A_2, A_3 lie in clockwise order. If $\mathbf{u}(A_{i+1})$ is ahead of $\mathbf{u}(A_{i-1})$, then $(A_{i-1}, A_i, A_{i+1}) \in \mathsf{T}^P$.*

Clearly, Lemma 2.8 is equivalent to Lemma 2.6, so its proof is omitted. Note that T^P is well-defined on P. When P is clear from the context, we may simply write T^P as T.

Next, let us introduce a function f on ∂P^3. For a tuple of points (X_1, X_2, X_3), we define $f(X_1, X_2, X_3)$ to be the unique point X under which $XX_1X_2X_3$ is a parallelogram. Equivalently, $f(X_1, X_2, X_3)$ is the symmetric point of X_2 with respect to the mid point of X_1, X_3.

Lemma 2.9 (Transformed premier properties)**.** *Suppose that $A_0A_1A_2A_3$ is an LMAP whose corners A_0, A_1, A_2, A_3 lie in clockwise order. For any corner A_i such that $\mathbf{u}(A_{i-1})$ is ahead of $\mathbf{u}(A_{i+1})$, the following hold. (All subscripts of A are taken module 4.)*

1. *Corner A_i lies in $f(\mathsf{T})$.*
2. *Let $u = \mathbf{u}(A_{i-1})$ and $u' = \mathbf{u}(A_{i+1})$. Corner A_i lies in*
$$block(u, u') := f(\{(X_1, X_2, X_3) \in \mathsf{T} \mid X_3 \in u, X_1 \in u'\}). \tag{3}$$
3. *Let $w = \mathbf{u}(A_{i+2})$. Corner A_i lies in*
$$sector(w) := f(\{(X_1, X_2, X_3) \in \mathsf{T} \mid X_2 \in w\}). \tag{4}$$

Proof. Since $A_0A_1A_2A_3$ is an LMAP and $\mathbf{u}(A_{i-1})$ is ahead of $\mathbf{u}(A_{i+1})$, we have

$$(A_{i+1}, A_{i+2}, A_{i+3}) \in \mathsf{T}$$

due to Lemma 2.8. Since $A_0A_1A_2A_3$ is a parallelogram,

$$A_i = f(A_{i+1}, A_{i+2}, A_{i+3}).$$

Together, $A_i \in f(\mathsf{T})$.

When $A_{i-1} \in u, A_{i+1} \in u'$, then

$$(A_{i+1}, A_{i+2}, A_{i+3}) \in \{(X_1, X_2, X_3) \in \mathsf{T} \mid X_3 \in u, X_1 \in u'\},$$

which implies that $f(A_{i+1}, A_{i+2}, A_{i+3}) \in block(u, u')$, i.e. $A_i \in block(u, u')$.

When $A_{i+2} \in w$, then

$$(A_{i+1}, A_{i+2}, A_{i+3}) \in \{(X_1, X_2, X_3) \in \mathsf{T} \mid X_2 \in w\},$$

which implies that $f(A_{i+1}, A_{i+2}, A_{i+3}) \in sector(w)$, i.e. $A_i \in sector(w)$. □

We call each region in $\{block(u, u') \mid u \text{ is ahead of } u'\}$ a *block*, and each region in $\{sector(w) \mid w \text{ is a unit of } P\}$ a *sector*. The blocks and sectors are planar regions, as illustrated in Figure 4. By Definition (3) and (4), all the blocks constitute a partition of $f(\mathsf{T})$ and so do all the sectors.

From the figure, we can simply observe that the blocks and sectors are well-structured.

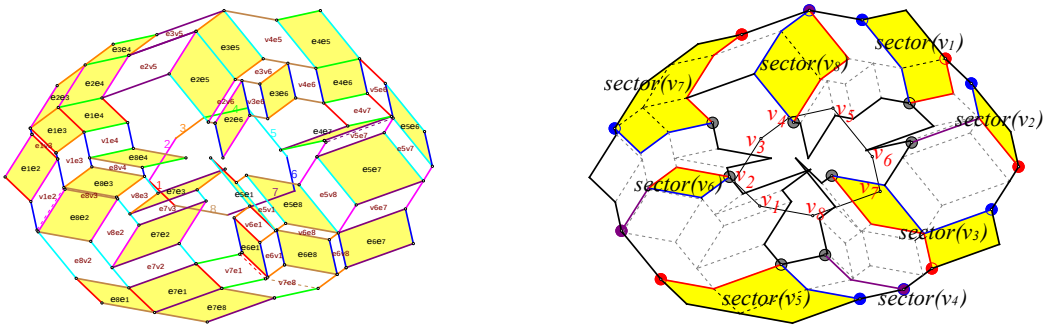

Figure 4: The block partition of $f(\mathsf{T})$ and the sector partition of $f(\mathsf{T})$.

2.3 Properties of $f(\mathsf{T})$ and an introduction of $Nest(p)$

Theorem 2.10.

Sector-continuity *For any vertex V, the intersection between $sector(V)$ and the boundary of P is continuous; it is either empty or a boundary-portion of P.*

Block-disjointness *The intersection of any pair of blocks lies in the interior of P.*

Reversibility-of-f *Let T^* denote the subset of T that is mapped to the boundary of P under f. Function f is a bijection from T^* to its image set $f(\mathsf{T}^*) = f(\mathsf{T}) \cap \partial P$.*

Interleavity-of-f *Region $f(\mathsf{T})$ has an "annular" appearance as shown in Figure 4, so it has two boundaries (which are polygonal closed curves); we call the inner one the "*inner boundary*" of $f(\mathsf{T})$. (See its explicit definition in Appendix E.1.) We claim that, the inner boundary of $f(\mathsf{T})$ interleaves ∂P, where "interleave" is defined as follows.*
Two oriented closed curves interleave *if, starting from any intersection between them, regardless of whether we travel around the first curve of a cycle or around the second curve of a cycle, we meet their intersections in identical order.*

Monotonicity-of-f *Let $f^{-1}()$ denote the reverse function of f on domain $f(\mathsf{T}) \cap \partial P$. Let $f_1^{-1}(X), f_2^{-1}(X), f_3^{-1}(X)$ respectively denote the 1st, 2nd, 3rd dimension of $f^{-1}(X)$. Notice that $f_2^{-1}()$ is a mapping from $f(\mathsf{T}) \cap \partial P$ to ∂P, we claim that $f_2^{-1}()$ is "circularly monotone". Specifically, if a point X travels in clockwise order around $f(\mathsf{T}) \cap \partial P$, point $f_2^{-1}(X)$ would shifts in clockwise order around the boundary of P non-strictly, and moreover, when X has traveled a cycle, $f_2^{-1}(X)$ also has traveled a cycle.*

Sector-monotonicity *$sector(v_1) \cap \partial P$, $sector(e_1) \cap \partial P$, ..., $sector(v_n) \cap \partial P$, $sector(e_n) \cap \partial P$ are disjoint and arranged in clockwise order on ∂P.*

These six properties of $f(\mathsf{T})$ are of great value for understanding the LMAPs, since set T is closely related to the LMAPs. As we show soon in the next subsection, by combining them with the premier properties, we can deduce two advanced properties of the LMAPs.

The elements in T that deserve special attention are those who are mapped to the boundary of P (which are defined as T^* in the theorem above). As the reader might noticed, all of the properties stated in Theorem 2.10 concern the properties of $f(\mathsf{T}^*)$, rather than $f(\mathsf{T})$.

Although, the statements of all these properties are succinct, their proofs are quite involved; more than a half of this paper is devoted to these proofs! However, the proofs are creative and highly modularized; lots of interesting lemmas are applied in the proofs. We outline the proofs in Subsection 3.4, where we also explain the inner connections of these properties.

We define $Nest(P)$ as the union of the boundaries of the blocks and sectors, or equivalently as the union of the boundaries of all the blocks and the n sectors $sector(v_1), \ldots, sector(v_n)$. The boundaries of the blocks and the n sectors are defined rigorously in Subsection 3.2 and 4.3.

Remark: Structure $Nest(P)$ is induced by the given polygon P, since all the blocks and sectors are well-defined on P. We name it $Nest(P)$ because that its shape resembles that of a bird nest; see Figure 1 for examples. This structure is a "visual description" of the transformed premier properties, since the blocks and sectors are bounding regions employed in these properties.

Terminologically, $Nest(P)$ is a "subdivision" over the exterior of P (due to the BLOCK-DISJOINTNESS). Moreover, it is an "arrangement" of certain line segments, each of which is parallel to an edge of P. In addition, it has $\Theta(n^2)$ line segments and hence is of size $\Theta(n^2)$.

2.4 Advanced properties of the LMAPs

To understand the properties of LMAPs, in particular the advanced properties stated below, we should now introduce a classification of the corners of the LMAPs.

Definition 2.11. Assume that $A_0A_1A_2A_3$ is a parallelogram inscribed on P, whose corners A_0, A_1, A_2, A_3 lie in clockwise order. Consider any corner, e.g. A_i.

Corner A_i is *broad* if $\mathbf{u}(A_{i+1})$ is ahead of $\mathbf{u}(A_{i-1})$.

Corner A_i is *narrow* if its opposite corner is broad; or if $\mathbf{u}(A_{i-1})$ is ahead of $\mathbf{u}(A_{i+1})$.

Corner A_i is *even* if it is neither broad nor narrow.

Figure 5 illustrates the broad, narrow and even corners.

Note 1 For all inscribed parallelograms, all their corners are classified to broad, narrow or even. The opposite corner of a broad, narrow, even corner is narrow, broad, even respectively.

Note 2 The premier properties provide bounds for each broad corner when its neighboring corners are fixed (on some units); whilst the transformed premier properties provide bounds for each narrow corner when its neighboring corners are fixed or its opposite corner is fixed.

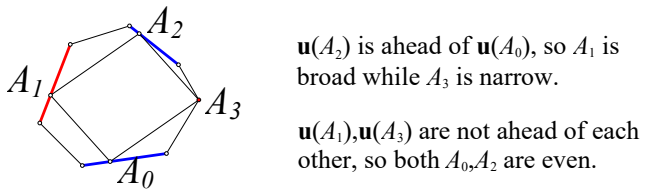

Figure 5: Illustration of broad, narrow and even corners.

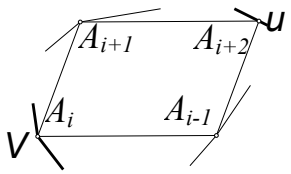

Figure 6: Illu. of Lemma 2.12.2

Lemma 2.12 (ADVANCED PROPERTIES OF THE LMAPS)**.** *Suppose that $Q = A_0A_1A_2A_3$ is an LMAP whose corners A_0, A_1, A_2, A_3 lie in clockwise order.*

1. *If A_i is a narrow corner which lies on point X, the other three corners $A_{i+1}, A_{i+2}, A_{i+3}$ lie on $f_1^{-1}(X), f_2^{-1}(X), f_3^{-1}(X)$ respectively.*
   Note: since A_i is narrow, $\mathbf{u}(A_{i-1})$ must be ahead of $\mathbf{u}(A_{i+1})$, and it follows that A_i lies in $f(\mathsf{T})$ according to the transformed premier properties (Lemma 2.9.1). Moreover, we also know that A_i lies on the boundary of P, since all LMAPs are inscribed on P. Therefore, $X \in f(\mathsf{T}) \cap \partial P$. Therefore, $f^{-1}(X)$ is well-defined according to REVERSIBLITY-OF-f .

2. *If corner A_i is broad and lies on vertex V while corner A_{i-1} is also broad, then A_{i-1} lies in*
$$\xi_V := \bigcup_{\text{unit } u \text{ intersects sector}(V) \text{ and } V \text{ is ahead of } u} \zeta(V, u). \tag{5}$$

Proof. 1. Since A_i is narrow, $\mathbf{u}(A_{i-1})$ must be ahead of $\mathbf{u}(A_{i+1})$. Then, by Lemma 2.8,

$$(A_{i+1}, A_{i+2}, A_{i+3}) \in \mathsf{T}.$$

Because $A_0A_1A_2A_3$ is a parallelogram, $(A_{i+1}, A_{i+2}, A_{i+3})$ is mapped to $A_i = X$ under function f. Therefore, $(A_{i+1}, A_{i+2}, A_{i+3})$ is a preimage of X in T under f. However, $f^{-1}(X)$ is the unique preimage of X in T under f. So, $(A_{i+1}, A_{i+2}, A_{i+3}) = f^{-1}(X)$.

2. See Figure 6. Let $u = \mathbf{u}(A_{i+2})$. Since A_i is broad, corner A_{i+2} is narrow. Applying the transformed premier properties, $A_{i+2} \in \mathit{sector}(\mathbf{u}(A_i)) = \mathit{sector}(V)$, which implies that unit u intersects $\mathit{sector}(V)$. Moreover, since A_{i-1} is broad, V is ahead of u. Together, $\zeta(V, u) \subseteq \xi_V$.

On the other hand, because A_{i-1} is broad, applying the premier property, we have

$$A_{i-1} \in \zeta\left(\mathbf{u}(A_i), \mathbf{u}(A_{i-2})\right) = \zeta(V, u).$$

Together, we get $A_{i-1} \in \xi_V$. □

Remark: The advanced property stated in Lemma 2.12.1 briefly says that all corners of an LMAP are settled as long as one of its narrow corner is settled. (Note that an LMAP may has no narrow corners.) This is useful in computing the LMAPs as shown in the next subsection. The REVERSIBLITY-OF-f plays an important role in deducing this advanced property.

The advanced property stated in Lemma 2.12.2 briefly says that if an LMAP has two broad corners and one of them lies on some vertex V, the other one could be bounded by a specific region defined as ξ_V. We should point out that these bounding regions are quite sharp; in fact, by applying the SECTOR-MONOTONICITY , we can further prove that $\xi_{v_1}, \ldots, \xi_{v_n}$ are boundary-portions of P that are disjoint and lie in clockwise order. (See Lemma 2.13.3 below.)

It is surprising that these advanced properties can be deduced from the original and transformed premier properties; the deduction is simple but not obvious.

2.5 The major procedure of our algorithm for computing the LMAPs

Lemma 2.13. *1. Any point X in $f(\mathsf{T}) \cap \partial P$ lies in a unique block and a unique sector. Moreover, suppose that X lies in $\mathit{block}(u, u')$ and $\mathit{sector}(w)$, then*

$$f_3^{-1}(X) \in u, f_2^{-1}(X) \in w, f_1^{-1}(X) \in u'. \tag{6}$$

2. Given a vertex V of P, we can determine whether $V \in f(\mathsf{T})$ and compute $f^{-1}(V)$ in $O(1)$ time if we have the information that tells

$$\text{“which block and sector does vertex } V \text{ lie in.”} \tag{7}$$

3. For each vertex V, the union ξ_V defined in (5) is a boundary-portion of P. Moreover, array ξ has the monotone property that its n elements $\xi_{v_1}, \ldots, \xi_{v_n}$ are disjoint (tough neighboring elements may share a common endpoint) and lie in clockwise order on ∂P.

4. Array ξ can be computed in linear time if we have the information that tells

$$\text{“which units are intersected by } \mathit{sector}(V) \text{ for each vertex } V\text{.”} \tag{8}$$

Note: According to the SECTOR-CONTINUITY , $\mathit{sector}(V) \cap \partial P$ is a boundary-portion, so the units intersected by $\mathit{sector}(V)$ are consecutive. Therefore, these units equal to an interval of units and can be stored implicitly in $O(1)$ space.

5. Given two vertices V, V' of P, in $O(\log n)$ time we can compute the parallelograms that are inscribed on P, not degenerated, and have a pair of neighboring corners lying on V, V'. (Note: Usually, such parallelogram is unique; but there are two exceptions. Exception 1: There would be two such parallelograms if P has an edge that is parallel to $\overline{VV'}$ and is longer than segment $\overline{VV'}$. Exception 2: There would be no such parallelograms if all the segments in P other than $\overline{VV'}$ that are parallel to $\overline{VV'}$ are shorter than segment $\overline{VV'}$.)

Proof or sketch of the proof.
1. Due to (3) and (4), $X = f(f_1^{-1}(X), f_2^{-1}(X), f_3^{-1}(X))$ lies in $block(\mathbf{u}(f_3^{-1}(X)), \mathbf{u}(f_1^{-1}(X)))$ and $sector(\mathbf{u}(f_2^{-1}(X)))$. So, X does lie in some block and sector. On the other hand, the Block-disjointness and the Sector-monotonicity implies that X cannot lie in multiple blocks or sectors. In addition, when X lies in $block(u, u')$ and $sector(w)$, we can conclude that $(\mathbf{u}(f_3^{-1}(X)), \mathbf{u}(f_1^{-1}(X)) = (u, u'))$ and $\mathbf{u}(f_2^{-1}(X)) = w$, which implies (6).

2. If V lies in no block and no sector, we can conclude that $V \notin f(\mathsf{T})$; otherwise, $V \in f(\mathsf{T})$. When the block and the sector containing V is known, we know exactly the units containing $f_1^{-1}(V), f_2^{-1}(V), f_3^{-1}(V)$. Then, to compute the exact positions of $f_1^{-1}(V), f_2^{-1}(V), f_3^{-1}(V)$, we only need to find three points X_1, X_2, X_3 within three given units so that $VX_1X_2X_3$ forms a parallelogram. Non-surprisingly, this can be done in $O(1)$ time. See the details in Appendix I.

3 & 4. According to the Sector-continuity , the units intersecting $sector(V)$ are consecutive, which implies that the units in set $U = \{u \mid u \text{ intersects } sector(V) \text{ and } V \text{ is ahead of } u\}$ are consecutive. Without loss of generality, let u_1, u_2 denote the clockwise first and last unit in U. We argue that ξ_V is a boundary-portion that starts at the starting point of $\zeta(V, u_1)$ and terminates at the terminal point of $\zeta(V, u_2)$, and thus it can be computed efficiently without computing the union of several portions. To prove this argument, we should prove and apply some monotone property of the ending points of $\{\zeta(V, u) \mid u \in U\}$. To prove the monotonicity of array ξ, we should further apply the Sector-monotonicity. We put the proofs in Appendix I.

5. It reduces to find a chord of P other than $\overline{VV'}$ but is a translation of $\overline{VV'}$, which can be found in $O(\log n)$ time by the Tentative Prune-and-Search technique. See Theorem 3.3 in [17]. □

We present the major procedure of our algorithm for computing the LMAPs in Algorithm 1. It computes the LMAPs with one anchored narrow corner or with two anchored broad corners.

Input: The information described in (7) and (8).
Output: All LMAPs with one anchored narrow corner or two anchored broad corners.
1 **foreach** *vertex* V *of* P **do**
2 Determine whether $V \in f(\mathsf{T})$ by checking weather V lies in some block;
3 If so, compute $f^{-1}(V)$ from (7) and output parallelogram $Vf_1^{-1}(V)f_2^{-1}(V)f_3^{-1}(V)$;
4 **end**
5 Compute array ξ from the information described in (8).
6 **foreach** *vertex pair* V, V' *such that* $V' \in \xi_V$ **do**
7 Compute and output all the parallelograms that are inscribed on P, not degenerated, and have two neighboring corners lying on V, V';
8 **end**

Algorithm 1: The major procedure of our algorithm for computing the LMAPs

Correctness: According to the advanced properties, the first loop in Algorithm 1 outputs all the *LMAPs with one anchored narrow corner*, while the second loop outputs all the *LMAPs with two anchored broad corners*. (Note that the algorithm may output some additional parallelograms that are not LMAPs; we only claim that certain LMAPs are outputted.)

Running time: Algorithm 1 runs in $O(n \log n)$ time. Specifically, Line 1-4 cost $O(n)$ time according to Lemma 2.13.2. Line 5 costs $O(n)$ time according to Lemma 2.13.4. Line 6-8 cost $O(n \log n)$ time according to Lemma 2.13.5 and the monotonicity of ξ stated in Lemma 2.13.3.

To complete our algorithm, a minor procedure should be added, which computes some remaining LMAPs (those who has an anchored even corner). It runs in $O(n \log n)$ time and is similar to the procedure for computing the LMAPs with two anchored broad corners. We present it in Subsection 4.2. Besides, a processing procedure should be add, which computes (7) and (8). This procedure costs $O(n \log^2 n)$ time and is outlined in 4.4.

3 Important Lemmas and Proving Techniques

In this section, we present the general method for proving the premier properties, as well as the general method for proving the properties of $f(\mathsf{T})$ stated in Theorem 2.10. Lots of lemmas are presented in this section, most of which are interesting in their own rights.

3.1 Techniques for proving the premier properties

We first state two key lemmas before we prove the premier properties.

Lemma 3.1. *Suppose that points X, X' lie in the same plane with two unparallel lines l, l'.*

1. *There is a unique pair of points Y, Y' such that*

$$Y \in l, Y' \in l' \text{and the mid point of } Y, Y' \text{ coincides with the mid point of } X, X'.$$

2. *There is a unique parallelogram (which may be degenerated), which has a pair of opposite corners lying on X, X' and has the other pair of opposite corners lying on l, l' respectively; and we denote this parallelogram by $\square(X, X', l, l')$.*

3. *Recall the distance function $dist_{l,l'}()$ defined in Definition 2.3. If X, X' lie in the same quadrant divided by l, l', then*

$$Area\left(\square(X, X', l, l')\right) = \left|dist_{l,l'}(X) - dist_{l,l'}(X')\right| / \sin\theta, \tag{9}$$

where θ denote the angle of the quadrant divided by l, l' and containing X, X'.
(Note: Here the constraint "X, X' lie in the same quadrant" is redundant. However, if we remove this constraint, we should define the distance from a point to a line in a signed version, in which the points on different sides of a line have different signs.)

Proof. 1. Let M be the mid point of X, X', and Y be the intersection of l and the reflecting line of l' around M, and Y' be the intersection of l' and the reflecting line of l around M. Then, (Y, Y') is clearly the unique pair of points that satisfies the conditions.

2. Claim 2 is a corollary of Claim 1.

3. We give the rigorous proof of Identity 9 in Appendix C. Here, we give its sketch. See Figure 7. Let O denote the intersection of l, l'. Let G, H denote the two points on l and l' such that $OGXH$ is a parallelogram, and G', H' the two points on l and l' such that $OG'X'H'$ is a parallelogram. Assume that $\square(X, X', l, l') = XYX'Y'$, where $Y \in l, Y' \in l'$. We can get that

$$\begin{aligned} Area(XYX'Y') &= Area(OYX'Y') - Area(GYX) - Area(HXY') - Area(OGXH) \\ &= Area(OYX'Y') - Area(H'X'Y') - Area(G'YX') - Area(OGXH) \\ &= Area(OG'X'H') - Area(OGXH). \end{aligned} \tag{10}$$

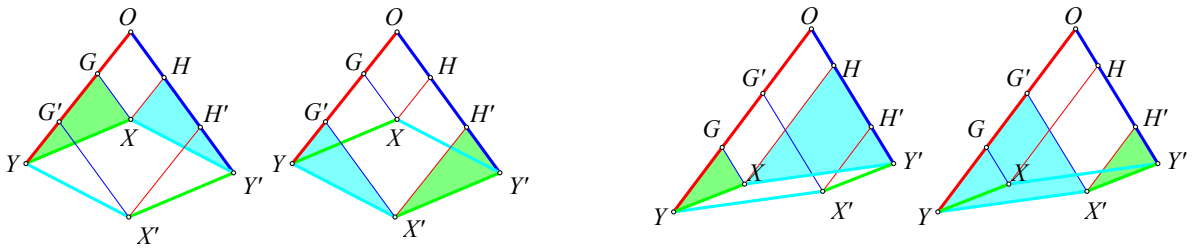

Figure 7: The geometric proof of Identity 9.

On the other hand, it can be simply computed that

$$Area(OGXH) = dist_{l,l'}(X)/sin\theta \quad \text{and} \quad Area(OG'X'H') = dist_{l,l'}(X')/sin\theta.$$

Together, we obtain Identity 9. □

Lemma 3.2. *Let ℓ_i, ℓ_j denote the extended lines of e_i, e_j, respectively. If $e_i \prec e_j$, then function $dist_{\ell_i,\ell_j}()$ is **strictly unimodal** on $[v_{j+1} \circlearrowright v_i]$. More specifically, i) $dist_{\ell_i,\ell_j}(X)$ strictly increases when point X travels from v_{j+1} to Z_i^j in clockwise along ∂P; and ii) $dist_{\ell_i,\ell_j}(X)$ strictly decreases when point X travels from Z_i^j to v_i in clockwise along ∂P.*

This lemma shows a unimodality of the distance function. We prove it in Appendix A.

Sketch of the proof of the premier properties. See Figure 8. Assume that $Q = A_0A_1A_2A_3$ is an LMAP. Assume that A_1, A_3 lie on units u and u' respectively, where u is ahead of u' .

Let a, a', b, b' respectively denote $back(u), back(u'), forw(u), forw(u')$. Note that $a \prec a'$ and $b \prec b'$, since u is ahead of u'. We shall prove that corner A_0 lies in $[Z_a^{a'} \circlearrowright Z_b^{b'}]$.

We prove it by contradiction. Suppose that A_0 lies in $(A_3 \circlearrowright Z_a^{a'})$, as shown in the figure; the proof is symmetric if A_0 lies in $(Z_b^{b'} \circlearrowright A_1)$. Let l, l' denote the extended lines of a, a', and let X be a point in $[A_0 \circlearrowright Z_a^{a'}]$. Denote $Q_X = \square(X, A_2, l, l')$ (recall the definition of $\square$ in Lemma 3.1) and denote by Y_X, Y'_X the opposite pair of corners of Q_X that lie on l, l'.

It is not difficult to prove that Y_X lie in edge a while Y'_X lie in edge a' as long as X is sufficiently close to A_0. Therefore, (i) Q_X is inscribed on P when X is sufficiently close to A_0.

By Lemma 3.1, $Area(Q_X)$ is in proportion to $dist_{l,l'}(X) - dist_{l,l'}(A_2)$. However, by Lemma 3.2, $dist_{l,l'}(X)$ strictly increases when X moves along $[A_0 \circlearrowright Z_a^{a'}]$. Together, we get (ii) the area of Q_X strictly increases when X moves along the boundary-portion $[A_0 \circlearrowright Z_a^{a'}]$.

Combining (i) and (ii), Q is not local maximal and hence is not an LMAP. □

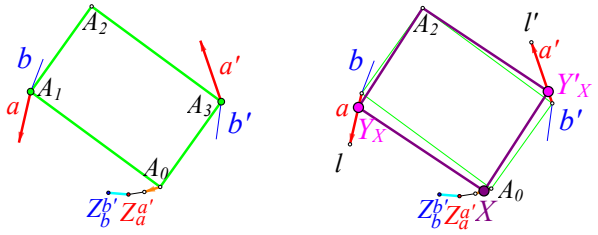

Figure 8: A sketch of the proof of the premier bounds.

Remark: In one sentence, the technique for proving the premier properties is as follows. If a corner A does not lie in some specific region, we apply Identity 9 to show that a strictly larger parallelogram can be found nearby *by adjusting the position of A while maintaining its opposite corner and adjusting the other two corners accordingly within the boundary of P.*

3.2 Geometric definition of the blocks and their borders

The following two subsections provide preliminary notations and lemmas for proving the properties of $f(\mathsf{T})$. In this subsection, we give an intuitive geometric definition for the blocks. Meanwhile we define the borders of the blocks and define the direction of the borders.

The blocks are important geometric objects in our paper. Previously, $block(u, u')$ is defined as the image set of $\mathsf{T}(u, u')$ under function f in Subsection 2.2, where

$$\begin{aligned} \mathsf{T}(u, u') &:= \{(X_1, X_2, X_3) \in \mathsf{T} \mid X_3 \in u, X_1 \in u'\} \\ &= \{(X_1, X_2, X_3) \mid X_3 \in u, X_2 \in \zeta(u, u'), X_1 \in u'\}. \end{aligned} \tag{11}$$

To give a geometric definition, we first state two formulas of the blocks.

Definition 3.3. For distinct units u, u', we define $u \oplus u' = \{\mathsf{M}(X,Y) \mid X \in u, X' \in u'\}$, where $\mathsf{M}(X,Y)$ denotes the mid point of point X and point Y.

Note: The shape of $u_1 \oplus u_2$ is a parallelogram, a segment, or a point. More specific, $e_i \oplus e_j$ equals an open parallelogram, whose four corners are respectively $\mathsf{M}(v_i, v_j)$, $\mathsf{M}(v_i, v_{j+1})$, $\mathsf{M}(v_{i+1}, v_j)$, $\mathsf{M}(v_{i+1}, v_{j+1})$; $e_i \oplus v_j$ equals the open segment $\overline{\mathsf{M}(v_i, v_j)\mathsf{M}(v_{i+1}, v_j)}$; $v_i \oplus e_j$ equals the open segment $\overline{\mathsf{M}(v_i, v_j)\mathsf{M}(v_i, v_{j+1})}$; $v_i \oplus v_j = \mathsf{M}(v_i, v_j)$. See Figure 9 for illustrations.

$$block(u, u') = \bigcup_{X \in u \oplus u'} \text{the reflection of } \zeta(u, u') \text{ around point } X. \tag{12}$$

$$block(u, u') = \bigcup_{X \in \zeta(u,u')} \text{the 2-scaling of } u \oplus u' \text{ about point } X. \tag{13}$$

The rigorous definition of "Reflecting" and "Scaling" is given in Definition 4.11. The proof of (12) and (13) follows from the definition of f and $block(u, u')$ and is presented in Appendix D.

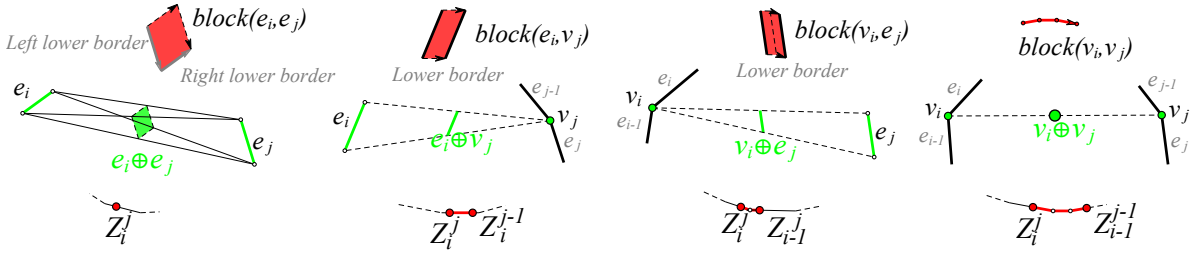

Figure 9: Illustration of $u \oplus u'$ and the geometric definition of the blocks.

We give the intuitive definition of blocks in the following. It is based on (12) and (13).

Definition 3.4 (Geometric definition of the blocks)**.** See Figure 9.

- When $e_i \prec e_j$, the 2-scaling of $e_i \oplus e_j$ about point Z_i^j is a parallelogram whose sides are congruent to either e_i or e_j; and we define this parallelogram to be $block(e_i, e_j)$.
  Each side of this parallelogram is called a *border* of $block(e_i, e_j)$. For those two borders that are congruent to e_i, we assume that they have the same direction as e_i. For those two borders that are congruent to e_i, we assume that they have the same direction as e_j.

- When v_i is ahead of v_j, the reflection of $\zeta(v_i, v_j)$ around $\mathsf{M}(v_i, v_j)$ is a polygonal curve, and we define it to be $block(v_i, v_j)$. We regard this curve as the only border of $block(v_i, v_j)$, and assume that its direction is from the reflection of Z_{i-1}^{j-1} to the reflection of Z_i^j.

- When v_i is ahead of e_j, $block(v_i, e_j)$ is the region bounded by the following curves:

  the 2-scaling of segment $v_i \oplus e_j$ about point Z_{i-1}^j;

  the 2-scaling of segment $v_i \oplus e_j$ about point Z_i^j.

  the reflection of $\zeta(v_i, e_j)$ around the mid point of v_i, v_j;

  the reflection of $\zeta(v_i, e_j)$ around the mid point of v_i, v_{j+1}.

  We call each of these curves a *border* of $block(v_i, e_j)$. The first two borders have the same direction as e_j; the other two goes from the reflection of Z_{i-1}^j to the reflection of Z_i^j.

- We define $block(e_i, v_j)$ and its related notions symmetric to $block(v_i, e_j)$.

Note: As we see, all the borders are arrangements of certain boundary-portions. Moreover, the direction of each border is the same as the original boundary-portion of this border.

3.3 Properties of the blocks and their bounding regions

In this subsection, we state some nontrivial properties of every single blocks. In particular, we introduce a new type of geometric objects $\{\chi_u^{u'} \mid u \text{ is ahead of } u'\}$, and state that $block(u,u')$ is bounded by $\chi_u^{u'}$. We call $\chi_u^{u'}$ the *bounding region* of $block(u,u')$. We also state two interesting properties of the bounding regions of the blocks.

Definition 3.5 (χ and $\widehat{\chi}$)**.** Consider two edges e_i, e_j such that $e_i \prec e_j$. See Figure 10 (a). Let $M = \mathsf{M}(v_i, v_{j+1})$. Make two rays at M, one with the opposite direction to e_j while the other with the same direction as e_i. We denote by χ_i^j the **open** region bounded by these two rays, and denote by $\widehat{\chi}_i^j$ the intersection of χ_i^j and ∂P;

Besides, consider any edge e_i. See Figure 10 (b). We denote by χ_i^j the **open** half-plane that is bounded by the extended line of e_i and lies the left of e_i, and $\widehat{\chi}_i^i$ the midpoint of e_i.

Note: The regions in $\{\widehat{\chi}_i^j \mid e_i \prec e_j \text{ or } e_i = e_j\}$ are boundary-portions of P, while regions in $\{\chi_i^j \mid e_i \prec e_j \text{ or } e_i = e_j\}$ are quadrants in the plane. (We regard the half-plane χ_i^i as a special quadrant whose apex lies at the midpoint of e_i.) In addition, $\chi_i^j \cap \partial P$ is always contained in $\widehat{\chi}_i^j$.

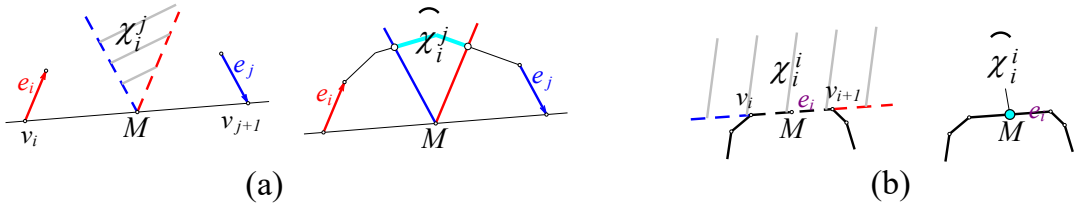

Figure 10: Illustration of the definition of χ_i^j and $\widehat{\chi}_i^j$.

Furthermore, we extend the definition of $\chi, \widehat{\chi}$ onto the pair of units. For a unit pair u, u' such that u is ahead of u', notice that $forw(u) \preceq back(u')$ and we define

$$\chi_u^{u'} = \chi_{forw(u)}^{back(u')}, \quad \widehat{\chi}_u^{u'} = \widehat{\chi}_{forw(u)}^{back(u')}. \tag{14}$$

Lemma 3.6. *Assume that unit u is ahead of unit u'.*

1. *(Bounding regions of blocks.) Region $block(u,u')$ is contained in region $\chi_u^{u'}$.*
2. *(Monotonicity of the borders.) Suppose we stand at some position in P's interior or boundary and in the opposite quadrant of $\chi_u^{u'}$, while point X travels along some border of $block(u,u')$. Then, point X is traveling in clockwise order around us.*
   *Note: when we discuss the opposite quadrant of χ_i^j, we assume that it is **open**.*
3. *(Local-reversibility of f.) Recall $\mathsf{T}(u,u')$ defined in (11) and recall that $block(u,u') = f(\mathsf{T}(u,u'))$. Function f is a bijection from $\mathsf{T}(u,u')$ to $block(u,u')$.*
4. *(Local-monotonicity of f.) For point X in $block(u,u')$, denote by $f_{u,u'}^{-1}(X)$ the unique preimage of X in $\mathsf{T}(u,u')$, and denote the 2nd point of $f_{u,u'}^{-1}(X)$ by $f_{u,u'}^{-1,2}(X)$.*
   We claim that, when point X travels in clockwise along a boundary-portion of P in $block(u,u')$, point $f_{u,u'}^{-1,2}(X)$ moves along ∂P in clockwise order non-strictly.

Lemma 3.7 (A peculiar property of χ). *For two edges e_i, e_j, we say $e_i \preceq e_j$ if $e_i = e_j$ or $e_i \prec e_j$. For every edge pair (e_i, e_j) such that $e_i \preceq e_j$, we call $[v_i \circlearrowright v_{j+1}]$ a* "small portion"*.*

For four edges $e_a, e_{a'}, e_b, e_{b'}$ such that $e_a \preceq e_{a'}$ and $e_b \preceq e_{b'}$ and that $e_a, e_{a'}, e_b, e_{b'}$ are not contained in any small portion, the intersection region $\chi_a^{a'} \cap \chi_b^{b'}$ lies in the interior of P.

Note that "small portion" is an important notion that is used frequently henceforth.

Lemma 3.8 (Monotonicity of $\widehat{\chi}$). *Consider two edges e_i, e_j such that $e_i \prec e_j$. See Figure 11. Let ρ denote $[v_i \circlearrowright v_{j+1}]$. We claim that*

$$(\widehat{\chi}_i^{j-1}).s \leq_\rho (\widehat{\chi}_i^j).s \leq_\rho (\widehat{\chi}_{i+1}^j).s, \tag{15}$$

$$(\widehat{\chi}_i^{j-1}).t \leq_\rho (\widehat{\chi}_i^j).t \leq_\rho (\widehat{\chi}_{i+1}^j).t, \tag{16}$$

where $(\widehat{\chi}_x^y).s$ and $(\widehat{\chi}_x^y).t$ denote the starting and terminal point of $\widehat{\chi}_x^y$, respectively, and where $\leq_\rho$ is defined as follows. For two points A, B on a boundary-portion ρ, we state that $A <_\rho B$ if A would be encountered earlier than B traveling along ρ; and that $A \leq_\rho B$ if $A = B$ or $A <_\rho B$.

More generally, consider m boundary-portions in a list $\widehat{\chi}_{u_1}^{u'_1}, \ldots, \widehat{\chi}_{u_m}^{u'_m}$, where $u_1, \ldots, u_m$ are units lying in clockwise order around ∂P, and $u'_1, \ldots, u'_m$ are units lying in clockwise order around ∂P, and u_k is ahead of u'_k for $1 \leq k \leq m$. We claim that the starting points of these portions lie in clockwise order around ∂P, and so do their terminal points.

The two properties of the bounding regions are well illustrated in the figure below.

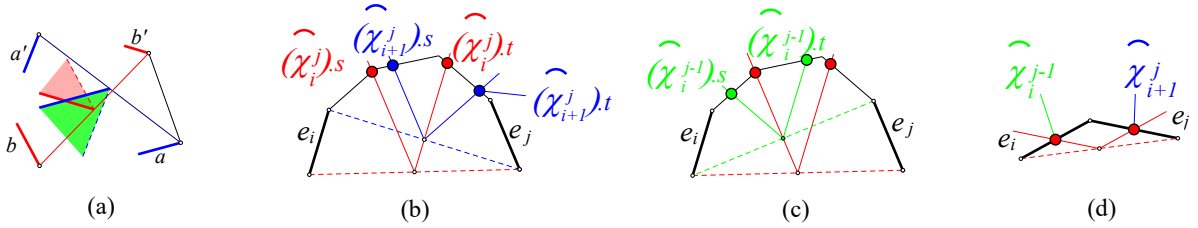

Figure 11: Illustration of the properties of χ and $\widehat{\chi}$.

Lemma 3.6 is proved in Appendix D — "Properties of a single block". Lemma 3.7 and Lemma 3.8 are proved in Appendix B — "Properties of the bounding regions".

3.4 Techniques for proving the properties of $f(\mathsf{T})$

Recall the properties of $f(\mathsf{T})$ stated in Theorem 2.10. We outline their proofs in this subsection.

The framework of our entire proof is illustrated in Figure 12. Among others, the Block-disjointness ad Interleavity-of-f are the most nontrivial; several lemmas are applied in proving them. These two properties are strongly connected; and their proofs are analogous.

The Local-reversibility of f (Lemma 3.6.3) is applied in proving Reversibility-of-f; and Local-monotonicity of f (Lemma 3.6.4) is applied in proving Monotonicity-of-f. The Sector-continuity is not drawn in this figure; this property is not related to others.

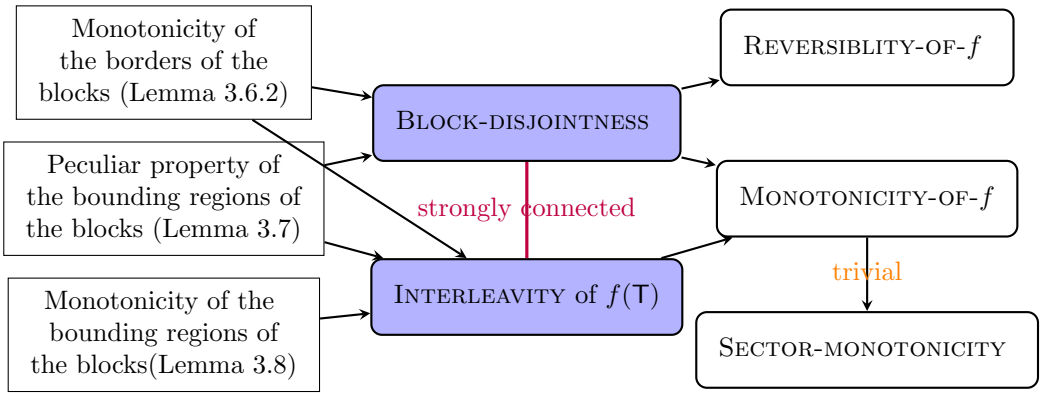

Figure 12: The structure of the proof. The Sector-continuity is not drawn in this picture because it is isolated.

Sketch of the proof of the BLOCK-DISJOINTNESS . Consider two blocks, e.g., $block(u, u')$ and $block(v, v')$. They are said *in-local-area*, if there exists (e_i, e_j) such that $e_i \preceq e_j$ and that

$$\text{the small portion } [v_i \circlearrowright v_{j+1}] \text{ contains } forw(u), back(u'), forw(v), back(v');$$

otherwise, they are said *in-global-area*.

Case 1: in-global-area. Then, $forw(u), back(u'), forw(v), back(v')$ are not contained in any small portion, and so

$$\chi_{forw(u)}^{back(u')} \cap \chi_{forw(v)}^{back(v')} \text{ lies in the interior of } P$$

according to the peculiar property of χ. On the other hand, according to Lemma 3.6.1,

$$block(u, u') \cap block(v, v') \subset \chi_u^{u'} \cap \chi_v^{v'} = \chi_{forw(u)}^{back(u')} \cap \chi_{forw(v)}^{back(v')}.$$

Together, the intersection of these two blocks lies in the interior of P.

Case 2: in-local-area. We claim that, *If $e_i \preceq e_j$, all blocks in set S are pairwise disjoint, where*

$$S = \{block(u, u') \mid u \text{ is ahead of } u', \text{ and } forw(u), back(u') \text{ lie in } [v_i \circlearrowright v_{j+1}]\}.$$

We can prove this claim by induction according to the following observation. See Figure 13. Let O denote the mid point of v_i, v_{j+1}. Then, *point X would move in clockwise order around O, if it travels along any border of any block in S.* This observation simply follows from the monotonicity of the borders of the blocks (Lemma 3.6.2). See the details in Subsection E.3.

In either case, the intersection of the two blocks lies in the interior of P. □

Next, we outline the proof of INTERLEAVITY-OF-f , which states that the inner boundary of $f(\mathsf{T})$ interleaves ∂P. Similar to the proof above, we shall handle a local case and a global case. Briefly, we argue that each local fraction of the inner boundary interleaves ∂P, while from a global viewpoint the local fractions are distributed far away from each other.

More specifically, our proof consists of four steps as follows.

1. We cut the inner boundary of $f(\mathsf{T})$ to $2q$ *fragments*, $\beta_1, \alpha_1, \ldots, \beta_q, \alpha_q$, where $q \geq 3$. See Figure 14 for an example, and see the definition of these fragments in Subsection E.4.

2. We choose $2q$ points $X_1, Y_1, \ldots, X_q, Y_q$ from the boundary of P which lie in clockwise order and "delimitate" the $2q$ fragments. By delimitate we mean that

   (i) for $1 \leq i \leq q$, the intersections between β_i and ∂P are contained in $[X_i \circlearrowright Y_i]$;

   (ii) for $1 \leq i \leq q$, the intersections between α_i and ∂P are contained in $[X_i \circlearrowright Y_{i+1}]$.

3. We prove that

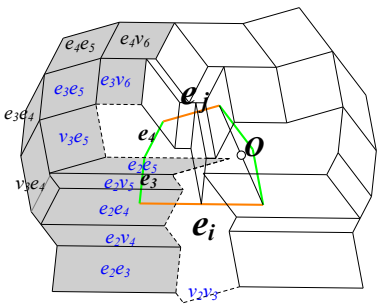

Figure 13: Blocks in local area are pairwise disjoint

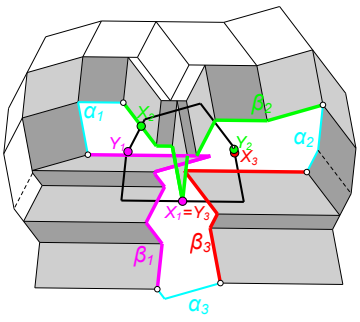

Figure 14: Split the inner bdry. of $f(\mathsf{T})$ to fragments.

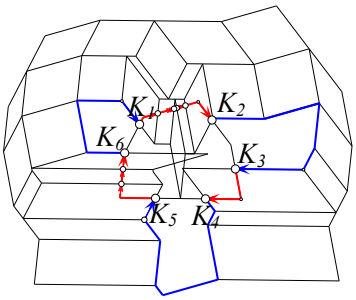

Figure 15: Illustration of the MONOTONICITY of f.

(iii) for $1 \leq i \leq q$, the concatenation of $\alpha_{i-1}, \beta_i, \alpha_i$ interleaves ∂P. ($\alpha_0 = \alpha_q$)

A directed curve $\mathcal{C}$ *interleaves* the curve ∂P, if $\mathcal{C}$ and ∂P are disjoint or the following is true: starting from their first intersecting point, regardless of whether we travel along $\mathcal{C}$ (in its positive direction) or along ∂P in clockwise, we would encounter the intersecting points between $\mathcal{C}$ and ∂P in the same order, where the *first* intersecting point refers to the one which will be encountered earlier than the others traveling along $\mathcal{C}$.

4. We prove the following lemma, which says that all the above imply Interleavity-of-f.

Lemma 3.9. *Assume that some closed curve can be cut to $2q$ fragments: $\beta_1, \alpha_1, \ldots, \beta_q, \alpha_q$, where $q \geq 3$, such that Property (iii) holds. Further assume that we can find $2q$ points $X_1, Y_1, \ldots, X_q, Y_q$ lying in clockwise order around P's boundary which "delimitate" the $2q$ fragments. Then, we can conclude that this curve interleaves ∂P.*

Step 2 corresponds to the global case; and Step 3 to the local case. In Step 2, the delimiting points are chosen from the endpoints of the boundary-portions in $\{\widehat{\chi}_i^j \mid e_i \preceq e_j\}$; and we apply the peculiarity and monotonicity of the bounding regions (Lemma 3.7 and Lemma 3.8) to prove (i) and (ii). In Step 3, we apply the monotonicity of the borders of the blocks to prove (iii). The proof of Lemma 3.9 is quite trivial. We give all the details in Subsection E.4.

Next, we prove Reversiblity-of-f from Block-disjointness .

Proof of the Reversiblity-of-f . For each unit pair (u, u') such that u is ahead of u', let us call $\mathsf{T}(u, u')$ a component of T. Clearly, each element of T belongs to exactly one component. Now, consider two elements of T^*. If they belong to the same component, their images under function f are distinct according to the Local-reversibility of f (Lemma 3.6.3). If they belong to distinct components, their images under function f do not coincide, because otherwise there would be two distinct blocks with an intersection on the boundary of P, which contradicts the Block-disjointness . Therefore, function f is a bijection from T^* to $f(\mathsf{T}^*)$. □

Next, we outline the proof of Monotonicity-of-f . See Figure 15 for an illustration.

Let σP denote the inner boundary of $f(\mathsf{T})$, and let $K_1, \ldots, K_m$ denote all the intersections between σP and ∂P, which lie in clockwise order around ∂P. Points $K_1, \ldots, K_m$ divide ∂P into m portions; and we call each of them a *K-portion*. We prove the following statements.

i) The *outer boundary* of $f(\mathsf{T})$ is a simple closed curve whose interior contains P.

ii) For every K-portion, it either lies entirely in $f(\mathsf{T})$, or lies entirely outside $f(\mathsf{T})$.

iii) For a K-portion that lies in $f(\mathsf{T})$, function $f_2^{-1}()$ is monotone on it, i.e. when point X travels in clockwise along this portion, $f_2^{-1}(X)$ shifts in clockwise around ∂P non-strictly.

iv) Points $f_2^{-1}(K_1), \ldots, f_2^{-1}(K_m)$ lie in clockwise order around ∂P.

Applying the last three statements, we obtain the Monotonicity-of-f as follows. According to ii), region $f(\mathsf{T}) \cap \partial P$ consists of those K-portions who lie entirely in $f(\mathsf{T})$. Now, suppose that a point X travels around $f(\mathsf{T}) \cap \partial P$ in clockwise; iii) assures that $f_2^{-1}(X)$ is monotone inside each K-portion, while iv) assures that $f_2^{-1}(X)$ is monotone between the K-portions.

The outline for proving these statements are as follows. Statement i) mainly follows from the Block-disjointness . Statement ii) follows from i) and the Interleavity-of-f . Statement iii) directly follows from the Local-monotonicity of f , since when X travels along a K-portion that lies in $f(\mathsf{T})$, it always travels in some blocks. To prove Statement iv), we should introduce a function g that is defined on σP. Briefly, for $X \in \sigma P$, we know X is an image of some tuple (X_1, X_2, X_3) in T; and we define $g(X) = X_2$. We can easily prove that

$g(X)$ is circularly monotone on σP. Moreover, since $K_1, \ldots, K_m$ lie in clockwise around ∂P, they lie in clockwise around σP according to INTERLEAVITY-OF-f , and thus $g(K_1), \ldots, g(K_m)$ lie in clockwise around ∂P according to the circularly monotone property. On the other hand, we have $f_2^{-1}(K_i) = g(K_i)$. Therefore, we obtain iv). See all the details in Subsection E.5.

Finally, we prove SECTOR-MONOTONICITY from MONOTONICITY-OF-f .

Proof of the SECTOR-MONOTONICITY . For any unit w,

$$\begin{aligned} \mathit{sector}(w) \cap \partial P &= \{f(X_1, X_2, X_3) \mid (X_1, X_2, X_3) \in \mathsf{T}^*, X_2 \in w\} \\ &= \left\{X \in f(\mathsf{T}) \cap \partial P \mid f_2^{-1}(X) \in w\right\} = \left\{X \in f(\mathsf{T}) \cap \partial P \mid \mathbf{u}(f_2^{-1}(X)) = w\right\}. \end{aligned}$$

Consider the points in $f(\mathsf{T}) \cap \partial P$. We know that $\mathbf{u}(f_2^{-1}())$ is a function on these points that maps them to the $2n$ units of P. From the MONOTONICITY-OF-f , $\mathbf{u}(f_2^{-1}())$ is circularly monotone on these points. So, $\mathbf{u}(f_2^{-1}())$ implicitly divides $f(\mathsf{T}) \cap \partial P$ into $2n$ parts which are disjoint and lie in clockwise order around ∂P. According to the equation above, these $2n$ parts are precisely $\mathit{sector}(v_1) \cap \partial P$, $\mathit{sector}(e_1) \cap \partial P$, ..., $\mathit{sector}(v_n) \cap \partial P$, $\mathit{sector}(e_n) \cap \partial P$. □

4 The Complete Algorithm

In subsection 2.5, we presented the *major procedure* of our algorithm for computing the LMAPs. To complete our algorithm we have to design two more procedures, one called *minor procedure*, which computes some LMAPs missed by the major procedure, and another called *preprocessing procedure*, which compute the information required by the major procedure, i.e., the information described in (7) and (8). We show the design of these two procedures in this section.

Lemma 4.1. *If an LMAP has a narrow corner whose two neighboring corners are both unanchored, this narrow corner must be anchored.*

Lemma 4.1 is proved in Appendix C together with the premier properties.

Lemma 4.2. *Assume Q is an LMAP. At least one of the following holds. 1) it has an anchored narrow corner; 2) it has two anchored broad corners; 3) it has an anchored even corner.*

Proof. Suppose Q is an LMAP. If a pair of its opposite corners are unanchored, one of the other corners must be narrow, and this narrow corner must be anchored due to the Lemma 4.1. Therefore, in this case Q has an anchored narrow corner. Now, assume that at least one corner is anchored among each pair of opposite corners. Suppose Q has an even corner A. Then, either A or A's opposite corer is anchored, so Q has an anchored even corner. Now, further assume that there is no even corner. Then, Q has at least two anchored corners that are narrow or broad. Thus, it either has an anchored narrow corner or has two anchored broad corners. □

The task of our minor procedure is to compute the LMAPs with an anchored even corner. Due to Lemma 4.2, the major procedure (which computes LMAPs with one anchored narrow corner or two anchored broad corners) and the minor one together compute all the LMAPs.

4.1 The generalized premier properties of the LMAPs

To compute the LMAPs with an anchored even corner, we have to apply some new properties of the LMAPs. The new properties are similar to the premier properties stated in Lemma 2.6, except that they bring us bounds on the even corners instead of the broad corners.

Lemma 4.3. *Suppose $A_0A_1A_2A_3$ is an LMAP and its corners A_0, A_1, A_2, A_3 lie in clockwise order. Consider an arbitrary corner A_i. Assume that A_{i+1}, A_{i-1} lie on unit u, u' respectively.*

- *(Bound on broad corners claimed in Lemma 2.6) Corner A_i must lie in $\zeta(u, u')$ if*

$$u \text{ is ahead of } u'. \tag{17}$$

- *(New claim - Bound on even corners) Corner A_i must lie in $\zeta(u, u')$ if*

$$u, u' \text{ are not ahead of each other.} \tag{18}$$

Recall that $\zeta(u, u')$ is defined as $[Z_{back(u)}^{back(u')} \circlearrowright Z_{forw(u)}^{forw(u')}]$ when u is ahead of u'. We extend the definition of $\zeta(u, u')$ right below so that it is defined for every pair of units u, u'. In particular, $\{\zeta(u, u') \mid u, u' \text{ are not ahead of each other}\}$ are used in the new claim in Lemma 4.3.

Definition 4.4. For any edge e_i, let δ_i denote the unique vertex of P that has the largest distance to the extended line of e_i. (The uniqueness is due to the assumption that edges of P are pairwise unparallel). For each unit pair (u, u') that are distinct, we define

$$\zeta(u, u') = [Z_a^{a'} \circlearrowright Z_b^{b'}], \text{ where } \begin{cases} e_a &= back(u) \\ e_{a'} &= \begin{cases} back(u'), & \text{if } back(u) \prec back(u'); \\ back(\delta_a), & \text{otherwise.} \end{cases} \\ e_{b'} &= forw(u') \\ e_b &= \begin{cases} forw(u), & \text{if } forw(u) \prec forw(u'); \\ forw(\delta_{b'}), & \text{otherwise.} \end{cases} \end{cases} \tag{19}$$

Note that this equation degenerates to (1) when u is ahead of u'.

The portions in $\{\zeta(u, u') \mid u, u' \text{ are not ahead of each other}\}$ are illustrated in Figure 16.

Remark: For convenience, all the properties stated in Lemma 4.3 are referred to as *generalized premier properties of the LMAPs*. We prove them all together in Appendix C.

Although, the proof of the bounds on the even corners are not substantially difficult than the proof of the previous bounds on the broad ones; fetching the bounds on the even corners are more difficult indeed. This can be perceived according to the definition of $\zeta(u, u')$.

In fact, we can prove that A_i lies in $\zeta(u, u')$ even if u' is ahead of u. This provides us bounds on the narrow corners. However, these bounds are useless and will not be proved in the paper.

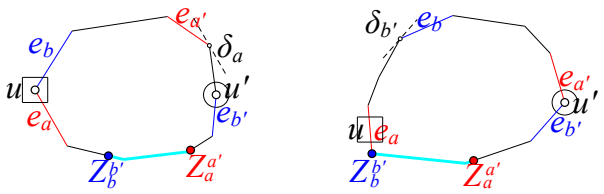

Figure 16: Definition of $\zeta(u, u')$ when u, u' are not ahead of each other.

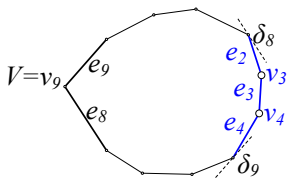

Figure 17: Definition of $\mathbb{H}_V$. Here, $\mathbb{H}_{v_9}$ contains the units in $(\delta_8 \circlearrowright \delta_9)$.

4.2 The minor procedure

Here, we design an algorithm for computing the LMAPs with an anchored even corner, which is referred to as *minor procedure*. Recall the notation δ introduced in Definition 4.4. For each vertex V, denote by $\mathbb{H}_V$ the set of units that lie in $(\delta_{back(V)} \circlearrowright \delta_{forw(V)})$. (See Figure 17.)

Lemma 4.5. *If $A_0A_1A_2A_3$ is an LMAP where A_0, A_1, A_2, A_3 lie in clockwise and A_i is an even corner, one of the following holds.*

(a) Corner A_{i+1} lies on some vertex V, while A_i lies in $\bigcup_{u\in\mathbb{H}_V}\zeta(V,u)$.

(b) Corner A_{i-1} lies on some vertex V, while A_i lies in $\bigcup_{u\in\mathbb{H}_V}\zeta(u,V)$.

Proof. Let $u^+ = \mathbf{u}(A_{i+1}), u^- = \mathbf{u}(A_{i-1})$. Units u^+, u^- are distinct and not ahead of each other because A_i is an even corner. A crucial observation is that one of the following holds:

(a') *u^+ is a vertex and $u^- \in \mathbb{H}_{u^+}$.*

(b') *u^- is a vertex and $u^+ \in \mathbb{H}_{u^-}$.*

Clearly, (a') implies (a). Suppose (a') is true. Let $V = u^+, u = u^-$. Then, $u \in \mathbb{H}_V$. Moreover, according to Lemma 4.3, A_i lies in $\zeta(u^+, u^-) = \zeta(V, u)$. Together, A_i lies in $\bigcup_{u\in\mathbb{H}_V}\zeta(V,u)$.

Symmetrically, (b') implies (b).

Next, we prove the preceding observation about u^+, u^-.

Case 1: u^+ is a vertex while u^- is an edge. In this case, we argue that $u^- \in \mathbb{H}_{u^+}$.
Assume $u^+ = v_i$. First, $u^- \notin \{e_i, e_{i-1}\}$. Second, because u^+ is not ahead of u^-, edge u^- is not contained in $[v_{i+1} \circlearrowleft \delta_{i-1}]$. Third, because u^- is not ahead of u^+, edge u^- is not contained in $[\delta_i \circlearrowleft v_{i-1}]$. Together, edge u^- can only lie in $(\delta_{i-1} \circlearrowleft \delta_i)$, i.e. $u^- \in \mathbb{H}_{u^+}$.

Case 2: u^+ is an edge while u^- is a vertex. Symmetric to Case 1, we have $u^+ \in \mathbb{H}_{u^-}$.

Case 3: u^+, u^- are both vertices, e.g., $u^+ = v_i, u^- = v_j$.

Assume $e_i \prec e_j$, otherwise it is symmetric. Then, $e_{j-1} \prec e_{i-1}$, because otherwise v_i is ahead of v_j.

Since $e_i \prec e_j$, we get $v_j \in (v_i \circlearrowleft \delta_i)$. Since $e_{j-1} \prec e_{i-1}$, we get $v_j \in (\delta_{i-1} \circlearrowleft v_i)$. Together, $v_j \in (\delta_{i-1} \circlearrowleft \delta_i)$, i.e. $u^- \in \mathbb{H}_{u^+}$.

□

The algorithm is presented in Algorithm 2, where

$$\kappa_V^+ := \bigcup\nolimits_{u\in\mathbb{H}_V}\zeta(V,u), \qquad \kappa_V^- := \bigcup\nolimits_{u\in\mathbb{H}_V}\zeta(u,V). \tag{20}$$

```
1 Compute array κ_V^+ and array κ_V^-;
2 foreach vertex pair V, V' such that V' ∈ κ_V^+ or V' ∈ κ_V^- do
3 |   Compute and output all the parallelograms that are inscribed on P, not degenerated,
  |   and have two neighboring corners lying on V, V';
4 end
```

Algorithm 2: Compute the LMAPs with an anchored even corner

Based on Lemma 4.5, this algorithm computes all the LMAPs with an anchored even corner. It runs in $O(n \log n)$ time according to Lemma 2.13.5 and the following lemma.

Lemma 4.6. *1. For each vertex V, the unions κ_V^+, κ_V^- are boundary-portions of ∂P. In addition, we can compute arrays κ^+, κ^- in linear time.*

2. Array κ^+ has the monotone property that its n elements $\kappa_{v_1}^+, \ldots, \kappa_{v_n}^+$ are disjoint and are arranged in clockwise order around P's boundary. (Note that neighboring elements may share a common endpoint.) Array κ^- has the same property. As a corollary, there are only $O(n)$ pairs of vertices V, V' such that $V' \in \kappa_V^+$ or $V' \in \kappa_V^-$.

These properties of κ^+, κ^- are similar to those of ξ, and are proved in Appendix I.

4.3 Prove the Sector-continuity & Compute $sector(V) \cap \partial P$

Assume that V is a fixed vertex. In this subsection we depict the morphology of $sector(V)$, informally define its two boundaries, and outline the proof of the SECTOR-CONTINUITY , which says that $sector(V) \cap \partial P$ is a boundary-portion of P. Moreover, we outline the algorithm for computing the endpoints of $sector(V) \cap \partial P$, which will be used in the preprocessing procedure.

This subsection is organized as follows. ① We introduce two special edges e_{s_V}, e_{t_V}. ② We introduce some directed segments called *roads* and define two particular *routes* consists of the roads, named $\mathcal{L}_V$ and $\mathcal{R}_V$. ③ We depict the morphology of $sector(V)$ by $\mathcal{L}_V, \mathcal{R}_V$: It is roughly a 2-scaling of the region that is bounded by $\mathcal{L}_V$ and $\mathcal{R}_V$. ④ We state some properties of the routes and thus prove the SECTOR-CONTINUITY . In addition, we show that computing the endpoints of $sector(V) \cap \partial P$ reduces to computing $\mathcal{L}_V^\star \cap \partial P$ and $\mathcal{R}_V^\star \cap \partial P$, where $\mathcal{L}_V^\star, \mathcal{R}_V^\star$ are the scaled versions of $\mathcal{L}_V, \mathcal{R}_V$ respectively. ⑤ We discuss how to compute $\mathcal{L}_V^\star \cap \partial P$ or $\mathcal{R}_V^\star \cap \partial P$.

① **Introduction of e_{s_V}, e_{t_V}.** We suspend their definitions for a while, since the definitions are slightly complicated and are unhelpful for depicting the morphology of $sector(V)$. For simplicity, we abbreviate these two edges by e_s, e_t. We promise that the following holds.

(i) $e_s \preceq e_t$, so $[v_s \circlearrowright v_{t+1}]$ is a small portion. Moreover, $[v_s \circlearrowright v_{t+1}]$ does not contain V.

Facts (i)-(viii) stated in this subsection are proved in Appendix F.

② **Definition of $\mathcal{L}_V, \mathcal{R}_V$.** Denote

$$\Delta_V = \left\{ (u, u') \mid \begin{array}{c} u, u' \text{ are units in } [v_s \circlearrowright v_{t+1}] \text{ such that} \\ u' \text{ is after but not right after } u \text{ (in clockwise)} \end{array} \right\}. \tag{21}$$

Recall the regions $\{u \oplus u' \mid u, u' \text{ are distinct}\}$ introduced in Definition 3.3. In particular, see Figure 18 (a) for an illustration of all those regions in $\{u \oplus u' \mid (u, u') \in \Delta_V\}$, and note that

(ii) regions in $\{u \oplus u' \mid (u, u') \in \Delta_V\}$ are pairwise disjoint. (This follows from $e_s \preceq e_t$.)

See Figure 18 (b). For any unit pair $(e_i, v_j) \in \Delta_V$, region $e_i \oplus v_j$ is a segment and we consider it has *the same* direction as e_i; for any unit pair $(v_i, e_j) \in \Delta_V$, region $v_i \oplus e_j$ is a segment and we consider it has *the opposite* direction to e_j; we call each such directed segment a *road*. see Figure 18 (c). Starting from $\mathsf{M}(v_s, v_{t+1})$, we can travel along several roads to reach $[v_s \circlearrowright v_{t+1}]$; and this would yields a directional zigzag polygonal curve. We call such a curve a *route*.

To define $\mathcal{L}_V$ and $\mathcal{R}_V$, we first state an interesting monotone property of the Z-points. (The bi-monotonicity of Z-points is proved in Appendix A.)

Lemma 4.7 (Bi-monotonicity of Z-points). *Assume that e_s, e_t are two edges such that $e_s \preceq e_t$. Consider all points in set $\{Z_i^j \mid (e_i, e_j) \in S\}$, where*

$$S = \{(e_i, e_j) \mid e_i \prec e_j, \text{ and } e_i, e_j \text{ both belong to } \{e_s, e_{s+1}, \ldots, e_t\}.\}$$

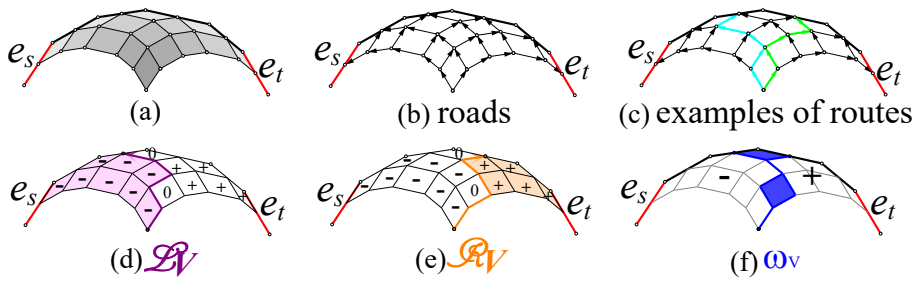

Figure 18: Illustration of $\mathcal{L}_V, \mathcal{R}_V$ and the region ω_V bounded by $\mathcal{L}_V, \mathcal{R}_V$ and ∂P.

We claim that all these Z-points lie in boundary-portion $\rho = [v_{t+1} \circlearrowleft v_s]$ and they have the following monotonicity. For $(e_i, e_j), (e_{i'}, e_{j'})$ in S such that $e_i \preceq e_{i'}$ and $e_j \preceq e_{j'}$, we have

$$Z_i^j \leq_\rho Z_{i'}^{j'}.$$

We now define $\mathcal{L}_V$ and $\mathcal{R}_V$. Denote $\rho = [v_{t+1} \circlearrowleft v_s]$. For any region $e_i \oplus e_j$ such that $(e_i, e_j) \in \Delta_V$, we mark it '-' if $Z_i^j <_\rho V$; '+' if $V <_\rho Z_i^j$; and '0' if $V = Z_i^j$. According to the bi-monotonicity of the Z-points, there exists a unique route, denoted by $\mathcal{L}_V$, which separates the regions marked by '-' from the regions marked by '+/0'. ($\mathcal{L}_V$ is defined explicitly before Lemma F.2.) Similarly, there exists a unique route, denoted by $\mathcal{R}_V$, which separates the regions marked by '+' from the regions marked by '-/0'. See Figure 18 (d),(e) for illustrations.

③ **Depiction of** *sector*(V)**.** Denote by ω_V the region bounded by $\mathcal{L}_V, \mathcal{R}_V$ and ∂P as shown in Figure 18 (e), which contains its boundaries $\mathcal{L}_V, \mathcal{R}_V$. Then, *sector*$(V)$ is (roughly) the 2-scaling of ω_V about V. More precisely, we prove that

$$\textit{sector}(V) = \text{2-scaling of } (\omega_V - \epsilon_V) \text{ about } V, \tag{22}$$

where ϵ_V denote the region united by regions in $\{u \oplus u' \mid (u, u') \in \Delta_V, u \text{ is not ahead of } u'\}$.

To prove Equation (22), we mainly apply the following facts.

(iii) $\textit{sector}(V) = \text{2-scaling of } \left(\bigcup_{u \text{ is ahead of } u', \zeta(u,u') \text{ contains } V} u \oplus u'\right)$ about V.

(iv) If u is ahead of u' and $\zeta(u, u')$ contains V, then $(u, u') \in \Delta_V$.

Fact (iii) follows from the definition of sectors; and (iv) follows from the definitions of e_s, e_t.

④ **The proof:** *sector*$(V) \cap \partial P$ **is a boundary-portion of** P**.**

(v) For each route, call its 2-scaling about V a *scaled-route*. Then, if we travel along a scaled-route, we will eventually get outside P and never return to P since then. (So there is at most one intersection between a scaled-route and ∂P.)

According to (v), we can prove the following fact about the 2-scaling of ω_V about V.

(vi) Let $\mathcal{L}_V^\star, \mathcal{R}_V^\star, \omega_V^\star$ denote the scaled version $\mathcal{L}_V, \mathcal{R}_V, \omega_V$. If the common starting point of $\mathcal{L}_V^\star, \mathcal{R}_V^\star$ lies in P, then $\omega_V^\star \cap \partial P = [\mathcal{L}_V^\star \cap \partial P \circlearrowleft \mathcal{R}_V^\star \cap \partial P]$; otherwise $\omega_V^\star \cap \partial P$ is empty.

On the other hand, according to (22), we can prove the following fact.

(vii) *sector*$(V) \cap \partial P$ is a boundary-portion that has the same endpoints as $\omega_V^\star \cap \partial P$.

Combine (vi) with (viii) and the immediate result is the SECTOR-CONTINUITY . Moreover, computing the endpoints of *sector*$(V) \cap \partial P$ reduces to computing $\mathcal{L}_V^\star \cap \partial P$ and $\mathcal{R}_V^\star \cap \partial P$.

⑤ **Compute** $\mathcal{L}_V^\star \cap \partial P$ **and** $\mathcal{R}_V^\star \cap \partial P$**.** Briefly, we can generate an arbitrary edge in $\mathcal{L}_V^\star$, and in $O(\log n)$ time decide whether it lies inside P, intersects P, or lies outside P. Therefore,

(viii) we can compute $\mathcal{L}_V^\star \cap \partial P$ (or $\mathcal{R}_V^\star \cap \partial P$) by a binary search, which costs $O(\log^2 n)$ time.

We attach the definitions of e_s, e_t below; see their demonstrations in Appendix F.

Definition 4.8 (e_s, e_t)**.** We say e_i is *smaller than* e_j, or e_j is *larger than* e_i, if e_i is enumerated earlier when we enumerate all edges in clockwise order from V's clockwise next edge to V's clockwise previous edge.

We define e_{s_V} to be the smallest edge e_i such that $\bigcup_{e_j : e_i \prec e_j} [v_{i+1} \circlearrowleft Z_i^j]$ contains V.

We define e_{t_V} to be the largest edge e_i such that $\bigcup_{e_k : e_k \prec e_i} [Z_k^i \circlearrowleft v_i]$ contains V.

Note 1 When we mention the two boundaries of *sector*(V), we refer to $\mathcal{L}_V^\star$ and $\mathcal{R}_V^\star$.

Note 2 The challenges in studying *sector*(V) lie in defining e_s, e_t properly and proving (i).

4.4 The preprocessing procedure

In the last subsection, we outline the algorithm for computing the endpoints of $sector(V) \cap \partial P$ for each vertex V. After computing these endpoints, we can easily compute the information "*which units does* $sector(V)$ *intersect and which sector does vertex* V *lie in*". The details of computing these information are provided in Appendix G.

In this subsection, we assume that V is a fixed vertex, and we show how do we compute "*which block does vertex* V *lie in*". Here we assume that $sector(w)$ contains V and w has been computed. This means that $V \in f(\mathsf{T})$ and there is a unique block containing V. (When no sector contains V, we determine that $V \notin f(\mathsf{T})$ and return "no block contains V".)

Let $block(u_1^*, u_2^*)$ denote the unique block that contains V; we shall compute (u_1^*, u_2^*).

The first step is the most tricky and important, in which we compute two critical edges e_{pV}, e_{qV} (abbreviated by e_p, e_q) to constrain the candidate space of (u_1^*, u_2^*).

(i) In $O(\log n)$ time, we can compute two edges e_p, e_q satisfying the following properties.

$$e_p \prec e_q \text{ and } V \text{ lies in } (v_p \circlearrowright v_{q+1}); \tag{23}$$

$$[v_p \circlearrowright V) \text{ contains } u_1^*; \text{ and } (V \circlearrowright v_{q+1}] \text{ contains } u_2^*. \tag{24}$$

Note: $[X \circlearrowright X')$ denotes $[X \circlearrowright X'] - \{X'\}$, and $(X \circlearrowright X']$ denotes $[X \circlearrowright X'] - \{X\}$.
The method for computing e_p, e_q are outlined later; we first assume that they are given.

In the next, we have to discuss two cases depending on whether V lies in $sector(v_k)$ for some vertex v_k or lies in $sector(e_k)$ for some edge e_k. Here, we assume that V lies in $sector(e_k)$ since this case is typical and more challenging. The other case is considered in Subsection H.3.

Consider any unit pair (u, u') such that

$$u \text{ is ahead of } u', \text{ and } u \text{ lies in } [v_p \circlearrowright V) \text{ while } u' \text{ lies in } (V \circlearrowright v_{q+1}]. \tag{25}$$

We regard this unit pair *active* if

$$\zeta(u, u') \text{ intersects } e_k. \tag{26}$$

(ii) The target unit pair (u_1^*, u_2^*) is active.

Based on (ii), the candidate space of (u_1^*, u_2^*) is further narrowed down. See Figure 19.
Next, we introduce some regions called *cells*. For each active unit pair (u, u'), we define

$$cell(u, u') := block(u, u') \cap sector(e_k), \tag{27}$$

and call it a *cell*. Note that $cell(u_1^*, u_2^*)$ is the only cell that contains V; otherwise there exist two blocks containing V. So, the question is: how do we find the unique cell that contains V?

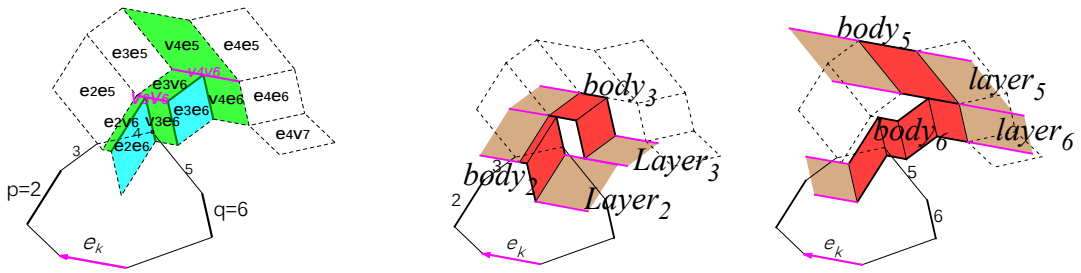

Figure 19: Illustration of the cells and layers. The left picture labels all the unit pairs satisfying (25); in which the ones in the colored region are those satisfying (26) too.

The idea is as follows. An edge e_j in $(v_p \circlearrowleft V)$ is said *active* if there is at least one unit u such that (e_j, u) is active; An edge e_j in $(V \circlearrowleft v_{q+1})$ is said *active* if there is at least one unit u such that (u, e_j) is active; for each active edge e_j, we define a region layer_j, which contains all the cells that are parallel to e_j. See illustrations in Figure 19 and see the rigorous definitions in (iii) and (iii') below. We observe that there is a monotonicity between the cells within the same layer; and there is a monotonicity between the layers; by utilizing these monotonicities, we can compute the layer that contains V and then the cell that contains V by a binary search.

(iii) Assume that e_j is an active edge in $(v_p \circlearrowleft V)$. Then, the unit set $\{u \mid (e_j, u) \text{ is active}\}$ consists of consecutive units. Moreover, let $u_s, \ldots, u_t$ denote the units in this set in clockwise order, then $cell(e_j, u_s), \ldots, cell(e_j, u_t)$ are all parallelograms with a pair of sides congruent to e_j, and they are contiguous and lie monotonously in the opposite direction of e_k. Denote by body_j the region united by these cells, which is a complex region that has two borders congruent to e_j. Denote by layer_j the extension of body_j by removing those two borders congruent to e_j, which contains body_j and two strip regions that are parallel to e_k. We call layer_j an *A-type layer*.

(iii') Assume that e_j is an active edge in $(V \circlearrowleft v_{q+1})$. Then, the unit set $\{u \mid (u, e_j) \text{ is active}\}$ consists of consecutive units. Moreover, let $u_s, \ldots, u_t$ denote the units in this set in clockwise order, then $cell(u_s, e_j), \ldots, cell(u_t, e_j)$ are all parallelograms with a pair of sides congruent to e_j, and they are contiguous and lie monotonously in the opposite direction of e_k. We define body_j and layer_j symmetric to (iii), and call layer_j a *B-type layer*.

(iv) The active edges in $(v_p \circlearrowleft V)$ are consecutive. The active edges in $(V \circlearrowleft v_{q+1})$ are consecutive. All the layers lie in the closed half-plane bounded by the extended line of e_k and containing P. Moreover, all the A-type layers are disjoint and lie monotonously in the direction perpendicular to e_k. (More specifically, for any two adjacent A-type layers layer_j and layer_{j+1}, they are disjoint, and layer_j lies in the area bounded by layer_{j+1} and the extended line of e_k.) Symmetrically, all the B-type layers have the same monotonicity.

Our result is the following.

(v) We can compute the unique cell that contains V in $O(\log^2 n)$ time.

In what follows we outline the method for computing (e_p, e_q) which verifies Fact (i).

Definition 4.9. Assume that $V = v_i$. Denote

$$\nabla_V = \big\{(u, u') \mid u \text{ is a unit in } (\delta_i \circlearrowleft v_i), u' \text{ is a unit in } (v_i \circlearrowleft \delta_{i-1}), \text{ and } u \text{ is ahead of } u'\big\}. \quad (28)$$

For $(e_a, e_{a'})$ in ∇_V, we call it a *turning pair*, if neither $(e_{a-1}, e_{a'})$ nor $(e_a, e_{a'+1})$ belongs to ∇_V. We denote by $\mathsf{TP}_1, \ldots, \mathsf{TP}_t$ all the turning pairs and assume that they are sorted in such a way that TP_1 is the topmost turning pair and TP_t is the leftmost turning pair. (See Figure 20.)

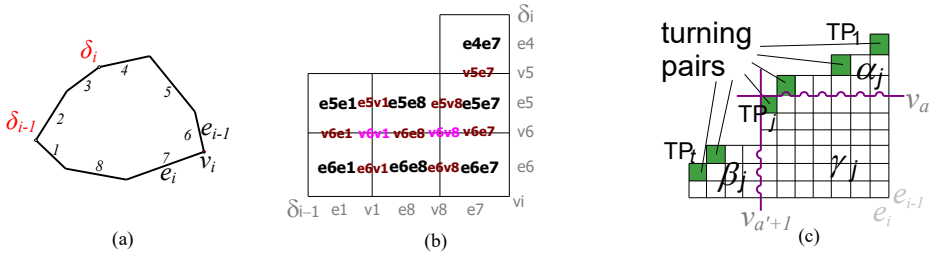

Figure 20: An illustration of set ∇_V and its turning pairs.

For each turning pair $\mathsf{TP}_j = (e_a, e_{a'})$, we define three subsets of ∇_V as follows. If we cut ∇_V along the horizontal line corresponding to v_a and the vertical line corresponding to $v_{a'+1}$, we get three chunks; the unit pairs in the top chunk are in α_j; those in the left chunk are in β_j; and the rest have a rectangular shape and they contain the unit pairs in γ_j. Formally,

$$\begin{aligned}
\alpha_j &= \{(u, u') \in \nabla_V \mid u \text{ lies in } (\delta_i \circlearrowleft v_a)\},\\
\beta_j &= \{(u, u') \in \nabla_V \mid u' \text{ lies in } (v_{a'+1} \circlearrowleft \delta_{i-1})\},\\
\gamma_j &= \left\{(u, u') \in \nabla_V \mid u \text{ lies in } [v_a \circlearrowleft v_i), u' \text{ lies in } (v_i \circlearrowleft v_{a'+1}]\right\}.
\end{aligned}$$

Two key observations are as follows, where $\widehat{\chi}[S] := \bigcup_{(u,u')\in S} \widehat{\chi}_u^{u'}$ for any subset S of ∇_V.

(vi) If $\mathit{block}(u_1^*, u_2^*)$ contains V, the unit pair (u_1^*, u_2^*) belongs to ∇_V (and so $V \in \widehat{\chi}(\nabla_V)$).

(vii) Denote $\alpha_{t+1} = \nabla_V$. Then, $\widehat{\chi}[\alpha_{j+1}] \cap \widehat{\chi}[\beta_j] = \varnothing$ for any $1 \leq j \leq t$.

Following (vi) and (vii), and noticing that $\varnothing = \alpha_1 \subset \alpha_2 \subset \ldots \subset \alpha_{t+1} = \nabla_V$, we get: There is a unique index in $1..t$, denoted by j^*, such that $V \notin \widehat{\chi}(\alpha_{j^*})$ but $V \in \widehat{\chi}(\alpha_{j^*+1})$. Moreover,

(viii) $(u_1^*, u_2^*) \notin \alpha_{j^*}$ and $(u_1^*, u_2^*) \notin \beta_{j^*}$ and thus $(u_1^*, u_2^*) \in \gamma_{j^*}$. In other words, by choosing $(e_p, e_q) = \mathsf{TP}_{j^*}$, condition (23) and (24) hold. In addition, we can compute j^* by a binary search and thus compute (e_p, e_q) in $O(\log n)$ time.

The proofs of (i)-(viii) are provided in Appendix H.

4.5 Summary, concluding remarks, and future direction

Theorem 4.10. *Given an n-sided convex polygon P, all the LMAPs in P can be computed in $O(n \log^2 n)$ time. Moreover, there are in total $O(n)$ LMAPs.*

1. Our algorithm is totally **practical**, although the proofs seems involved.

2. The overall reduction is **tricky**. Especially, it is not obvious that computing the LMAPs with two anchored broad corners reduces to computing the units intersecting the sectors.

3. Both the major and minor procedures presented in our paper run in $O(n \log n)$ time. However, they can actually be **optimized to run in purely linear time**. In other words, we can compute the LMAPs in $O(n)$ time after the preprocessing procedure. We do not present this optimization since it does not improve the total running time.

4. The bottleneck of our entire algorithm lies in two **highly-symmetric** preprocessing modules: computing the endpoints of $\mathit{sector}(V) \cap \partial P$ and computing the block that contains V for a given vertex V. Both of them run in $O(\log^2 n)$ time, and both contain a tricky preprocessing step, for computing s_V, t_V or p_V, q_V, which only costs $O(\log n)$ time. Besides, the "roads" and "routes" are analogues of the "cells" and "layers".

5. The properties of $Nest(P)$ are **just enough**; each of them has its particular value. According to these properties, the blocks and sectors are quite interesting geometric objects.

6. The bounding regions of blocks are the **major tools** in proving the properties of $Nest(P)$, and they are also important tools for computing e_{p_V}, e_{q_V}.

7. **Future direction.** It would be interesting to know whether we can find a space subdivision associated with a three dimensional convex polyhedron that is similar to $Nest(P)$. More generally, can we discover similar results in other geometry spaces?

   Besides, can we find more applications of $Nest(P)$?

Acknowledgements The author thank Andrew C. Yao, Haitao Wang, Danny Chen, Jian Li, Kevin Matulef for instructions, and appreciate the developers of Geometer's Sketchpad®.

Outline of the appendix The appendix is divided into nine sections.

Section A proves the properties of the distance function $dist_{l,l'}()$ and the Z-points; B proves the properties of the bounding regions of blocks; C proves the premier properties of the LMAPs.

Section D proves properties of every single block; E proves the properties of $Nest(P)$ stated in Theorem 2.10 (excluding the SECTOR-CONTINUITY); F proves properties of every single sector (including the SECTOR-CONTINUITY) and computes the endpoints of $sector(V) \cap \partial P$.

Sections G and H preprocess the information that are used in the major procedure. The last section presents the omitted details of our algorithm for computing the LMAPs.

Notations used in the appendix

Denote by ℓ_i the extended line of edge e_i.

Denote by $\mathsf{l}_{i,j}$ the intersection of ℓ_i and ℓ_j.

Denote by $e_i \not\prec e_j$ if edge e_i is not ahead of edge e_j.

Denote by $|AB|$ the distance between point A and point B.

Denote by $d_l(X)$ the distance from point X to line l.

Denote by $\mathsf{p}_i(X)$ the line at point X that is parallel to e_i.

Recall the backward and forward edge of units defined in Definition 2.5. Here, we define the backward and forward edge of points on ∂P. For any point $X \in \partial P$, its backward (resp. forward) edge is defined to be the backward (resp. forward) edge of the unit containing X. Formally, $back(X) := back(\mathbf{u}(X)), forw(X) := forw(\mathbf{u}(X))$.

Definition of Reflection and Scaling

Definition 4.11. See Figure 21. For any figure F on the plane, we define its *reflection around point O* as another figure which is congruent to F and is centrally-symmetric to F about point O; so a point belongs to the reflection if and only if the point symmetric to it about O belongs to F. We define F's *k-scaling about point O* to be figure F', which contains point X if and only if F contains point $(X - O)/k + O$.

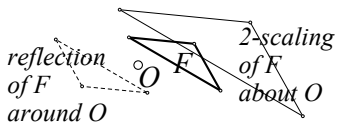

Figure 21: Reflection and scaling.

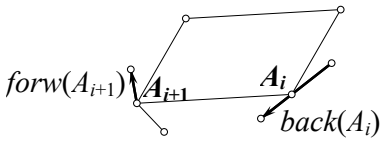

Figure 22: Illustration of Lemma 4.12.

Statement of two trivial facts

Lemma 4.12. *1. Assume $A_0A_1A_2A_3$ is an inscribed parallelogram, where A_0, A_1, A_2, A_3 lie in clockwise. For any two neighboring corners A_i, A_{i+1}, we have $back(A_i) \prec forw(A_{i+1})$.*

2. No parallelogram is inscribed on a small portion. (Recall "small portions" in Lemma 3.7.)

Proof. See Figure 22. Claim 1 is trivial as shown in the figure. We only prove Claim 2.

Assume that points A, B, C, D lie in clockwise order on a small portion and that they constitute a parallelogram. Denote $e_a = forw(A)$, $e_d = back(D)$. We know $e_a \preceq e_d$ from the assumption of A, B, C, D. On the other hand, we have $e_d \prec e_a$ by Claim 1. Contradictory! □

A The distance function $dist_{l,l'}()$ and the Z-points

Recall that $dist_{l,l'}(X)$ denotes the distance from point X to lines (l, l') and is defined as the product of the distance from X to l and the distance from X to l'. This appendix exhibits a few properties of this distance function $dist_{l,l'}$ and of the Z-points, which are frequently applied in proving the properties of the blocks and sectors.

Lemma A.1 (***Strict concavity*** of $dist_{l,l'}()$)**.** *Assume that l, l' are fixed unparallel lines. Assume that points B, B' lie on l, l', respectively, and that none of them lie on the intersection of l, l'. Then, on segment $\overline{BB'}$, function $dist_{l,l'}()$ is strictly concave and maximized at $\mathsf{M}(B, B')$.*

Proof. Suppose that X is a point on segment $\overline{BB'}$ and its distance to point B is x, as shown in Figure 23 (a). Obviously, $dist_{l,l'}(X) = x \sin\angle B \cdot (|BB'| - x) \sin\angle B' = k \cdot x(|BB'| - x)$, where k is a constant. Therefore, it is strictly concave on BB' and maximized at $x = \frac{1}{2}|BB'|$. □

The next lemma simply follows the strict concavity of $dist_{l,l'}$. (Proof omitted.)

Lemma A.2. *Let l, l', B, B' be the same as the above lemma. Further assume that $\overline{XX'}$ is a segment on $\overline{BB'}$ such that $X \neq X'$ and B, X, X', B' lie in order. The following hold.*

1. *If $|BX'| \leq \frac{1}{2}|BB'|$, then $dist_{l,l'}(Y)$ consistently decreases when point Y moves from X' to X in a straight line.*
2. *If X' has a larger distance to (l, l') than any other point on $\overline{XX'}$, then $|BX'| \leq \frac{1}{2}|BB'|$.*
3. *The order between $|BX|, |X'B'|$ is the same as the order between $dist_{l,l'}(X), dist_{l,l'}(X')$.*

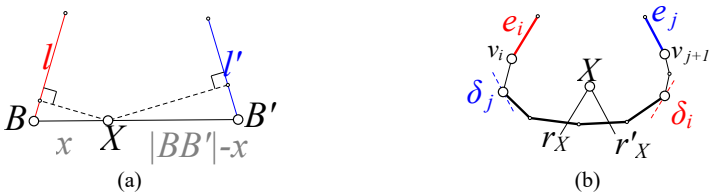

Figure 23: Illustration of the proofs of Lemma A.1 and Lemma A.3

The next lemma shows that the Z-points $\{Z_i^j\}$ are well-defined.

Lemma A.3. *For two edges e_i, e_j such that $e_i \prec e_j$, in the closed domain P, the function $dist_{\ell_i,\ell_j}()$ achieves maximum value at a unique point (which is defined as Z_i^j). Moreover, this point lies in the boundary-portions $[\delta_i \circlearrowright \delta_j]$ and $(v_{j+1} \circlearrowright v_i)$.*

Proof. Suppose to the contrary that $dist_{\ell_i,\ell_j}()$ achieves maximum value at X_1 and X_2. According to the concavity of $dist_{\ell_i,\ell_j}$, there must be a point X_3 on segment $\overline{X_1X_2}$ which has a larger distance to (ℓ_i, ℓ_j) than X_1 and X_2. Because P is convex, $\overline{X_1X_2}$ is contained in P, and so does X_3. Therefore, $dist_{\ell_i,\ell_j}()$ does not achieve maximum value at X_1 and X_2. This is contradictory! Therefore, it achieves maximum value at a unique point in P.

For any point X in P, let r_X denote the ray at X that has the opposite direction to e_i, and let r'_X denote the ray at X that has the same direction as e_j. See Figure 23 (b). We have:

(i): When $X \notin [\delta_i \circlearrowright \delta_j]$, a segment fraction of r_X or r'_X is contained in P.

(ii): Any point on r_X or r'_X beside X has a larger distance to (ℓ_i, ℓ_j) than point X.

Together, $dist_{\ell_i,\ell_j}()$ can only achieve its maximum value at $[\delta_i \circlearrowright \delta_j]$. In other words, point Z_i^j lies in $[\delta_i \circlearrowright \delta_j]$. Furthermore, because $[\delta_i \circlearrowright \delta_j]$ is contained in $[v_{j+1} \circlearrowright v_i]$ while Z_i^j certainly does not lie on v_{j+1} or v_i, point Z_i^j lies in $(v_{j+1} \circlearrowright v_i)$. □

Proof of bi-monotonicity of Z-points stated in Lemma 4.7.

Assume that $e_s \prec e_t$, otherwise $e_s = e_t$ and the lemma is trivial.

Assume that $(e_i, e_j) \in S$. According to Lemma A.3, point Z_i^j lies in $[\delta_i \circlearrowright \delta_j]$. Since $e_s \prec e_t$, we have $[\delta_i \circlearrowright \delta_j] \subseteq [v_{t+1} \circlearrowright v_s]$. Together, Z_i^j lies in $\rho = [v_{t+1} \circlearrowright v_s]$.

To prove the monotonicity of the Z-points, we only need to prove the following facts:

If (e_i, e_j) belongs to S and e_i, e_j are not adjacent, then

$$Z_i^{j-1} \leq_\rho Z_i^j \text{ and } Z_i^j \leq_\rho Z_{i+1}^j.$$

We prove the first inequality; the proof of the second is symmetric.

See Figure 24 (a). Suppose to the contrary that $Z_i^j <_\rho Z_i^{j-1}$. The line connecting these two Z-points intersects with $\ell_i, \ell_j, \ell_{j-1}$, and we denote the intersections by A, B, C, respectively. Applying the concavity of $dist_{\ell_i,\ell_j}()$ on segment $\overline{AB}$ (Lemma A.2.2), we get $|AZ_i^j| \leq \frac{1}{2}|AB|$. Applying the concavity of $dist_{\ell_i,\ell_{j-1}}()$ on segment $\overline{AC}$, we get $|AZ_i^{j-1}| \geq \frac{1}{2}|AC|$. Together, we get $|AC| < |AB|$. This is contradictory with the assumption of A, B, C. □

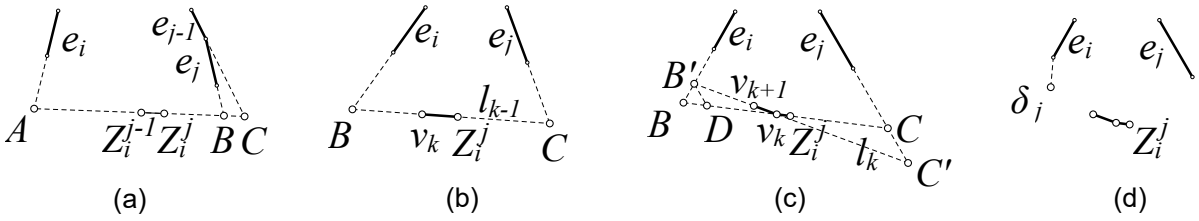

Figure 24: Illustration of the proofs of Lemma 4.7 and Lemma 3.2

Proof of the unimodality of $dist_{\ell_i,\ell_j}()$ stated in Lemma 3.2.

We prove ii), which says that $dist_{\ell_i,\ell_j}(X)$ strictly decreases when point X travels from Z_i^j to v_i in clockwise along ∂P; the proof of i) is symmetric.

Let us first consider the traveling process of X from Z_i^j to v_k, where v_k denote the clockwise first vertex in $[Z_i^j \circlearrowright \delta_j]$ that is not equal to Z_i^j. See Figure 24 (b). Let $B = \mathsf{l}_{k-1,i}, C = \mathsf{l}_{k-1,j}$. By the definition of Z_i^j, its distance to (ℓ_i, ℓ_j) is superior to all the other points on $\overline{v_k Z_i^j}$, which implies that $|Bv_k| < |BZ_i^j| \leq \frac{1}{2}|BC|$ due to Lemma A.2.2. According to Lemma A.2.1, this inequality implies that when X travels from Z_i^j to v_k, its distance to (ℓ_i, ℓ_j) strictly decreases.

Now, let us further consider the traveling process of X from v_k to v_{k+1}. See Figure 24 (c). Let $B' = \mathsf{l}_{k,i}$ and $C' = \mathsf{l}_{k,j}$. Assume that $\mathsf{p}_j(B')$ intersects ℓ_{k-1} at point D. Because $B'D$ is parallel to CC', we get $|B'v_k| : |C'v_k| = |Dv_k| : |Cv_k| < |Bv_k| : |Cv_k|$; because $|Bv_k| < \frac{1}{2}|BC|$, we get $|Bv_k| < |Cv_k|$; together, $|B'v_k| < |C'v_k|$. Therefore, $|B'v_{k+1}| < |B'v_k| < \frac{1}{2}|B'C'|$. Then, according to Lemma A.2.1, $dist_{\ell_i,\ell_j}(X)$ strictly decreases when X travels from v_k to v_{k+1}.

By induction, before X arrives at δ_j, its distance to (ℓ_i, ℓ_j) strictly decreases.

Finally, consider the traveling process from δ_j to v_i. See Figure 24 (d). In this last traveling process, $dist_{\ell_i,\ell_j}(X)$ strictly decreases because both $d_{\ell_i}(X)$ and $d_{\ell_j}(X)$ strictly decreases. □

The next lemma provide useful bounds of the Z-points.

Lemma A.4. *Assume that $e_i \prec e_j$.*

1. *When point Z_i^j lies on edge e_k, it must lie on the mid point of $\mathsf{l}_{i,k}$ and $\mathsf{l}_{j,k}$.*
2. *Point Z_i^j always lies in or on the boundary of the opposite quadrant of χ_i^j.*

Proof. 1. Suppose to the contrary that $Z_i^j \neq \mathsf{M}(\mathsf{I}_{i,k}, \mathsf{I}_{j,k})$, as shown in Figure 25 (a). There exists a point, denoted by N, which lies on e_k and between Z_i^j and $\mathsf{M}(\mathsf{I}_{i,k}, \mathsf{I}_{j,k})$. According to the strict concavity of $dist_{\ell_i,\ell_j}()$ on $\overline{\mathsf{I}_{i,k}\mathsf{I}_{j,k}}$, $dist_{\ell_i,\ell_j}(N) > dist_{\ell_i,\ell_j}(Z_i^j)$. This means that Z_i^j is not the point in P with the maximum distance to (ℓ_i, ℓ_j), which is contradictory!

2. See Figure 25 (b). Let $M = \mathsf{M}(v_i, v_{j+1})$. Let H_1 denote the closed half-plane bounded by $\mathsf{p}_i(M)$ and containing v_{j+1}, and let H_2 denote the closed half-plane bounded by $\mathsf{p}_j(M)$ and containing v_i; we shall prove that Z_i^j lies in $H_1 \cap H_2$.

Consider the backward edge of Z_i^j, denoted by e_b. Because Z_i^j has a larger distance to (ℓ_i, ℓ_j) than all of the other points in P, it has a larger distance to (ℓ_i, ℓ_j) than all of the points on e_b. Then, from the concavity of $dist_{\ell_i,\ell_j}()$ on segment $\overline{\mathsf{I}_{j,b}\mathsf{I}_{i,b}}$, we have $|\mathsf{I}_{i,b}Z_i^j| \geq \frac{1}{2}|\mathsf{I}_{j,b}\mathsf{I}_{i,b}|$, which implies that $d_{\ell_i}(Z_i^j) \geq \frac{1}{2}d_{\ell_i}(\mathsf{I}_{j,b})$. Moreover, $\frac{1}{2}d_{\ell_i}(\mathsf{I}_{j,b}) \geq \frac{1}{2}d_{\ell_i}(v_{j+1}) = d_{\ell_i}(M)$. So, $d_{\ell_i}(Z_i^j) \geq d_{\ell_i}(M)$, which implies that $Z_i^j \in H_1$. Symmetrically, $Z_i^j \in H_2$. Therefore, $Z_i^j \in H_1 \cap H_2$. □

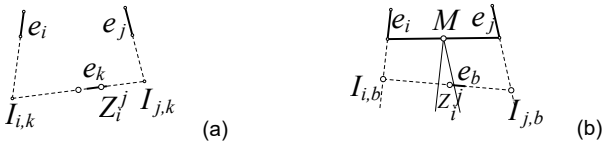

Figure 25: Illustration of the proof of Lemma A.4

At the end of this appendix, we consider the computational aspect of the Z-points.

Lemma A.5. *Consider two edges e_i, e_j such that $e_i \prec e_j$.*

1. *If the unit containing Z_i^j is known, we can compute the exact position of Z_i^j in $O(1)$ time.*
2. *Recall that Z_i^j lies in $(v_{j+1} \circlearrowleft v_i)$ (Lemma A.3). We can distinguish the following cases in $O(1)$ time for a given vertex v_k in $(v_{j+1} \circlearrowleft v_i)$.*

   (i) Z_i^j lies on v_k; (ii) Z_i^j lies in $(v_{j+1} \circlearrowleft v_k)$; (iii) Z_i^j lies in $(v_k \circlearrowleft v_i)$.

Proof. 1. If the unit containing Z_i^j is a vertex, the position Z_i^j can be computed directly; otherwise, Z_i^j can be computed in $O(1)$ time according to Lemma A.4.1.

2. We say that point X *dominates* point X', if X has a larger distance to (ℓ_i, ℓ_j) than X'.
The unimodality of $dist_{\ell_i,\ell_j}$ stated in Lemma 3.2 implies the following facts:

- "Z_i^j lies on v_k" if and only if "v_k dominates all points on e_{k-1} and e_k."
- "Z_i^j lies in $(v_{j+1} \circlearrowleft v_k)$" if and only if "there is a point on e_{k-1} which dominates v_k."
- "Z_i^j lies in $(v_k \circlearrowleft v_i)$" if and only if "there is a point on e_k which dominates v_k."

Thus, it reduces to solve the following queries:
Does v_k dominate each point on e_{k-1}?
Does v_k dominate each point on e_k?
We can answer these queries in $O(1)$ time by applying the concavity of $dist_{\ell_i,\ell_j}$. □

Lemma A.6. *Given m pairs of edges $(a_1, b_1), \ldots, (a_m, b_m)$ such that $a_i \prec b_i$ for $1 \leq i \leq m$, and that $a_1, \ldots, a_m$ lie in clockwise order around ∂P and $b_1, \ldots, b_m$ lie in clockwise order around ∂P, we can compute the positions of $Z_{a_1}^{b_1}, \ldots, Z_{a_m}^{b_m}$ all together in $O(m+n)$ time.*

Proof. By Lemma A.5.1, to compute $Z_{a_1}^{b_1}, \ldots, Z_{a_m}^{b_m}$, we only need to determine the respective units that they lie on. Moreover, due to the bi-monotonicity of the Z-points, $Z_{a_1}^{b_1}, \ldots, Z_{a_m}^{b_m}$ lie in clockwise order, so the units they lie on are monotonous in clockwise order. So, we can walk around the boundary of P to compute these Z-points in order, and it costs $O(m+n)$ time. □

B Properties of the bounding regions

Here, we prove the properties of the bounding regions, including the peculiar property of χ stated in Lemma 3.7 and the monotonicity of $\widehat{\chi}$ stated in Lemma 3.8.

Definition B.1. See Figure 26. For edge pair (e_i, e_j) such that $e_i \preceq e_j$, we denote by hp_i^j the **open** half-plane delimited by the extended line of $v_{j+1}v_i$ and lies on the right side of $\overrightarrow{v_{j+1}v_i}$.

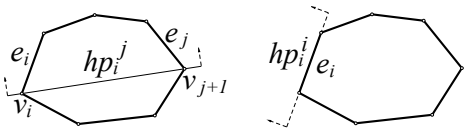

Figure 26: Illustration of the definition of $\{\mathsf{hp}_i^j \mid e_i \preceq e_j\}$.

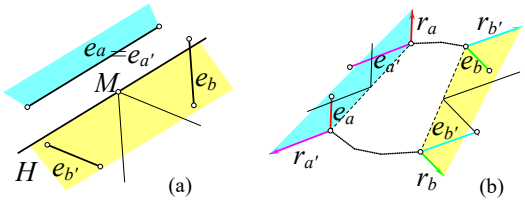

Figure 27: Trivial cases of the peculiar property of χ

Note that χ_i^j is always a subregion of hp_i^j.

Restatement of Lemma 3.7: *For four edges $e_a, e_{a'}, e_b, e_{b'}$ such that $e_a \preceq e_{a'}$ and $e_b \preceq e_{b'}$ and that $e_a, e_{a'}, e_b, e_{b'}$ are not contained in any small portion, $\chi_a^{a'} \cap \chi_b^{b'}$ lies in the interior of P.*

Proof. We first consider several trivial cases, in which $\chi_a^{a'}$ has no intersection with $\chi_b^{b'}$.

Recall that $\mathsf{p}_i(X)$ denotes the line at point X that is parallel to e_i.

- Case 1: $a = a'$. See Figure 27 (a). Let M denote the apex of $\chi_b^{b'}$, which equals $\mathsf{M}(v_b, v_{b'+1})$. Let H denote the open half-plane delimited by $\mathsf{p}_a(M)$ and not containing e_a.

  Since $e_a, e_{a'}, e_b, e_{b'}$ are not contained in any small portion, we know $e_a \prec e_b$ while $e_{b'} \prec e_a$. Since $e_a \prec e_b$, the boundary of $\chi_b^{b'}$ that is parallel to e_b lies in H. Since $e_{b'} \prec e_a$, the boundary of $\chi_b^{b'}$ that is parallel to $e_{b'}$ lies in H. Together, quadrant $\chi_b^{b'}$ lies in H.

  Moreover, $\chi_a^{a'}$ clearly has no intersection with H. Therefore, $\chi_a^{a'} \cap \chi_b^{b'} = \varnothing$.

- Case 2: $b = b'$. This case is symmetric to Case 1.

- Case 3: $e_a, e_{a'}, e_b, e_{b'}$ are distinct edges and lie in clockwise order on ∂P. See Figure 27 (b). We make four rays. Ray r_a locates at $v_{a'+1}$ and has the same direction as e_a. Ray $r_{a'}$ locates at v_a and has the opposite direction to $e_{a'}$. Ray r_b locates at $v_{b'+1}$ and has the same direction as e_b. Ray $r_{b'}$ locates at v_b and has the opposite direction to $e_{b'}$. Let Π_1 denote the region bounded by $r_{a'}, \overline{v_a v_{a'+1}}, r_a$ and containing $\chi_a^{a'}$. Let Π_2 denote the region bounded by $r_{b'}, \overline{v_b v_{b'+1}}, r_b$ and containing $\chi_b^{b'}$. Assume that Π_1, Π_2 do not contain the boundaries. Since $e_a, e_{a'}, e_b, e_{b'}$ are not containing in any small portion, we have $e_{b'} \prec e_a$ while $e_{a'} \prec e_b$. This further implies that Π_1, Π_2 are disjoint. Therefore, $\chi_a^{a'}, \chi_b^{b'}$ are disjoint, since they are respectively subregions of Π_1, Π_2.

In the preceding cases, $\chi_a^{a'} \cap \chi_b^{b'}$ is empty and hence it lies in the interior of P.

When none of the preceding cases occur, two cases remain:

- Case 4: $e_a \prec e_b \preceq e_{a'} \prec e_{b'} \prec e_a$.

- Case 5: $e_b \prec e_a \preceq e_{b'} \prec e_{a'} \prec e_b$.

Assume that Case 4 occurs; the other case is symmetric. See Figure 28.

Let $C = v_{b'+1}, D = v_a, E = v_b, F = v_{a'+1}$, and G denote the intersection of CE and DF. It is obvious that $\triangle EFG \subseteq P$. Therefore, to prove that $\chi_a^{a'} \cap \chi_b^{b'}$ lies in the interior of P reduces to prove that it lies in the interior of $\triangle EFG$, and this further reduces to prove the following.

i. $\chi_a^{a'} \cap \chi_b^{b'}$ lies in half-plane $\mathsf{hp}_a^{a'}$.

ii. $\chi_a^{a'} \cap \chi_b^{b'}$ lies in half-plane $\mathsf{hp}_b^{b'}$.

iii. $\chi_a^{a'} \cap \chi_b^{b'}$ lies in half-plane h, where h denotes the open half-plane bounded by the extended line of $\overline{EF}$ and containing G. (In other words, h is the complementary half-plane of $\mathsf{hp}_b^{a'}$.)

Formula $\chi_a^{a'} \subseteq \mathsf{hp}_a^{a'}$ implies (i); $\chi_b^{b'} \subseteq \mathsf{hp}_b^{b'}$ implies (ii). We prove (iii) in the following.

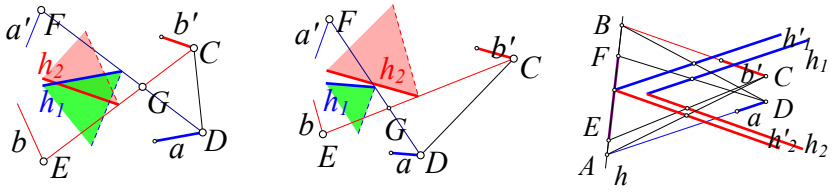

Figure 28: Nontrivial cases of the peculiar property of χ

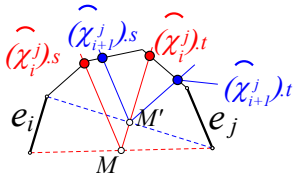

Figure 29: Proof of the monotonicity of $\widehat{\chi}$

See the right picture. Denote by h_1 the open half-plane bounded by $\mathsf{p}_a(\mathsf{M}(D,F))$ and containing e_a, and h_2 the open half-plane bounded by $\mathsf{p}_{b'}(\mathsf{M}(E,C))$ and containing $e_{b'}$. By the definitions of $\chi_a^{a'}$ and $\chi_b^{b'}$, we have $\chi_a^{a'} \subseteq h_1$ and $\chi_b^{b'} \subseteq h_2$. Assume that the extended line of $\overline{EF}$ intersects $\ell_a, \ell_{b'}$ at A, B respectively. Denote by h_1' the open half-plane bounded by $\mathsf{p}_a(\mathsf{M}(D,B))$ and containing e_a, and h_2' the open half-plane bounded by $\mathsf{p}_{b'}(\mathsf{M}(A,C))$ and containing $e_{b'}$. Because P is convex, points E, F both lie on $\overline{AB}$, which implies that $h_1 \subseteq h_1'$ and $h_2 \subseteq h_2'$. Moreover, from the definition of h_1', h_2', their boundaries pass through the mid point of A, B. So, the apex of quadrant $h_1' \cap h_2'$ locates on $\overline{AB}$. Further, since $e_{b'} \prec e_a$, h_1' is parallel to e_a and h_2' is parallel to e_b, we have $h_1' \cap h_2' \subseteq h$. Altogether, $\chi_a^{a'} \cap \chi_b^{b'} \subseteq h_1 \cap h_2 \subseteq h_1' \cap h_2' \subseteq h$. □

Proof of the monotonicity of $\widehat{\chi}$. See the statement of this monotonicity in Lemma 3.8.

When $j = i+1$, we have: (i) $\widehat{\chi}_i^{j-1}$ contains a single point, which is the midpoint of e_i; (ii) $\widehat{\chi}_{i+1}^{j}$ contains a single point, which is the midpoint of e_j; (iii) $\widehat{\chi}_i^{j}$ starts at the midpoint of e_i and terminates at the midpoint of e_j. See Figure 11 (d). Together, we get (15) and (16).

Now, assume that $j \neq i+1$. See Figure 29. Let $M = \mathsf{M}(v_i, v_{j+1}), M' = \mathsf{M}(v_{i+1}, v_{j+1})$, and recall that ρ denote $[v_i \circlearrowright v_{j+1}]$.

First, consider the two starting points $(\widehat{\chi}_i^{j}).s$ and $(\widehat{\chi}_{i+1}^{j}).s$. Clearly, their distance to line ℓ_j are respectively equal to the distance from M, M' to that line. Moreover, since $e_i \prec e_j$, the distance from M to ℓ_j is larger than the distance from M' to ℓ_j. Therefore, $(\widehat{\chi}_i^{j}).s$ is further than $(\widehat{\chi}_{i+1}^{j}).s$ from line ℓ_j. This further implies that $(\widehat{\chi}_i^{j}).s \preceq_\rho (\widehat{\chi}_{i+1}^{j}).s$.

Then, consider the two terminal points $(\widehat{\chi}_i^{j}).t$ and $(\widehat{\chi}_{i+1}^{j}).t$. Observe that

$$\overline{M', (\widehat{\chi}_i^{j}).t} \text{ is parallel to } e_i \text{ while } \overline{M', (\widehat{\chi}_{i+1}^{j}).t} \text{ is parallel to } e_{i+1}, \text{ while } e_i \prec e_{i+1},$$

we get $(\widehat{\chi}_i^{j}).t \preceq_\rho (\widehat{\chi}_{i+1}^{j}).t$.

Symmetrically, $(\widehat{\chi}_i^{j-1}).s \preceq_\rho (\widehat{\chi}_i^{j}).s$ and $(\widehat{\chi}_i^{j-1}).t \preceq_\rho (\widehat{\chi}_i^{j}).t$. Altogether, we get (15) and (16).

Next, we prove the general case. For $1 \leq k \leq m$, denote $a_k = forw(u_k)$ and $a'_k = back(u'_k)$. From the assumption of $\{u_k\}$ and $\{u'\}$, lists $\{a_k\}$ and $\{a'_k\}$ have the following properties: (i) $a_k \preceq a'_k$ for $1 \leq k \leq m$; (ii) $a_1, \ldots, a_m$ lie in clockwise order; (iii) $a'_1, \ldots, a'_m$ lie in clockwise order. According to these properties and by applying (15), (16), the starting points of $\widehat{\chi}_{a_1}^{a'_1}, \ldots, \widehat{\chi}_{a_m}^{a'_m}$ lie in clockwise order around ∂P, whilst the terminal points of $\widehat{\chi}_{a_1}^{a'_1}, \ldots, \widehat{\chi}_{a_m}^{a'_m}$ lie in clockwise order around ∂P. We complete the proof by recalling that $\widehat{\chi}_{u_k}^{u'_k} = \widehat{\chi}_{a_k}^{a'_k}$. □

C *Corner-stones:* the premier properties of the LMAPs

In this appendix, we prove Identity 9 rigorously, and then apply it to prove Lemma 4.1 and the generalized premier properties of the LMAPs (stated in Lemma 4.3).

We state one lemma before we prove the main results of this appendix.

Lemma C.1. *Suppose two lines l, l' intersect at O, and points X, X' lie in the same quadrant divided by l, l'. Let Y, Y' be the pair of points such that $Y \in l, Y' \in l'$ and that the mid point of Y, Y' coincides with the mid point of X, X' (which is unique due to Lemma 3.1.1). Then,*

1. *"$dist_{l,l'}(X) < dist_{l,l'}(X')$" if and only if "$X$ lies in the interior of $\triangle OYY'$".*
2. *"$dist_{l,l'}(X) = dist_{l,l'}(X')$" if and only if "$Y, X, Y', X'$ lie in the same line".*

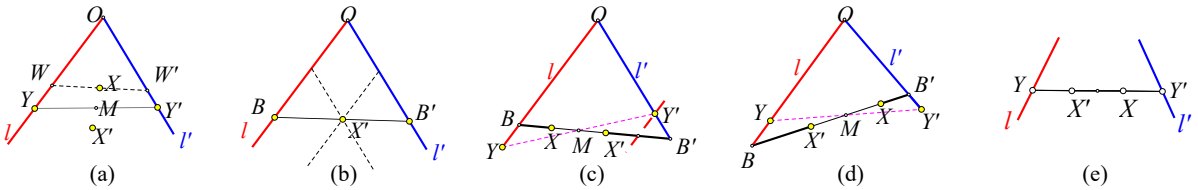

Figure 30: Illustration of the proof of Lemma C.1.

Proof. For convenience, denote $M = \mathsf{M}(X, X')$.

First, we argue that X lies in the interior of $\triangle OYY'$ when $dist_{l,l'}(X) < dist_{l,l'}(X')$.

Since $dist_{l,l'}(X) < dist_{l,l'}(X')$, there are three cases as follows.

Case 1: $d_l(X) \le d_l(X')$ and $d_{l'}(X) \le d_{l'}(X')$, and at least one inequality is strictly less.

See Figure 30 (a). Let W denote the intersection between l and the reflection of l' around X. Let W' denote the intersection between l' and the reflection of l around X. By this definition, segment WW' contains X (as its midpoint). So, it reduces to show that WW' lies in interior of $\triangle OYY'$. Notice that

$$d_{l'}(W) = 2d_{l'}(X) \le d_{l'}(X) + d_{l'}(X') = 2d_{l'}(M) = d_{l'}(Y),$$

$$d_l(W') = 2d_l(X) \le d_l(X) + d_l(X') = 2d_l(M) = d_l(Y').$$

We get that $|OW| \le |OY|$ and $|OW'| \le |OY'|$, and at least one inequality is strictly less. This further implies that segment WW' is contained in the interior of $\triangle OYY'$.

Case 2: $d_l(X) < d_l(X')$ and $d_{l'}(X) > d_{l'}(X')$.

Assume that the extended line of X, X' intersects l, l' at B, B' respectively. We point out that *segment BB' lies in the quadrant bounded by l, l' and containing X, X'.*

This statement follows from the assumption $d_l(X) < d_l(X')$ and $d_{l'}(X) > d_{l'}(X')$, and is illustrated in Figure 30 (b). We omit its trivial proof.

Now, see Figure 30 (c). Since X, X' both lie on segment BB' and since $dist_{l,l'}(X) < dist_{l,l'}(X')$, we have $|XB| < |X'B'|$ according to Lemma A.2.3.

Since $|XB| < |X'B'|$ and $|MX| = |MX'|$, we get $|MB| < |MB'|$. Therefore, $d_l(B') > 2d_l(M) = d_l(Y')$, which implies that Y' lies between O, B'. Similarly, B lies between O, Y. Therefore, segment BM is contained in the interior of $\triangle OYY'$. Moreover, notice that segment BM contains point X in this case. Therefore, X lies in the interior of $\triangle OYY'$.

Case 3: $d_l(X) > d_{l'}(X')$ and $d_{l'}(X) < d_{l'}(X')$.
It is symmetric to Case 2 and we omit its proof. See Figure 30 (d) for an illustration.

Similar to the preceding argument, we can prove: When $dist_{l,l'}(X) > dist_{l,l'}(X')$, point X' lies in the interior of $\triangle OYY'$ (and thus point X does not lie in the interior of $\triangle OYY'$); and when $dist_{l,l'}(X) = dist_{l,l'}(X')$, points Y, X, Y', X' lie in the same line. (See Figure 30 (e).)
Combining all the three arguments, we obtain the claims of this lemma. □

Proof of Identity 9. Assume that $\square(X, X', l, l') = XYX'Y'$, where Y, Y' lie on l, l', respectively.
First, consider the case where $dist_{l,l'}(X) = dist_{l,l'}(X')$. According to Lemma C.1, points Y, X, Y', X' lie in the same line, which implies $Area(XY'X'Y) = 0$ and hence Identity 9 holds.
Next, consider the case where $dist_{l,l'}(X) < dist_{l,l'}(X')$. (The other case where $dist_{l,l'}(X) > dist_{l,l'}(X')$ is symmetric.) See Figure 7. We state two facts.

(i) Point X lies in the quadrilateral $OYX'Y'$.

(ii) $\triangle GXY$ is congruent to $\triangle H'Y'X'$ while $\triangle HXY'$ is congruent to $\triangle G'YX'$.

Proof: Since $dist_{l,l'}(X) < dist_{l,l'}(X')$, point X lies in $\triangle OYY'$ by Lemma C.1, which further implies Fact (i). Fact (ii) simply follows from the fact that $XYX'Y'$ is a parallelogram.
Fact (i) and Fact (ii) together guarantee the correctness of Equation 10. As a result,

$$Area(XY'X'Y) = Area(OH'X'G') - Area(OHXG). \tag{29}$$

Notice that $d_l(X) = |XG| \cdot \sin\theta$ and $d_{l'}(X) = |XH| \cdot \sin\theta$. Therefore,

$$Area(OHXG) = |XG| \cdot |XH| \cdot \sin\theta = d_l(X)d_{l'}(X)/\sin\theta = dist_{l,l'}(X)/\sin\theta.$$

Similarly,

$$Area(OH'X'G') = dist_{l,l'}(X')/\sin\theta.$$

Finally, by substituting the last two equations into (29), we obtain Identity 9. □

Recall that Lemma 4.1 states the following. *A narrow corner of an LMAP must be anchored if neither of two its neighboring corners is anchored.*

Proof of Lemma 4.1. Assume that $Q = A_0A_1A_2A_3$ is an LMAP, where A_0, A_1, A_2, A_3 lie in clockwise order. Moreover, assume that A_3, A_1 lie on e_i, e_j, respectively, where $e_i \prec e_j$. We shall prove that the narrow corner A_0 is anchored.
Suppose to the contrary that A_0 is not anchored but lies on an edge, e.g. e_k. See Figure 31. Denote by B the one among $\mathsf{l}_{i,k}, \mathsf{l}_{j,k}$ which is closer to A_0; let B be any of them for a tie.
Suppose point X is restricted on $\overline{A_0B}$ and is distinct from A_0. Denote $Q_X = \square(X, A_2, \ell_i, \ell_j)$, which is the unique parallelogram that has a pair of opposite corners lying on X, A_2 and has the other pair of opposite corners lying on ℓ_i, ℓ_j. Let $d()$ denotes $dist_{\ell_i,\ell_j}()$ for short. Then,

$d(A_2) > d(A_0)$,	according to Lemma C.1;
$d(A_0) > d(X)$,	according to the concavity of $d()$ on $\overline{\mathsf{l}_{i,k}, \mathsf{l}_{j,k}}$;
$Area(Q_X) = c \cdot \lvert d(A_2) - d(X)\rvert$,	
$Area(Q_{A_0}) = c \cdot \lvert d(A_2) - d(A_0)\rvert$,	due to (9), and note that c is a positive constant.

Therefore, $Area(Q_X) > Area(Q_{A_0})$.
Moreover, because A_1, A_3 are unanchored, Q_X is inscribed on P when X is sufficiently close to A_0. Therefore, there is an inscribed parallelogram Q_X nearby Q_{A_0} with a larger area; so $Q = Q_{A_0}$ is not local maximal and hence is not an LMAP. Contradictory! Therefore, the narrow corner A_0 must be anchored. □

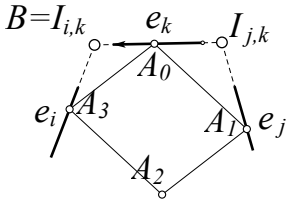

Figure 31: Lemma 4.1

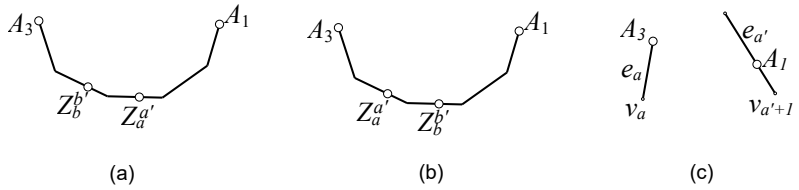

Figure 32: Proofs of the premier properties (I)

Next, we prove the generalized premier properties of the LMAPs stated in Lemma 4.3.

Proof. Recall that $Q = A_0A_1A_2A_3$ is an LMAP, where the corners A_0, A_1, A_2, A_3 lie in clockwise order, and where A_2 is **broad or even**. Let $u = \mathbf{u}(A_3), u' = \mathbf{u}(A_1)$ and let a, a', b, b' be defined according to (19). We shall prove that $A_2 \in [Z_a^{a'} \circlearrowleft Z_b^{b'}]$.

First, we state three arguments and argue that they together imply the consequence.

(i) At least one point in $Z_a^{a'}, Z_b^{b'}$ lies in $(A_1 \circlearrowleft A_3)$.

(ii) When point $Z_a^{a'}$ lies in $(A_1 \circlearrowleft A_3)$, corner A_2 is not contained in $(A_1 \circlearrowleft Z_a^{a'})$.

(iii) When point $Z_b^{b'}$ lies in $(A_1 \circlearrowleft A_3)$, corner A_2 is not contained in $(Z_b^{b'} \circlearrowleft A_3)$.

Noticing that A_2 always lies in $(A_1 \circlearrowleft A_3)$, combining these arguments, we immediately get $A_2 \in [Z_a^{a'} \circlearrowleft Z_b^{b'}]$. To see this clearly, we discuss three cases depending on whether $Z_a^{a'}$ and $Z_b^{b'}$ lie in $\rho = (A_1 \circlearrowleft A_3)$. The case where only one of them lie in ρ is trivial; let us assume that both of them lie in ρ. There could be two subcases. Either $Z_a^{a'} \leq_\rho Z_b^{b'}$ or $Z_b^{b'} <_\rho Z_b^{b'}$, as shown in Figure 32 (a) and (b). In the first subcase, by (ii) and (iii), A_2 can only lie in $[Z_a^{a'} \circlearrowleft Z_b^{b'}]$. In the second subcase, by (ii) and (iii), A_2 cannot lie in ρ, which means that this subcase would not happen. (In fact, it would not happen according to the bi-monotonicity of Z-points.)

Argument (i) follows from the following three facts.

(1.) $back(A_3) \prec back(A_1)$ or $forw(A_3) \prec forw(A_1)$.

(2.) If $back(A_3) \prec back(A_1)$, point $Z_a^{a'}$ lies in $(A_1 \circlearrowleft A_3)$.

(3.) If $forw(A_3) \prec forw(A_1)$, point $Z_b^{b'}$ lies in $(A_1 \circlearrowleft A_3)$.

Proof of (1.): Since A_1, A_3 are opposite corners of a parallelogram inscribed on P, we get

$$back(A_1) \neq back(A_3) \text{ and } forw(A_1) \neq forw(A_3).$$

Moreover, since A_2 is broad or even, $\mathbf{u}(A_1)$ is not ahead of $\mathbf{u}(A_3)$. Therefore,

$$back(\mathbf{u}(A_1)) \not\prec back(\mathbf{u}(A_3)) \text{ or } forw(\mathbf{u}(A_1)) \not\prec forw(\mathbf{u}(A_3)),$$

$$i.e., back(A_1) \not\prec back(A_3) \text{ or } forw(A_1) \not\prec forw(A_3).$$

Together, we get (1.).
Proof of (2.): Assume that $back(A_3) \prec back(A_1)$. Then, $e_{a'} = back(A_1)$ due to (19), which implies that $(v_{a'+1} \circlearrowleft v_a) \subseteq (A_1 \circlearrowleft A_3)$, as illustrated in Figure 32 (c). Moreover, we have $Z_a^{a'} \in (v_{a'+1} \circlearrowleft v_a)$ by Lemma A.3. Together, $Z_a^{a'} \in (A_1 \circlearrowleft A_3)$. Proof of (3.) is symmetric.

In the following, we prove (ii). The proof of (iii) is symmetric.

We prove (ii) by contradiction. Suppose to the contrary that $Z_a^{a'}$ lies in $(A_1 \circlearrowleft A_3)$ and A_2 lies in $(A_1 \circlearrowleft Z_a^{a'})$. We shall show that there exists a parallelogram inscribed on P, nearby Q, and with an area larger than Q. We need to discuss two cases as below; note that $back(u) \neq back(u')$ since $back(u) = back(A_3) \neq back(A_1) = back(u')$.

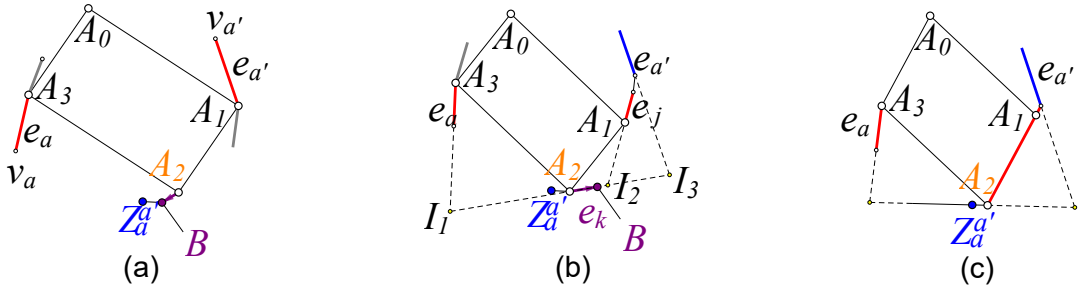

Figure 33: Proofs of the premier properties (II)

Case 1: $back(u) \prec back(u')$. See Figure 33 (a). In this case $e_{a'} = back(u') = back(A_1)$ due to (19). Let B be any point that lies in $(A_2 \circlearrowright Z_a^{a'})$ and $forw(A_2)$ simultaneously, let X denote a point restricted in segment $\overline{A_2B}$ and is distinct from A_2, and denote $Q_X = \square(X, A_0, \ell_a, \ell_{a'})$.

First, $dist_{\ell_a,\ell_{a'}}(A_2) > dist_{\ell_a,\ell_{a'}}(A_0)$ by Lemma C.1. Second, $dist_{\ell_a,\ell_{a'}}(X) > dist_{\ell_a,\ell_{a'}}(A_2)$ due to the strict unimodality of $dist_{\ell_a,\ell_{a'}}()$. Then, applying (9), we get $Area(Q_X) > Area(Q_{A_2})$.

So, we only need to show that *when X is sufficiently close to A_2, parallelogram Q_X is inscribed on P*. This reduces to prove that when X moves from A_2 to B along edge $forw(A_2)$,

(I) the corner of Q_X that is inscribed on ℓ_a moves toward v_a; and

(II) the corner of Q_X that is inscribed on $\ell_{a'}$ moves toward $v_{a'}$.

We prove (I) in the following; (II) is symmetric. Because A_1, A_2 are neighboring corners of Q, we have $back(A_1) \prec forw(A_2)$ by Lemma 4.12.1. It implies that X gets away from $\ell_{a'}$ during its movement. So, the center of Q_X gets away from $\ell_{a'}$, since it moves in the same direction as X. Therefore, the reflection of $\ell_{a'}$ around the center of Q_X gets away from $\ell_{a'}$; i.e. the corner of Q_X which is inscribed on ℓ_a gets away from $\ell_{a'}$. This further implies (I) since $e_a \prec e_{a'}$.

Case 2: $back(u') \prec back(u)$. In this case, we first claim (III) $back(A_2) \neq back(A_1)$; the proof is given later. See Figure 33 (b). Denote $e_j = back(A_1), e_k = back(A_2)$. Let B be any point in e_k but not in $[A_2 \circlearrowright Z_a^{a'}]$, let X denote a point restricted on segment $\overline{A_2B}$ and is distinct from A_2, and denote $Q_X = \square(X, A_0, \ell_a, \ell_j)$. Assume that ℓ_k intersects $\ell_a, \ell_j, \ell_{a'}$ at $\mathsf{I}_1, \mathsf{I}_2, \mathsf{I}_3$, respectively.

Applying the strict unimodality of $d_{\ell_a,\ell_{a'}}$, we know $d_{\ell_a,\ell_{a'}}(X)$ strictly decreases when X moves from A_2 to B. This implies that $|A_2\mathsf{I}_3| \leq |A_2\mathsf{I}_1|$ according to Lemma A.2.2, which further implies that $|A_2\mathsf{I}_2| \leq |A_2\mathsf{I}_1|$. Based on the last inequality and by applying Lemma A.2.1, we get: when X moves from A_2 to B, distance $dist_{\ell_a,\ell_j}(X)$ strictly decreases. Therefore, $dist_{\ell_a,\ell_j}(X) < dist_{\ell_a,\ell_j}(A_2)$. Moreover, based on Identity 9 and Lemma C.1, $Area(Q_X)$ is in proportion to $dist_{\ell_a,\ell_j}(A_0) - dist_{\ell_a,\ell_j}(X)$. Therefore, we get $Area(Q_X) > Area(Q_{A_2})$.

In addition, similar to Case 1, we know that parallelogram Q_X is inscribed on P when X is sufficiently close to A_2. Therefore, $Q = Q_{A_2}$ is not an LMAP.

Finally, we prove (III) by contradiction.

Suppose to the contrary that $back(A_2) = back(A_1)$, as shown in Figure 33 (c).

Since $back(A_2) = back(A_1)$, we get

$$forw(A_1) = back(A_2). \tag{30}$$

Since A_2, A_3 are neighboring corners of parallelogram Q, by applying Lemma 4.12.1, we have

$$back(A_2) \prec forw(A_3). \tag{31}$$

Combining (30) and (31),

$$forw(A_1) \prec forw(A_3), \text{ i.e. } forw(u') \prec forw(u) \tag{32}$$

Further, since $back(u') \prec back(u)$, corner A_2 is narrow, which contradicts the assumption. □

D Properties of a single block

In this appendix, we prove the equation of $block(u, u')$ stated in (12) and prove the properties of blocks stated in Lemma 3.6. The proof of (13) is similar to that of (12) and is omitted.

Proof of (12).

$$\begin{aligned} block(u,u') &= f(\mathsf{T}(u,u')) = \bigcup\nolimits_{X_3\in u, X_1\in u', X_2\in\zeta(u,u')} f(X_1,X_2,X_3) \\ &= \bigcup\nolimits_{X_3\in u, X_1\in u'} \bigcup\nolimits_{X_2\in\zeta(u,u')} \text{the reflection of } X_2 \text{ around } \mathsf{M}(X_3,X_1) \\ &= \bigcup\nolimits_{X_3\in u, X_1\in u'} \text{the reflection of } \zeta(u,u') \text{ around } \mathsf{M}(X_3,X_1) \\ &= \bigcup\nolimits_{X\in u\oplus u'} \text{the reflection of } \zeta(u,u') \text{ around point } X \end{aligned}$$

□

Proof of Lemma 3.6.1. To prove this statement, we need to prove the following formulas:
$block(e_i, e_j) \subset \chi_i^j$, $block(e_i, v_{j+1}) \subset \chi_i^j$, $block(v_i, e_j) \subset \chi_i^j$, $block(v_i, v_{j+1}) \subset \chi_i^j$.
Above all, we note that the regions $\{\chi_i^j \mid e_i \prec e_j\}$ do **not** contain their boundaries.

- $block(e_i, e_j) \subset \chi_i^j$: Point Z_i^j lies in or on the boundary of the opposite quadrant of χ_i^j (by Lemma A.4.2), whereas $e_i \oplus e_j$ is clearly contained in χ_i^j. So, the 2-scaling of $e_i \oplus e_j$ about point Z_i^j, which is equal to $block(e_i, e_j)$ due to (13), is contained in χ_i^j.

- $block(e_i, v_{j+1}) \subset \chi_i^j$: Denote by H_1 the closed half-plane bounded by $\mathsf{p}_j(\mathsf{M}(v_i, v_{j+1}))$ and not containing e_j, and H_2 the closed half-plane bounded by $\mathsf{p}_i(\mathsf{M}(v_i, v_{j+2}))$ and not containing e_i. See Figure 34 (a). According to Lemma A.4.2, $Z_i^j \in H_1$, $Z_i^{j+1} \in H_2$. So, $\zeta(e_i, v_{j+1}) = [Z_i^j \circlearrowleft Z_i^{j+1}]$ is contained in quadrant $H_1 \cap H_2$. Therefore, for each point $X \in e_i \oplus v_{j+1}$, the reflection of $\zeta(e_i, v_{j+1})$ around X is contained in χ_i^j. Applying (12), $block(e_i, v_{j+1}) = \left(\bigcup_{X\in e_i\oplus v_{j+1}} \text{the reflection of } \zeta(e_i, v_{j+1}) \text{ around } X\right)$ is contained in χ_i^j.

- $block(v_i, e_j) \subset \chi_i^j$. This one is symmetric to the preceding one.

- $block(v_i, v_{j+1}) \subset \chi_i^j$: To prove this formula, we first state the following.

  (1) Z_{i-1}^j lies in the opposite quadrant of χ_i^j.
  (2) Z_i^{j+1} lies in the opposite quadrant of χ_i^j.

  We show the proof of (1); the proof of (2) is symmetric. Consider two cases.

  Case 1: $i \neq j$. See Figure 34 (b). Because v_i is ahead of v_{j+1}, we have $e_{i-1} \prec e_j$. This implies that $\mathsf{M}(v_{i-1}, v_{j+1})$ lies in the opposite quadrant of χ_i^j, which further implies that the opposite quadrant of χ_{i-1}^j and its boundary are contained in the opposite quadrant of χ_i^j. Moreover, Z_{i-1}^j lies in or on the boundary of the opposite quadrant of χ_{i-1}^j by Lemma A.4.2. Together, we get (1).

  Case 2: $i = j$. Point Z_{i-1}^i lie in $(v_{i+1} \circlearrowleft v_{i-1})$ by Lemma A.3, whereas $(v_{i+1} \circlearrowleft v_{i-1})$ is contained in the opposite quadrant of χ_i^i due to the definition of χ_i^i. So we get (1).

  Since $\zeta(v_i, v_{j+1}) = [Z_{i-1}^j \circlearrowleft Z_i^{j+1}]$, (1) and (2) together imply that $\zeta(v_i, v_{j+1})$ lies in the opposite quadrant of χ_i^j. Therefore, the reflection of $\zeta(v_i, v_{j+1})$ around $\mathsf{M}(v_i, v_{j+1})$, which equals $block(v_i, v_{j+1})$ due to (12), is contained in χ_i^j.

□

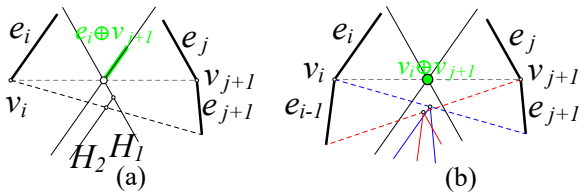

Figure 34: Proof of Lemma 3.6.1

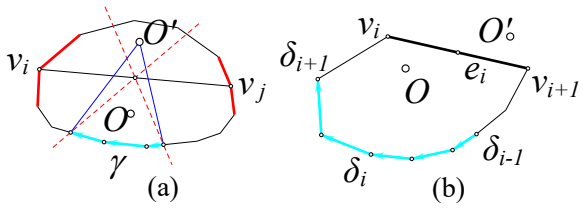

Figure 35: Proof of Lemma 3.6.2

Proof of the MONOTONICITY OF THE BORDERS. Let O be an arbitrary point in the closed domain P and also in the opposite quadrant of $\chi_u^{u'}$. Let X be a point. We shall prove that

(1) *when X travels along any border of $block(u, u')$, it is traveling in clockwise around O.*

Case 1: both u, u' are edges. Since $block(u, u') \subset \chi_u^{u'}$, all points in the opposite quadrant of $\chi_u^{u'}$, including O, are on the right of each border of $block(u, u')$. This implies (1).

Case 2: both u, u' are vertices. In this case $block(u, u')$ has a unique border, which equals the reflection of $\zeta(u, u')$ around $\mathsf{M}(u, u')$. Thus, it reduces to show that

(2) *when X travels along $\zeta(u, u')$, it is traveling in clockwise around O', where O' denotes the reflection of O around $\mathsf{M}(u, u')$.*

Assume that $(u, u') = (v_i, v_j)$. We consider two cases.

- Case 2.1: $j \neq i + 1$. See Figure 35 (a). Let γ denote the intersection between ∂P and the opposite quadrant of $\chi_u^{u'}$. We state the following which together imply (2).

  (i) Boundary-portion $\zeta(v_i, v_j)$ is contained in boundary-portion γ.

  (ii) when point X travels along γ, it is traveling in clockwise around O'.

  Proof of (i): In proving $block(u, u') \subset \chi_u^{u'}$ we proved that $\zeta(v_i, v_j)$ is contained in the opposite quadrant of $\chi_{v_i}^{v_j}$. Therefore, it is contained in γ.

  Proof of (ii): Since O' is the reflection of O around $\mathsf{M}(u, u')$ while O lies in the opposite quadrant of $\chi_u^{u'}$, point O' lies in $\chi_u^{u'}$. This further implies (ii).

- Case 2.1: $j = i + 1$. See Figure 35 (b). We state the following which together imply (2).

  (i) $\zeta(u, u') \subseteq [\delta_{i-1} \circlearrowright \delta_{i+1}]$.

  (ii) When point X travels along $[\delta_{i-1} \circlearrowright \delta_i]$, it is traveling in clockwise around O'.

  (iii) When point X travels along $[\delta_i \circlearrowright \delta_{i+1}]$, it is traveling in clockwise around O'.

  Fact (i) follows from Lemma A.3; we prove (ii) in the following; (iii) is symmetric to (ii).

  Consider any edge in $[\delta_{i-1} \circlearrowright \delta_i]$, e.g. e_k. We argue that when X travels along e_k, it is traveling in clockwise around O'. Let $d(Y)$ denote the signed version distance from point Y to ℓ_k, so that the points on the right of e_k have positive values.

  Because e_k lies in $[\delta_{i-1} \circlearrowright \delta_i]$, point v_i has the largest distance to ℓ_k in P. Moreover, we know $O \neq v_i$ since O lies in the opposite quadrant of $\chi_u^{u'}$. Therefore, $d(v_i) > d(O)$.

  Because P is convex, we know $d(v_{i+1}) \geq 0$.

  Finally, since O' is the reflection of O around $\mathsf{M}(v_i, v_{i+1})$, we get $d(O') = 2d(\mathsf{M}(v_i, v_{i+1})) - d(O) = d(v_i) + d(v_{i+1}) - d(O) > 0$. So, O' is on the right of e_k. Thus we prove the argument.

Case 3: u, u' are a vertex and an edge. $block(u, u')$ has four borders; two are congruent to the only edge in u, u' and two are reflections of $\zeta(u, u')$. Similar to Case 1, (1) is correct for the former two borders; similar to Case 2, (1) is correct for the other two borders. □

Before we prove the LOCAL-REVERSIBILITY OF f , we state the following (trivial) fact.

(a) *Suppose that u, u' are distinct units and point O lies in $u \oplus u'$. Then, there exists only one pair of points (X, X') such that $\mathsf{M}(X, X') = O$ and X, X' lie on u, u' respectively.*

Proof of the LOCAL-REVERSIBILITY OF f . Assume that $A = (A_1, A_2, A_3), B = (B_1, B_2, B_3)$ are distinct tuples of points in $\mathsf{T}(u, u')$. We shall prove that $f(A) \neq f(B)$.

For convenience, denote by $r(X, O)$ the reflection of X around O.

Case 1: $A_2 = B_2$. Clearly, $(A_1, A_3) \neq (B_1, B_3)$. Applying Fact (a) above, $\mathsf{M}(A_1, A_3) \neq \mathsf{M}(B_1, B_3)$. Therefore, $f(A) = r(A_2, \mathsf{M}(A_1, A_3)) = f(B_2, \mathsf{M}(A_1, A_3)) \neq r(B_2, \mathsf{M}(B_1, B_3)) = f(B)$.

Case 2: $A_2 \neq B_2$. Because $A, B \in \mathsf{T}(u, u')$, points A_2, B_2 lie in $\zeta(u, u')$. So, $\zeta(u, u')$ is not a single point, and so there is at least one vertex among u, u'. When u, u' are both vertices, we have $A_1 = B_1 = u'$ and $A_3 = B_3 = u$ and hence $\mathsf{M}(A_1, A_3) = \mathsf{M}(B_1, B_3)$, which means $r(A_2, \mathsf{M}(A_1, A_3)) \neq r(B_2, \mathsf{M}(B_1, B_3))$, i.e. $f(A) \neq f(B)$. Now, assume that u, u' are an edge and a vertex, e.g. $(u, u') = (v_i, e_j)$. In order to show that $f(A), f(B)$ are distinct in this case, we argue that their distances to line ℓ_j differ. By Lemma A.3, $\zeta(v_i, e_j) = [Z^j_{i-1} \circlearrowleft Z^j_i] \subseteq [v_{j+1} \circlearrowleft \delta_j]$. This implies that all points on $\zeta(v_i, e_j)$ have different distances to ℓ_j. So, A_2, B_2 have different distances to ℓ_j. Moreover, $\mathsf{M}(A_1, A_3)$ and $\mathsf{M}(B_1, B_3)$ both lie on segment $v_i \oplus e_j$ and thus have the same distance to ℓ_j. So, $f(A) = r(A_2, \mathsf{M}(A_1, A_3))$ and $f(B) = r(B_2, \mathsf{M}(B_1, B_3))$ have different distances to ℓ_j. □

Proof of the LOCAL-MONOTONICITY OF f . Let $(J_X, K_X, L_X) = f^{-1}_{u,u'}(X)$ for any point X in $\mathit{block}(u, u')$. Note that $J_X \in u', K_X \in \zeta(u, u'), L_X \in u$ since $(J_X, K_X, L_X) \in \mathsf{T}(u, u')$. We shall prove that when point X travels (in clockwise) along a boundary-portion of ∂P that lies in $\mathit{block}(u, u')$, point K_X moves along ∂P in clockwise non-strictly.

Case 1: Both u, u' are edges. K_X is invariant in this case since $K_X \in \zeta(u, u')$ and $\zeta(u, u') = Z^{u'}_u$.

Case 2: u, u' are a vertex and an edge. Without loss of generality, assume that $(u, u') = (v_i, e_j)$. Denote by $d(X)$ the distance from point X to ℓ_j. Suppose that ρ is a boundary-portion of P that lies in $\mathit{block}(u, u')$. We first state some arguments.

(i) When point X travels along ρ in clockwise, $d(X)$ (non-strictly) decreases.

(ii) For any point X in $\mathit{block}(v_i, e_j) \cap \partial P$, quantity $d(X) + d(K_X)$ is a constant.

(iii) Suppose that point Y is in a movement in which its position is restricted on $\zeta(v_i, e_j)$, and we observe that $d(Y)$ (non-strictly) increases during the movement of Y. We can conclude that point Y moves in clockwise (non-strictly) along $\zeta(v_i, e_j)$.

We can prove our result by combining (i), (ii) and (iii). Suppose point X travels along ρ. Then, $d(X)$ non-strictly decreases due to (i). So, $d(K_X)$ non-strictly increases due to (ii). Applying (iii) for $Y = K_X$, point K_X travels along $\zeta(v_i, e_j)$ in clockwise non-strictly.

We prove (i), (ii), and (iii) in the following. Since $\mathit{block}(v_i, e_j) \subset \chi^j_i$, $\mathit{block}(v_i, e_j) \cap \partial P \subseteq (v_i \circlearrowleft v_{j+1})$, which implies $\rho \subseteq (v_i \circlearrowleft v_{j+1})$, which further implies (i).

Because $f(J_X, K_X, L_X) = X$, we have $\mathsf{M}(X, K_X) = \mathsf{M}(J_X, L_X)$. Because $J_X \in u'$ and $L_X \in u$, their mid point $\mathsf{M}(J_X, L_X)$ lies in $u \oplus u' = v_i \oplus e_j$. Therefore, $\mathsf{M}(X, K_X)$ lies on $v_i \oplus e_j$. and hence $d(\mathsf{M}(X, K_X))$ is a constant. Further, since X, K_X both lie on ∂P, they lie on the same side of ℓ_j, so $d(X) + d(K_X) = 2d(\mathsf{M}(X, K_X))$. Together, we get (ii).

By Lemma A.3, $\zeta(v_i, e_j) = [Z^j_{i-1} \circlearrowleft Z^j_i] \subseteq [v_{j+1} \circlearrowleft \delta_j]$, which implies that $d(Y)$ strictly increases when point Y travels along $\zeta(v_i, e_j)$ in clockwise. This further implies (iii).

Case 3 u, u' are both vertices. Note that $\mathit{block}(u, u')$ is a curve in this case. Under our assumption that edges are pairwise nonparallel, there is no boundary-portion lying in $\mathit{block}(u, u')$. □

E *Roof garden:* Proof of the properties of $Nest(P)$

In the appendix, we provide the details for proving the properties of $Nest(P)$. The outline of the proof was already given in Subsection 3.4.

E.1 Rigorous definition of the inner boundary of $f(\mathsf{T})$

Here, we define the *inner boundary* of $f(\mathsf{T})$ (denoted by σP) rigorously.

Briefly, we shall introduce the *frontier blocks*, which are those blocks that lie on the inner side of $f(\mathsf{T})$, and define *bottom border* of each frontier block; the inner boundary of $f(\mathsf{T})$ is then defined as the concatenation of the bottom borders of the frontier blocks.

First, we define a circular list of unit pairs, called *frontier-pair-list*, which is used to indicate the frontier blocks. Specifically, for each unit pair (u, u') in this list, we call $block(u, u')$ a *frontier block*. This list is defined as FPL generated by Algorithm 3. See Figure 36 for an illustration.

```
Let FPL be empty, let i = 1, and let e_j be the previous edge of δ_1;
repeat
    Add unit pair (e_i, e_j) to the tail of FPL;
    if e_i ≺ e_{j+1} then
        Add unit pair (e_i, v_{j+1}) to the tail of FPL and increase j by 1;
    else
        if i + 1 ≠ j then
            Add unit pair (v_{i+1}, e_j) to the tail of FPL and increase i by 1;
        else Add unit pair (v_{i+1}, v_{j+1}) to the tail of FPL and increase i, j both by 1;
    end
until i = 1 and e_j is the previous edge of δ_1;
```

Algorithm 3: An algorithm for defining FPL

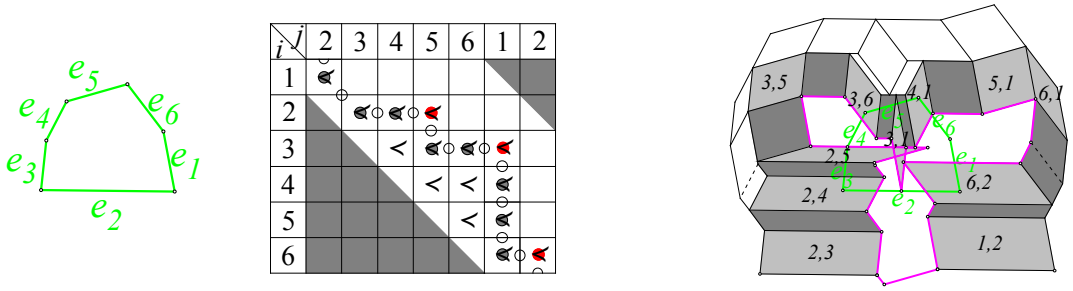

Figure 36: The left picture shows P. The table in the middle exhibits the relationship "ahead of" between the edges of P, where the solid circles indicate edge pairs in the frontier-pair-list, and the hollow circles indicate other unit pairs in the frontier-pair-list. The right picture shows $f(\mathsf{T})$, where the grey blocks indicate the frontier blocks, and the pink curve indicates σP.

Definition E.1 (Lower borders and Bottom borders)**.** See Figure 9.

Recall the geometric definition of the blocks and their borders in Subsection 3.2.

The *left lower border* of $block(e_i, e_j)$ refers to the 2-scaling of $v_i \oplus e_j$ about Z_i^j.

The *right lower border* of $block(e_i, e_j)$ refers to the 2-scaling of $e_i \oplus v_{j+1}$ about Z_i^j.

The *lower border* of $block(v_i, e_j)$ refers to the reflection of $\zeta(v_i, e_j)$ around $\mathsf{M}(v_i, v_{j+1})$.

The *lower border* of $block(e_i, v_j)$ refers to the reflection of $\zeta(e_i, v_j)$ around $\mathsf{M}(v_i, v_j)$.

For (u, u') in FPL, we define the *bottom border* of $block(u, u')$ as follows.

- When u, u' comprise two vertices, $block(u, u')$ has a single border (which is the block itself) and we define this border as the *bottom border* of $block(u, u')$.
- When u, u' comprise an edge and a vertex, we define the *bottom border* of $block(u, u')$ to be the lower border of $block(u, u')$.
- When u, u' comprise two edges, e.g. $u = e_i, u' = e_j$, we define the bottom border of $block(u, u')$ to be

$$\begin{cases} \text{an empty set,} & \text{if } (e_{i-1}, e_j) \in \mathsf{FPL}, (e_i, e_{j+1}) \in \mathsf{FPL}. \\ \text{its right lower border,} & \text{if } (e_{i-1}, e_j) \in \mathsf{FPL}, (e_i, e_{j+1}) \notin \mathsf{FPL}; \\ \text{its left lower border,} & \text{if } (e_{i-1}, e_j) \notin \mathsf{FPL}, (e_i, e_{j+1}) \in \mathsf{FPL}; \\ \text{the concatenation of its two lower borders,} & \text{if } (e_{i-1}, e_j) \notin \mathsf{FPL}, (e_i, e_{j+1}) \notin \mathsf{FPL}; \end{cases}$$

By the geometric definition of the blocks, the bottom borders of the frontier blocks are end-to-end connected, which means that the starting point of the next border is the terminal point of the previous border; we define their concatenation as the *inner boundary of* $f(\mathsf{T})$.[1]

E.2 Introduction of extremal pairs

Here, we introduce a notion that is especially important in the following two subsections. It is called *extremal pairs* and is related to the *small portions*.

Definition E.2. The edge pair $(e_c, e_{c'})$ is *extremal*, if $e_c \prec e_{c'}$ and

$$\text{the small portion } [v_c \circlearrowleft v_{c'+1}] \text{ is not contained in any other small portions.}$$

Equivalent, we call $(e_c, e_{c'})$ an *extremal pair* if

$$e_{c'} = back(\delta_c) \text{ and } e_c = forw(\delta_{c'}).$$

For instance, in Figure 36, the three edge pairs indicated by red solid circles are extremal. Note that all of the extremal pairs are contained in the frontier-pair-list.

Lemma E.3. *There exist at least three extremal pairs.*

Proof. First, we state two arguments:

i For any edge e_i, let $e_j = back(\delta_i)$ and $e_k = forw(\delta_j)$, then (e_k, e_j) is extremal.

ii For any edge e_i, let $e_h = forw(\delta_i)$ and $e_l = back(\delta_h)$, then (e_h, e_l) is extremal.

We only prove (i); (ii) is symmetric.
See Figure 37 (1). To prove that (e_k, e_j) is extremal, we need to prove that

$$e_j = back(\delta_k) \text{ and } e_k = forw(\delta_j).$$

We know $e_k = forw(\delta_j)$ from assumption. To prove that $e_j = back(\delta_k)$, we only need to prove that

$$e_k \prec e_j \text{ and } e_{j+1} \prec e_k.$$

[1] **Note**: According to this definition, when $(e_{i-1}, e_j) \notin \mathsf{FPL}, (e_i, e_{j+1}) \notin \mathsf{FPL}$, the bottom border of $block(e_i, e_j)$ does not contain its "corner point", i.e. the common endpoint of its two lower borders, since the lower borders of $block(e_i, e_j)$ do not contain their endpoints. For example, in Figure 36, the lowermost corner of $block(3, 1)$, the leftmost corner of $block(6, 2)$, and the rightmost corner of $block(2, 5)$ are not contained in the bottom borders. Therefore, none of them are not contained in σP. If we count them in to σP, the description of some lemmas or proofs would be confused. For example, in Figure 36, the lowermost corner of $block(3, 1)$ lies exactly on ∂P. If this point is counted in to the intersection of σP and ∂P, the INTERLEAVITY-OF-f would be confused.

Since $e_k = forw(\delta_j)$, we get $e_k \prec e_j$.

Suppose $e_{j+1} \not\prec e_k$. Then, $e_k \prec e_{j+1}$, and so $e_i \prec e_{j+1}$. However, we know $e_{j+1} \prec e_i$ since $e_{j+1} = forw(\delta_i)$. Contradictory! Therefore, $e_{j+1} \prec e_k$.

Now, assume that $(e_a, e_{a'})$ is extremal. Let $e_b = forw(\delta_{a'+1}), e_{b'} = back(\delta_b)$. Let $e_{c'} = back(\delta_{a-1}), e_c = forw(\delta_{c'})$. By (i) and (ii), $(e_b, e_{b'})$ and $(e_c, e_{c'})$ are extremal. Moreover, they are clearly distinct. (See Figure 37 (2).) So, there are at least three extremal pairs. □

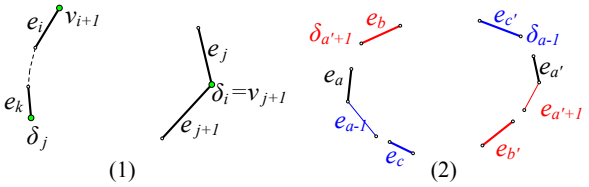

Figure 37: Illustration of Lemma E.3

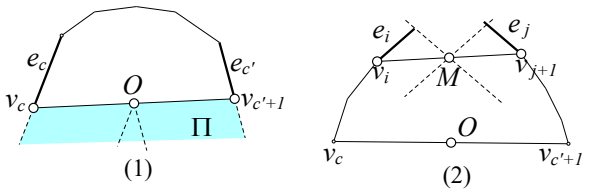

Figure 38: Illustration of Lemma E.4

The next lemma is fundamental to prove Block-disjointness and Interleavity-of-f. It reveals some common properties of the blocks within a local area.

Lemma E.4. *Consider any extremal pair, e.g.* (e_c, e'_c). *Denote*

$$\Delta(c, c') := \{(u, u') \mid \text{unit } u \text{ is ahead of } u', \text{ and } forw(u), back(u') \in \{e_c, e_{c+1}, \ldots, e_{c'}\}\}, \quad (33)$$

1. *Blocks in* $\{block(u, u') \mid (u, u') \in \Delta(c, c')\}$ *do not intersect the opposite quadrant of* $\chi_c^{c'}$.
2. *When point* X *travels along any border of any block in* $\{block(u, u') \mid (u, u') \in \Delta(c, c')\}$, *it is traveling in clockwise order around* $O = \mathsf{M}(v_c, v_{c'+1})$.
   Note: In most cases, X is traveling in clockwise order "strictly"; which means that the orientation of OX strictly increases during the traveling process. However, in a special case, where X travels along the two lower borders of $block(c, c')$, the orientation of OX may not strictly increase but just keep invariant during the traveling process. This occurs when $Z_c^{c'}$ lies on the boundary of the opposite quadrant of $\chi_c^{c'}$. (Recall that $Z_c^{c'}$ lies in or on the boundary of the opposite quadrant of $\chi_c^{c'}$ as stated in Lemma A.4.2.)

Proof. Let (u, u') be an arbitrary unit pair in $\Delta(c, c')$, and denote

$$e_i = forw(u), e_j = back(u').$$

Because $(u, u') \in \Delta(c, c')$, we get:

$$e_i, e_j \text{ belong to } \{e_c, \ldots, e_{c'}\} \text{ and } e_i \preceq e_j. \quad (34)$$

We shall prove that

1. $block(u, u')$ is disjoint with the opposite quadrant of $\chi_c^{c'}$.
2. When X travels along any border of $block(u, u')$, it is traveling in clockwise around O.

Proof of 1: See Figure 38 (1). Let Π denote the region that lies on the right of e_c and on the right of $e_{c'}$ and on the right of $\overrightarrow{v_c v_{c'+1}}$. According to (34) and the definition of hp_j^i,

$$\text{the half-plane } \mathsf{hp}_i^j \text{ is disjoint with } \Pi.$$

Further, since $block(u, u') \subset \chi_u^{u'} = \chi_i^j \subseteq \mathsf{hp}_i^j$,

$$block(u, u') \text{ is disjoint with } \Pi.$$

Further, since the opposite quadrant of $\chi_c^{c'}$ is a subregion of Π,

$$block(u, u') \text{ is disjoint with the opposite quadrant of } \chi_c^{c'}.$$

Proof of 2: We assume that $(u, u') \neq (e_c, e_{c'})$; the case $(u, u') = (e_c, e_{c'})$ is easier.

Since $(u, u') \neq (e_c, e_{c'})$, we claim that $(i, j) \neq (c, c')$. The prove is as follows.

Suppose to the contrary that $(i, j) = (c, c')$. Then,

$$(u, u') \in \{(e_c, e_{c'}), (e_c, v_{c'+1}), (v_c, e_{c'}), (v_c, v_{c'+1})\}.$$

Since $(e_c, e_{c'})$ is a extremal pair, e_c is not ahead of $v_{c'+1}$, v_c is not ahead of $e_{c'}$, and v_c is not ahead of $v_{c'+1}$. However, u is ahead of u'. Therefore, $(u, u') = (e_c, e_{c'})$, which is contradictory.

See Figure 38 (2). Let $M = \mathsf{M}(v_i, v_{j+1})$. Because (34),

$$d_{\ell_j}(v_c) \geq d_{\ell_j}(v_i) \text{ and } d_{\ell_j}(v_{c'+1}) \geq d_{\ell_j}(v_{j+1}).$$

At least one of these inequalities is unequal since $(i, j) \neq (c, c')$. So,

$$d_{\ell_j}(v_c) + d_{\ell_j}(v_{c'+1}) > d_{\ell_j}(v_i) + d_{\ell_j}(v_{j+1}).$$

Notice that, in this inequality, the left and right part equal to $2 \cdot d_{\ell_j}(O)$ and $2 \cdot d_{\ell_j}(M)$, respectively. Therefore, $d_{\ell_j}(O) > d_{\ell_j}(M)$. Symmetrically, $d_{\ell_i}(O) > d_{\ell_i}(M)$.

The last two inequalities imply that O lies in the opposite quadrant of $\chi_i^j = \chi_u^{u'}$. Further, due to the monotonicity of the borders (Lemma 3.6.2), we obtain fact 2. □

E.3 Proof details: Block-disjointness

Here, we prove the following claim which is stated without proof in Subsection 3.4.

(i) *If $e_i \preceq e_j$, all blocks in set S are pairwise disjoint, where*

$$S = \{block(u, u') \mid u \text{ is ahead of } u', \text{ and } forw(u), back(u') \text{ lie in } [v_i \circlearrowleft v_{j+1}]\}.$$

Recall that

$$\Delta(c, c') := \left\{(u, u') \mid u \text{ is ahead of } u', \text{ and } forw(u), back(u') \text{ lie in } [v_c \circlearrowleft v_{c'+1}]\right\}.$$

Clearly, we only have to prove the case where (e_i, e_j) is extremal. Therefore, we prove the following claim instead.

(ii) *If $(e_c, e_{c'})$ is extremal, all blocks in $\{block(u, u') \mid (u, u') \in \Delta(c, c')\}$ are pairwise disjoint.*

Proof. For simplicity, we introduce some temporary notations in this proof.

We denote $BLOCK[S] = \{block(u, u') \mid (u, u') \in S\}$.

We call $BLOCK[S]$ a "*tiling*", if all blocks in $BLOCK[S]$ are pairwise disjoint.

For an edge pair $(e_a, e_{a'})$ such that $e_a \prec e_{a'}$, we denote

$$\mathsf{U}(a, a') = \left\{(u, u') \mid u \text{ is ahead of } u' \text{ and } u, u' \text{ lie in } (v_a \circlearrowleft v_{a'+1})\right\}.$$

For three distinct points O, X, Y, assume that there is a ray at O which rotates from OX to OY in clockwise; we denote by $\mathsf{SWEPT}_O(X, Y)$ the region swept by this ray.

First, we state that

(iii) *for each edge pair $(e_a, e_{a'})$ in $\Delta(c, c')$, $BLOCK[\mathsf{U}(a, a')]$ is a tiling.*

We prove statement (iii) by using induction on the number of edges k in $(v_a \circlearrowright v_{a'})$.

Initial: $k = 2$, i.e., $a' = a + 1$.

$BLOCK[\mathsf{U}(a, a')]$ contains only one block (which is $block(e_a, e_{a+1})$), and so is a tiling.

Induction: $k > 2$. By the induction hypothesis, $BLOCK[\mathsf{U}(a, a'-1)]$ and $BLOCK[\mathsf{U}(a+1, a')]$ are both tilings, and we shall prove that $BLOCK[\mathsf{U}(a, a')]$ is also a tiling.

See the left picture in Figure 39. We divide the unit pairs in $\mathsf{U}(a, a')$ into four parts distinguished by whether $\mathsf{U}(a, a'-1), \mathsf{U}(a+1, a')$ contain them. Formally,

$$U_{10} = \mathsf{U}(a, a'-1) - \mathsf{U}(a+1, a'), \qquad U_{01} = \mathsf{U}(a+1, a') - \mathsf{U}(a, a'-1),$$
$$U_{11} = \mathsf{U}(a, a'-1) \cap \mathsf{U}(a+1, a'), \qquad U_{00} = \mathsf{U}(a, a') - \mathsf{U}(a, a'-1) - \mathsf{U}(a+1, a').$$

Denote the regions occupied by $BLOCK[U_{00}]$, $BLOCK[U_{01}]$, $BLOCK[U_{10}]$, $BLOCK[U_{11}]$ by $R_{00}, R_{01}, R_{10}, R_{11}$, respectively. It is easy to show that the blocks in $BLOCK[U_{00}]$ are disjoint (since U_{00} only contain four unit pairs as shown below). Moreover, by the induction hypothesis, $BLOCK[U_{01}]$, $BLOCK[U_{10}]$, $BLOCK[U_{11}]$ are all tilings. Therefore, we only need to prove that $R_{00}, R_{01}, R_{10}, R_{11}$ are pairwise disjoint.

Because $BLOCK[\mathsf{U}(a, a'-1)]$ is a tiling, R_{11}, R_{10} are disjoint. Similarly, R_{11}, R_{01} are disjoint. Next, we prove that R_{01}, R_{10} are disjoint. Let $O = \mathsf{M}(v_a, v_{a'+1})$. Let A be an arbitrary point in the opposite quadrant of $\chi_c^{c'}$, and let B be the terminal point of the lower border of $block(v_{a+1}, e_{a'-1})$ (or equivalently, let B be the starting point of the lower border of $block(e_{a+1}, v_{a'})$). By Lemma E.4, we have $R_{01} \subset \mathsf{SWEPT}_O(B, A)$ and $R_{10} \subset \mathsf{SWEPT}_O(A, B)$. Further, since $\mathsf{SWEPT}_O(B, A)$ is disjoint with $\mathsf{SWEPT}_O(A, B)$, regions R_{01}, R_{10} are disjoint.

Next, we argue that R_{00} is disjoint with the other three regions. Let Π denote the region bounded by the right lower border of $block(e_a, e_{a'-1})$, the left lower border of $block(e_{a+1}, e_{a'})$, and the lower border of $block(v_{a+1}, v_{a'})$. Notice that

$$U_{00} = \{(e_a, e_{a'}), (v_{a+1}, e_{a'}), (e_a, v_{a'}), (v_{a+1}, v_{a'})\}.$$

Clearly, R_{00} is contained in Π, whereas the other regions are disjoint with Π. (We omit some details due to the length of the paper.) Therefore, R_{00} is disjoint with the others.

Finally, we prove (ii) by applying (iii). For convenience, let $(b, b'), (d, d')$ respectively denote the previous and next extremal pair of (c, c') in the frontier-pair-list. Consider the unit pairs in $\Delta(c, c') - \mathsf{U}(c, c')$. A part of them is contained in $\mathsf{U}(b, b')$, while the other part is contained in $\mathsf{U}(d, d')$. For convenience, denote these two part of unit pairs by S_1 and S_2. Formally,

$$S_1 = (\Delta(c, c') - \mathsf{U}(c, c')) \cap \mathsf{U}(b, b'), \qquad S_2 = (\Delta(c, c') - \mathsf{U}(c, c')) \cap \mathsf{U}(d, d')$$

See the right picture in Figure 39 for illustration, where R_1, R_2 respectively denote the regions occupied by $BLOCK[S_1]$, $BLOCK[S_2]$.

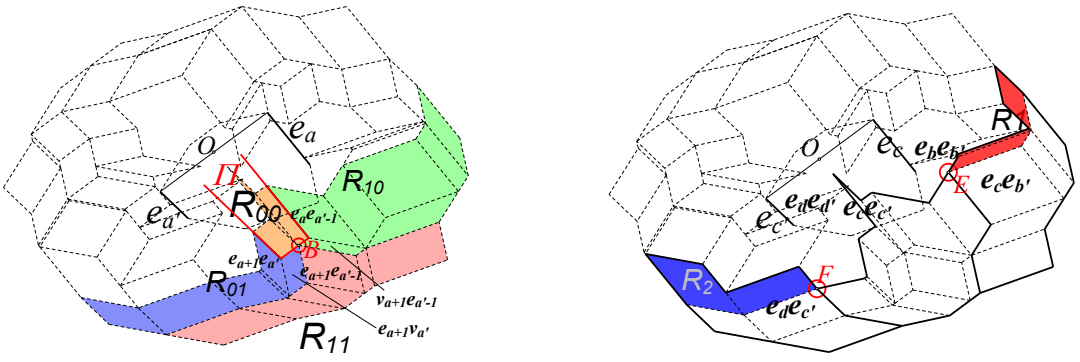

Figure 39: Illustration of the proof of the BLOCK-DISJOINTNESS in the local area

By (iii), $BLOCK[\mathsf{U}(c,c')]$ is a tiling. Therefore, to prove that $BLOCK[\Delta(c,c')]$ is a tiling, we only need to prove the following.

(a) The blocks in $BLOCK[S_1]$ are disjoint with the blocks in $BLOCK[\Delta(c,c') - S_1]$.

(b) The blocks in $BLOCK[S_2]$ are disjoint with the blocks in $BLOCK[\Delta(c,c') - S_2]$.

We only show the proof of (a); the proof of (b) is symmetric. Clearly, (a) follows from

(a1) The blocks in $BLOCK[S_1]$ are disjoint with the blocks in $BLOCK[\Delta(c,c') - \mathsf{U}(b,b')]$.

(a2) The blocks in $BLOCK[S_1]$ are disjoint with the blocks in $BLOCK[\mathsf{U}(b,b') - S_1]$.

Proof of (a1): Let $O = \mathsf{M}(v_c, v_{c'+1})$ and let E be the common endpoint of the two lower borders of $block(e_c, e_{b'})$. By Lemma E.4, the blocks in $BLOCK[S_1]$ lie in $\mathsf{SWEPT}_O(A,E)$ while the blocks in $BLOCK[\Delta(c,c') - \mathsf{U}(b,b')]$ lie in $\mathsf{SWEPT}_O(E,A)$. Therefore, we obtain (a1).
Proof of (a2): According to (ii), $BLOCK[\mathsf{U}(b,b')]$ is also a tiling, which implies (a2). □

E.4 Proof details: Interleavity-of-f

Recall that σP denote the inner boundary of $f(\mathsf{T})$. Here, we show that it interleaves ∂P, which is outlined in Subsection 3.4.

Step 1: We cut the curve σP to several fragments.

Definition E.5 (Cut σP to fragments)**.** For each extremal pair $(e_c, e_{c'})$, denote

$$\sigma(c,c') = \begin{array}{c}\text{the concatenation of the bottom borders of the}\\ \text{frontier blocks in } \{block(u,u') \mid (u,u') \in \Delta(c,c')\}.\end{array} \tag{35}$$

See Figure 13 for an illustration. In this figure, (e_e, e_5) is extremal. The grey blocks indicate $\{block(u,u') \mid (u,u') \in \Delta(2,5)\}$, in which the ones with blue labels are frontier blocks; and the dotted line indicates $\sigma(2,5)$. Notice that $\sigma(c,c')$ is a *directional* curve and is a fraction of σP.

Assume that there are in total q extremal pairs and denote them by $(e_{c_1}, e_{c'_1}), \ldots, (e_{c_q}, e_{c'_q})$ in clockwise order. We define

$$\alpha_i = \text{the fragment of } \sigma P \text{ that is contained commonly by } \sigma(c_i, c'_i) \text{ and } \sigma(c_{i+1}, c'_{i+1}). \tag{36}$$

$$\beta_i = \text{the fragment that belongs to } \sigma(c_i, c'_i) \text{ but does not belong to } \alpha_i \text{ or } \alpha_{i-1}. \tag{37}$$

See Figure 40. Clearly, σP is the concatenation of the $2q$ fragments $\beta_1, \alpha_1, \ldots, \beta_q, \alpha_q$.

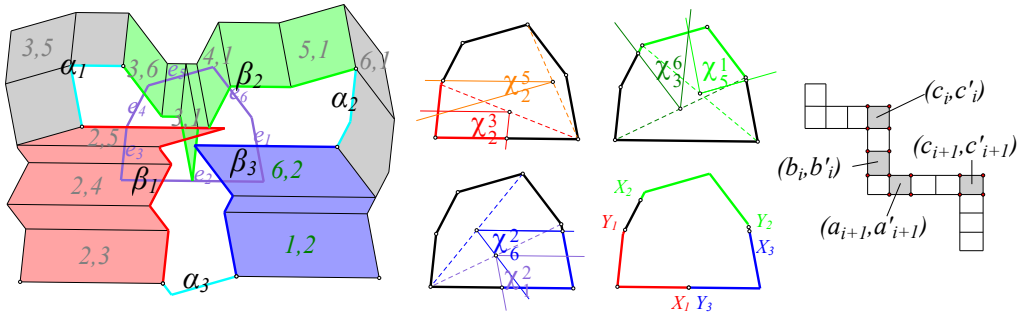

Figure 40: Illustration of the proof of the Interleavity-of-f . The left picture illustrates the definition of the fragments $\beta_1, \alpha_1, \ldots, \beta_q, \alpha_q$; the middle pictures illustrate how do we find $2q$ points to delimit these $2q$ fragments; the right picture illustrates the definitions of (a_i, a'_i) and (b_i, b'_i).

Step 2: We define $2q$ points $X_1, Y_1, \ldots, X_q, Y_q$ and prove that they delimit the $2q$ fragments.

Notice that β_i begins with the bottom border of $\mathit{block}(e_{a_i}, e_{a'_i})$, and ends with the bottom border of $\mathit{block}(e_{b_i}, e_{b'_i})$, where

$$(a_i, a'_i) = (c_i, c'_{i-1} + 1), \qquad (b_i, b'_i) = (c_{i+1} - 1, c'_i).$$

Recall $\widehat{\chi}$ defined in (14). We denote

$$X_i = \text{the starting point of } \widehat{\chi}^{a'_i}_{a_i}, \quad Y_i = \text{the terminal point of } \widehat{\chi}^{b'_i}_{b_i}. \tag{38}$$

(0) *The $2q$ points $X_1, Y_1, \ldots, X_q, Y_q$ lie in clockwise order around ∂P.*

(i) *For $1 \le i \le q$, the intersections between β_i and ∂P are contained in $[X_i \circlearrowright Y_i]$.*

(ii) *For $1 \le i \le q$, the intersections between α_i and ∂P are contained in $[X_i \circlearrowright Y_{i+1}]$.*

Proof. (0): Consider two neighboring extremal pairs $(e_{c_i}, e_{c'_i}), (e_{c_{i+1}}, e_{c'_{i+1}})$. Since they are neighboring extremal pairs, edges $b_i, b'_i, a_{i+1}, a'_{i+1}$ are not in a small portion; as illustrated in the right of Figure 40. Therefore, by applying the peculiar property of the bounding regions, $\widehat{\chi}^{b'_i}_{b_i}$ and $\widehat{\chi}^{a'_{i+1}}_{a_{i+1}}$ are disjoint (although they may share a common endpoint). Combining this with the monotonicity of the $\widehat{\chi}$ (see Lemma 3.8), the q portions $[X_1 \circlearrowright Y_1], \ldots, [X_q \circlearrowright Y_q]$ are disjoint and lie in clockwise order, which implies that $X_1, Y_1, \ldots, X_q, Y_q$ lie in clockwise order.

(i): Consider a frontier block whose bottom border is a fraction of β_i, for example, $\mathit{block}(u, u')$.

By the monotonicity of the $\widehat{\chi}$ and the definition of X_i, Y_i, portion $[X_i \circlearrowright Y_i]$ contains $\widehat{\chi}^{u'}_u$.

By Lemma 3.6.1, $\mathit{block}(u, u') \subset \chi^{u'}_u$. So, the intersections between the bottom border of $\mathit{block}(u, u')$ and ∂P are contained in $\chi^{u'}_u \cap \partial P$ and thus contained in $\widehat{\chi}^{u'}_u$.

Together, these intersections are contained in $[X_i \circlearrowright Y_i]$, which implies (i).

(ii): This statement can be proved the same way as (i), and we omit its proof. □

Step 3: We prove the following statement.

(iii) *For $1 \le i \le q$, the concatenation of $\alpha_{i-1}, \beta_i, \alpha_i$ interleaves ∂P. ($\alpha_0 = \alpha_q$)*

Proof. We argue that, for each extremal pair $(e_c, e_{c'})$, the curve $\sigma(c, c')$ interleaves ∂P. This implies (iii) since the concatenation of $\alpha_{i-1}, \beta_i, \alpha_i$ is exactly $\sigma(c_i, c'_i)$.

For ease of discussion, assume that $\sigma(c, c')$ and ∂P have a finite number of intersections $\mathsf{I}_1, \ldots, \mathsf{I}_x$, where $\mathsf{I}_1, \ldots, \mathsf{I}_x$ are sorted by the priority on $\sigma(c, c')$. Denote $O = \mathsf{M}(v_c, v_{c'+1})$. By Lemma E.4, rays $OI_1, \ldots, OI_x$ are in clockwise order. Further, because O lies in P, points $\mathsf{I}_1, \ldots, \mathsf{I}_x$ lie in clockwise order around ∂P. This means that $\sigma(c, c')$ interleaves ∂P. □

Step 4: We prove Lemma 3.9.

Proof. Index $\beta_1, \alpha_1, \ldots, \alpha_q$ the 1st, 2nd, etc., the $2q$-th *fragment*. Assume that at least one fragment in $\alpha_1, \ldots, \alpha_q$ intersects with ∂P (otherwise the consequence is trivial). Without loss of generality, assume that α_q intersects with ∂P.

Let $(\mathcal{C} - \alpha_q)$ denote the concatenation of the first $2q - 1$ fragments. We state that

(a) *The curve α_q interleaves ∂P.*

(b) *The curve $(\mathcal{C} - \alpha_q)$ interleaves ∂P.*

(c) *We can find two points A, B on ∂P such that the points in $\alpha_q \cap \partial P$ are restricted in $[A \circlearrowright B]$ while the points in $(\mathcal{C} - \alpha_q) \cap \partial P$ are restricted in $[B \circlearrowright A]$.*

Notice that $\mathcal{C}$ is the concatenation of α_q and $(\mathcal{C} - \alpha_q)$, statements (a), (b), and (c) together imply our result. Statement (a) simply follows from (iii); we prove (b) and (c) below.

For convenience, we regard X_1 the starting point of the closed curve ∂P. For two points A, A' on ∂P, we say that A lies *behind* A' if $A = A'$ or, A is encountered later than A' traveling around ∂P starting from X_1. We say that fragment γ lies *behind* fragment γ', if all of the points in $\gamma \cap \partial P$ lie behind all of the points in $\gamma' \cap \partial P$. Statement (b) is implied by (1).

(1) *for $1 < k < 2q$, the k-th fragment lies behind the first $k-1$ fragments.*

Case 1: $k = 2$. By (i) and (ii), $\alpha_1 \cap \partial P$ and $\beta_1 \cap \partial P$ are contained in $[X_1 \circlearrowright Y_2]$. Moreover, by (iii), the points in $\alpha_1 \cap \partial P$ lie behind the points in $\beta_1 \cap \partial P$, i.e. the 2-nd fragment α_1 lies behind the 1-st fragment β_1.

Case 2: the k-th fragment is β_i. Similar to Case 1, β_i lies behind the $(k-1)$-th fragment α_{i-1}. By (i) and (ii), the first $k-2$ fragments have their intersections with ∂P lying in $[X_1 \circlearrowright Y_{i-1}]$ while $\beta_i \cap \partial P$ lie in $[X_i \circlearrowright Y_i]$, so the k-th fragment β_i lies behind the first $k-2$ fragments. Together, the k-th fragment lies behind all the first $k-1$ fragments.

Case 3: the k-th fragment is α_i, and $k > 2$. Similar to Case 1, α_i lies behind the $(k-1)$-th fragment β_i and the $(k-2)$-th fragment α_{i-1}. Similar to Case 2, α_i also lies behind the first $k-3$ fragments. Together, the k-th fragment lies behind all the first $k-1$ fragments.

Proof of (c): The two points A, B are just defined as the first and last points of $\alpha_q \cap \partial P$. (Recall that we assume $\alpha_q \cap \partial P \neq \varnothing$.)

Clearly, $\alpha_q \cap \partial P$ are contained in $[A \circlearrowright B]$. We shall prove that $(\mathcal{C} - \alpha_q) \cap \partial P \subset [B \circlearrowright A]$, i.e. for each fragment beside the last one, its intersections with ∂P are restricted in $[B \circlearrowright A]$.

First, consider the four fragments $\alpha_1, \beta_1, \alpha_{q-1}, \beta_q$. By (iii), the concatenation of $\alpha_q, \beta_1, \alpha_1$, or $\alpha_{q-1}, \beta_q, \alpha_q$ interleaves ∂P. So, for the four fragments, their intersections with ∂P do not lie in $(A \circlearrowright B)$, and hence these intersections are restricted in $[B \circlearrowright A]$.

Then, consider any fragment (denoted by γ) beside the above four and beside α_n.

By (i) and (ii), we get: (c1) the intersections in $\gamma \cap \partial P$ lie in $[X_2 \circlearrowright Y_{q-1}]$.

Moreover, we argue that: (c2) $[X_2 \circlearrowright Y_{q-1}] \subseteq [B \circlearrowright A]$. Applying (ii), $\alpha_q \cap \partial P$ are contained in $[X_q \circlearrowright Y_1]$, and so $[A \circlearrowright B] \subseteq [X_q \circlearrowright Y_1]$. However, due to (0), $[X_q \circlearrowright Y_1] \subseteq [Y_{q-1} \circlearrowright X_2]$. Therefore, $[A \circlearrowright B] \subseteq [Y_{q-1} \circlearrowright X_2]$. Equivalently, $[X_2 \circlearrowright Y_{q-1}] \subseteq [B \circlearrowright A]$.

Combining (c1) and (c2), the intersections in $\gamma \cap \partial P$ are restricted in $[B \circlearrowright A]$. □

E.5 Proof details: Monotonicity-of-f

Here, we attach the proof of the following statements which were stated in Subsection 3.4.

i) The *outer boundary* of $f(\mathsf{T})$ is a simple closed curve whose interior contains P.

iv) Recall that $K_1, \ldots, K_m$ denote all the intersections of σP and ∂P, and they lie in clockwise order around ∂P. Then, points $f_2^{-1}(K_1), \ldots, f_2^{-1}(K_m)$ lie in clockwise order around ∂P.

First, we formally define the outer boundary and give a note about the definition of $f_2^{-1}(K_i)$.

Definition E.6 (Outer boundary of $f(\mathsf{T})$)**.** See Figure 41. For each i, we know $block(v_i, v_{i+1})$ is a curve, and we define this curve as the "*top border*" of $block(v_i, v_{i+1})$. For each i, we know $block(e_i, e_{i+1})$ is a parallelogram with four borders, we define the "*top border*" of $block(e_i, e_{i+1})$ to be the concatenation of those two borders that are not its lower borders.

We define the *outer boundary* of $f(\mathsf{T})$ as the concatenation of the top borders of

$$block(e_1, e_2), block(v_2, v_3), \ldots, block(e_i, e_{i+1}), block(v_{i+1}, v_{i+2}), \ldots, block(e_n, e_1), block(v_1, v_2).$$

A special Note: Function $f_2^{-1}()$ is currently **not** well-defined on $K_1, \ldots, K_m$. The reason is that, the points $K_1, \ldots, K_m$ are in fact not contained in $f(\mathsf{T})$. [2] However, we can extend the scope of definition of $f_2^{-1}()$ so that this function is defined on the K-points. Notice that each K-point (e.g. K_i) comes from the bottom border of some block (e.g. $block(u, u')$). Recall the function $f_{u,u'}^{-1,2}()$ defined in Lemma 3.6, which was previously defined on $block(u, u')$. The scope of the definition of $f_{u,u'}^{-1,2}()$ can be easily extended (see below) so that it is also defined on the lower border of $block(u, u')$. Then, we can define $f_2^{-1}(K_i)$ as $f_{u,u'}^{-1,2}(K_i)$.

Assume that point X lies on the lower border of $block(u, u')$.

Case 1: $u = e_i, u' = e_j$. We define $f_{u,u'}^{-1,2}(X) = Z_i^j$.

Case 2: $u = e_i, u' = v_j$. In this case, X must be the reflection of some point X' on $\zeta(v_i, v_j)$ around $\mathsf{M}(v_i, v_j)$; and we define $f_{u,u'}^{-1,2}(X) = X'$.

Case 3: $u = v_i, u' = e_j$. In this case, X must be the reflection of some point X' on $\zeta(v_i, e_j)$ around $\mathsf{M}(v_i, v_{j+1})$; and we define $f_{u,u'}^{-1,2}(X) = X'$.

Case 4: $u = v_i, u' = v_j$. We can ignore this case since $block(v_i, v_j)$ does not have a lower border.

Now, we complete the proof of Statement (i) and (iv).

Proof of (i). We first argue that all top borders lie outside P. First, consider the top border of $block(v_i, v_{i+1})$. We know that it is $block(v_i, v_{i+1})$ itself, and hence lies in hp_i^i, and so lies outside P. Second, consider the top border of $block(e_i, e_{i+1})$. We know that it is the concatenation of two borders, one is parallel to e_i and the other is parallel to e_{i+1}. Because $block(e_i, e_{i+1})$ lies in χ_i^{i+1}, the former border lies on the left of e_i while the latter one lies on the left of e_{i+1}; so both borders lie outside P; therefore, the top border of $block(e_i, e_{i+1})$ lies outside P.

Moreover, by BLOCK-DISJOINTNESS , the borders of the blocks do not intersect in the exterior of P. Therefore, the outer boundary does not intersect itself. Together, we get (i). □

Proof of (iv). The main idea of this proof is already given in Subsection 3.4. Here, we give the rigorous definition of function g. See Figure 42. Function g is a piecewise function on σP. (Note that σP may intersect itself and so there could be several points on σP which lie on the same position; we regard σP as a curve rather than a set of points.) For any point X on σP that comes from the bottom border of $block(u, u')$, we define $g(X) = f_{u,u'}^{-1,2}(X)$.

According to the definition of $f_{u,u'}^{-1,2}()$, this function is monotone on the lower border of $block(u, u')$. Therefore, function g is circularly monotone on curve σP. □

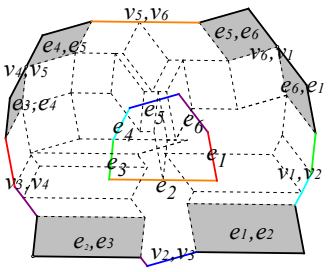

Figure 41: Outer boundary of $f(\mathsf{T})$.

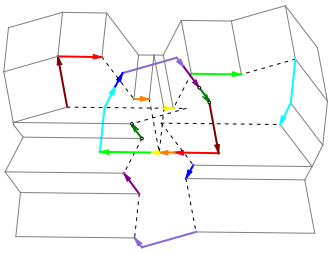

Figure 42: Function g on the inner boundary.

[2] Consider any frontier block, e.g. $block(u, u')$. Case 1: u, u' are both vertices. Then, u' must be the clockwise next vertex of u. So $block(u, u')$ lies outside P (which was proved later in this page) and hence has no intersection with ∂P. Case 2: u, u' comprise at least one edge. In this case, by the definition of $block(u, u')$, the lower border of $block(u, u')$ is not contained in this block; thus the bottom border of $block(u, u')$ is not contained in this block. So, the K-points coming from the bottom border of $block(u, u')$ are not contained in $f(\mathsf{T})$.

F Properties of a single sector

This appendix provides the details omitted in Subsection 4.3.

Assume that V is a fixed vertex throughout this section. Recall the "smaller" order between edges defined in Definition 4.8. We denote by $e_i \preceq_V e_j$ if e_i is smaller than or identical to e_j.

Definition F.1. Recall δ_i defined in Definition 4.4. For any edge e_i, denote

$$\begin{array}{rcccl} \mathsf{UZ}_i^+ & = & \bigcup_{e_j:e_i\prec e_j}[v_{i+1} \circlearrowleft Z_i^j] & = & [v_{i+1} \circlearrowleft Z_i^{back(\delta_i)}], \\ \mathsf{UZ}_i^- & = & \bigcup_{e_k:e_k\prec e_i}[Z_k^i \circlearrowleft v_i] & = & [Z_{forw(\delta_i)}^i \circlearrowleft v_i]. \end{array} \tag{39}$$

Recall that e_{s_V} is defined to be the smallest edge e_i such that UZ_i^+ contains V.
Recall that e_{t_V} is defined to be the largest edge e_i such that UZ_i^- contains V.

Notice that portion $\mathsf{UZ}_{back(V)}^+$ always contains V. So, there is at least one element in UZ^+ which contains V. Therefore, e_s is well-defined. Notice that portion $\mathsf{UZ}_{forw(V)}^-$ always contains V. So, there is at least one element in UZ^- which contains V. Therefore, e_t is well-defined.

We give a demonstration of the definitions of e_s, e_t in Figure 43.

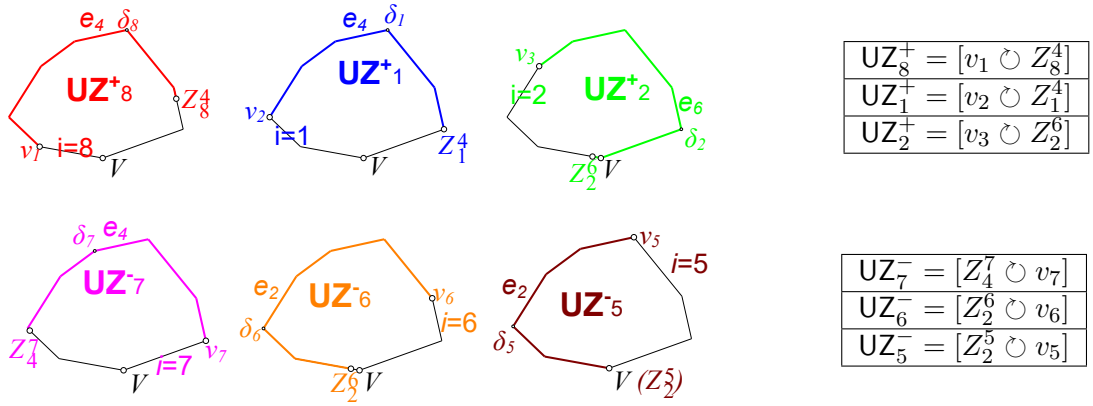

Figure 43: Demonstration of the definitions of s_V and t_V. Here, $s_V = 2, t_V = 5$.

F.1 The relationship between e_s, e_t and V

Fact (i) *$e_s \preceq e_t$, so $[v_s \circlearrowleft v_{t+1}]$ is a small portion. Moreover, $[v_s \circlearrowleft v_{t+1}]$ does not contain V.*

Proof. The proof consists of three parts.

Part 1) We argue that $e_s \preceq_V e_t$. Without loss of generality, here we assume $V = v_1$.

To prove this argument, we introduce two auxiliary edges,

$$e_{s^*} = forw(\delta_n) \text{ and } e_{t^*} = back(\delta_1).$$

First, we state that

$$e_s \preceq_V e_{s^*} \text{ and } e_{t^*} \preceq_V e_t. \tag{40}$$

Proof of (40): See Figure 44 (a).

Point $Z_{s^*}^n$ lies in $(v_1 \circlearrowleft v_{s^*})$ according to Lemma A.3.

This implies that $[v_{s^*+1} \circlearrowleft Z_{s^*}^n]$ contains v_1.

However, $[v_{s^*+1} \circlearrowleft Z_{s^*}^n] \subseteq \mathsf{UZ}_{s^*}^+$ by the definition of $\mathsf{UZ}_{s^*}^+$.

Therefore, $V = v_1 \in \mathsf{UZ}_{s^*}^+$, which implies $e_s \preceq_V e_{s^*}$ according to the definition of s.

Symmetrically, we have $V \in \mathsf{UZ}_{t^*}^-$ and thus $e_{t^*} \preceq_V e_t$.

Next, we apply (40) to prove $e_s \preceq_V e_t$. We discuss two cases as follows.

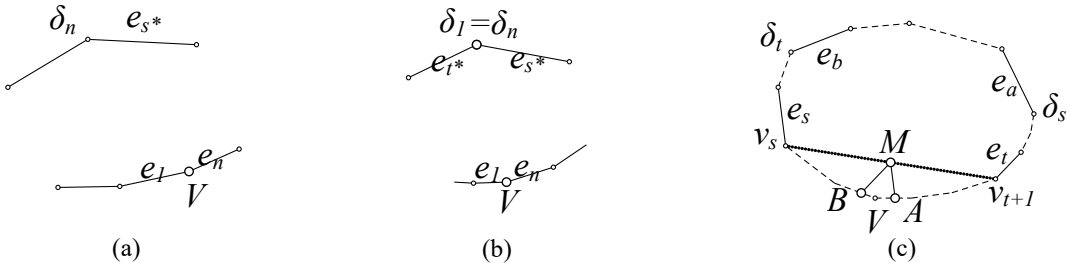

Figure 44: Illustration of the proof of the relationship between e_s, e_t and V

Case 1 $\delta_1 \neq \delta_n$. In this case, $e_{s^*} \leq_V e_{t^*}$. We get $e_s \leq_V e_t$ by combining (40) with $e_{s^*} \leq_V e_{t^*}$.

Case 2 $\delta_1 = \delta_n$. See Figure 44 (b).

In this case, edge e_{s^*} is the next edge of e_{t^*}, so $e_{t^*} \prec e_{s^*}$, and so $Z_{t^*}^{s^*}$ is defined.

Case 2.1 $Z_{t^*}^{s^*}$ lies in $[V \circlearrowright \delta_1]$. In this case, we first argue that $e_s \leq_V e_{t^*}$.
Since $V \in [\delta_1 \circlearrowright Z_{t^*}^{s^*}]$, whereas $[\delta_1 \circlearrowright Z_{t^*}^{s^*}] = [v_{t^*+1} \circlearrowright Z_{t^*}^{s^*}] \subseteq \mathsf{UZ}_{t^*}^+$, we get $V \in \mathsf{UZ}_{t^*}^+$, which implies that $e_s \leq_V e_{t^*}$ according to the definition of s.
Then, combining $e_s \leq_V e_{t^*}$ with $e_{t^*} \leq_V e_t$ stated in (40), we get $e_s \leq_V e_t$.

Case 2.2 $Z_{t^*}^{s^*}$ lies in $[\delta_1 \circlearrowright V]$. In this case, we first argue that $e_{s^*} \leq_V e_t$.
Since $V \in [Z_{t^*}^{s^*} \circlearrowright \delta_1]$, whereas $[Z_{t^*}^{s^*} \circlearrowright \delta_1] = [Z_{t^*}^{s^*} \circlearrowright v_{s^*}] \subseteq \mathsf{UZ}_{s^*}^-$, we get $V \in \mathsf{UZ}_{s^*}^-$, which implies that $e_{s^*} \leq_V e_t$ according to the definition of t.
Then, combining $e_{s^*} \leq_V e_t$ with $e_s \leq_V e_{s^*}$ stated in (40), we get $e_s \leq_V e_t$.

Part 2) We argue that $[v_s \circlearrowright v_{t+1}]$ does not contain V.

By the definition of UZ^+, we get $V \notin \mathsf{UZ}_{forw(V)}^+$, which means $e_s \neq forw(V)$. Symmetrically, $e_t \neq back(V)$. Therefore, V is distinct from v_s, v_{t+1}. Moreover, because $e_s \leq_V e_t$, we get $V \in [v_{t+1} \circlearrowright v_s]$. Therefore, $V \in (v_{t+1} \circlearrowright v_s)$. So, $[v_s \circlearrowright v_{t+1}]$ does not contain V.

Part 3) We argue that $e_s \preceq e_t$.

Suppose to the contrary that $e_t \prec e_s$. See Figure 44 (c). Denote $e_a = back(\delta_s), e_b = forw(\delta_t)$. Denote $\rho = [\delta_s \circlearrowright \delta_t]$ if $\delta_s \neq \delta_t$; otherwise, let ρ denote the entire boundary of P and assume that it starts and terminates at δ_s. Consider the positions of Z_s^a and Z_b^t. Clearly, both of them lie in ρ. We state that the following which contradict each other.

$$\text{(I) } Z_b^t \leq_\rho Z_s^a, \qquad \text{and} \qquad \text{(II) } Z_s^a <_\rho Z_b^t.$$

Proof of (I): By definition of s, V is contained in $\mathsf{UZ}_s^+ = [v_{s+1} \circlearrowright Z_s^a]$, so $V \leq_\rho Z_s^a$. By definition of t, V is contained in $\mathsf{UZ}_t^- = [Z_b^t \circlearrowright v_t]$, so $Z_b^t \leq_\rho V$; together, we get (I).

Proof of (II): Let $M = \mathsf{M}(v_s, v_{t+1})$. Denote by A the intersection of $\mathsf{p}_s(M)$ and $[v_{t+1} \circlearrowright v_s]$, and B the intersection of $\mathsf{p}_t(M)$ and $[v_{t+1} \circlearrowright v_s]$. The following arguments together imply (II).

$$\text{(II.1) } Z_s^a \text{ lies in } (\delta_s \circlearrowright A); \quad \text{(II.2) } Z_b^t \text{ lies in } (B \circlearrowright \delta_t); \quad \text{and (II.3) } A <_\rho B.$$

We prove (II.1) in the next; (II.2) is symmetric to (II.1); (II.3) simply follows from $e_t \prec e_s$.

Proof of (II.1): Denote by h the open half-plane delimited by $\mathsf{p}_s(M)$ and containing v_{t+1}. Because δ_s has larger distance to ℓ_s than point v_{t+1}, the mid point of v_s, δ_s is contained in h, which further implies that the opposite quadrant of χ_s^a, together with its boundary, are contained in h. However, according to Lemma A.4.2, Z_s^a lies in or on the boundary of the opposite quadrant of χ_s^a. Therefore, Z_s^a lies in h, which implies that Z_s^a lies in $(\delta_s \circlearrowright A)$. □

$$\text{Recall } \Delta_V = \left\{ (u,u') \mid \begin{array}{c} u,u' \text{ are units in } [v_s \circlearrowleft v_{t+1}] \text{ such that} \\ u' \text{ is after but not right after } u \text{ (in clockwise)} \end{array} \right\}.$$

Fact (ii) *Regions in* $\{u \oplus u' \mid (u,u') \in \Delta_V\}$ *are pairwise disjoint.*

Proof. We prove it by contradiction. Suppose that X is a point that lies in two regions in $\{u \oplus u' \mid (u,u') \in \Delta_V\}$. Then, there are two pairs of points $(A,A'),(B,B')$ such that

$$1)\ (\mathbf{u}(A),\mathbf{u}(A')) \in \Delta_V \text{; and } 2)\ (\mathbf{u}(B),\mathbf{u}(B')) \in \Delta_V \text{; and } 3)\ \mathsf{M}(A,A') = \mathsf{M}(B,B') = X.$$

Due to 1) and 2) and the definition of Δ_V, points A, A', B, B' lie in $[v_s \circlearrowleft v_{t+1}]$. Due to 3), $ABA'B'$ is a parallelogram. We also note that $[v_s \circlearrowleft v_{t+1}]$ is a small portion according to Fact (i). Thus, there is a parallelogram inscribed on a small portion, which contradicts Lemma 4.12.2. □

F.2 The morphology of *sector*(V)

Fact (iii) $sector(V) = $ 2-scaling of $\left(\bigcup_{u \text{ is ahead of } u', \zeta(u,u') \text{ contains } V} u \oplus u' \right)$ about V.

Proof:

$$\begin{aligned} sector(V) &= f\left(\{(X_1,X_2,X_3) \in \mathsf{T} \mid X_2 = V\}\right) \quad \text{(By definition (4))} \\ &= f\left(\bigcup_{u \text{ is ahead of } u'} \left\{(X_1,X_2,X_3) \mid X_1 \in u', X_2 = V, X_2 \in \zeta(u,u'), X_3 \in u\right\} \right) \\ &= f\left(\bigcup_{u \text{ is ahead of } u', V \in \zeta(u,u')} \left\{(X_1,V,X_3) \mid X_3 \in u, X_1 \in u'\right\} \right) \\ &= \bigcup_{u \text{ is ahead of } u', V \in \zeta(u,u')} f(\{(X_1,V,X_3) \mid X_3 \in u, X_1 \in u'\}) \\ &= \bigcup_{u \text{ is ahead of } u', V \in \zeta(u,u')} \text{2-scaling of } (u \oplus u') \text{ about } V \\ &= \text{2-scaling of } \left(\bigcup_{u \text{ is ahead of } u', V \in \zeta(u,u')} u \oplus u' \right) \text{ about } V. \quad \square \end{aligned}$$

Fact (iv) *If* u *is ahead of* u' *and* $\zeta(u,u')$ *contains* V*, then* $(u,u') \in \Delta_V$.

Proof. Let $e_a = back(u), e_{a'} = back(u'), e_b = forw(u), e_{b'} = forw(u')$.
Note that $\zeta(u,u') = [Z_a^{a'} \circlearrowleft Z_b^{b'}] \subseteq [v_{b+1} \circlearrowleft Z_b^{b'}] \subseteq \mathsf{UZ}_b^+$.
So, we have $V \in \mathsf{UZ}_b^+$ when $V \in \zeta(u,u')$. This implies that $e_s \preceq_V e_b$, i.e. $e_s \preceq_V forw(u)$.
Symmetrically, we have $V \in \mathsf{UZ}_{a'}^-$ when $V \in \zeta(u,u')$, which implies that $back(u') \preceq_V e_t$.
Therefore, $e_s \preceq_V forw(u) \preceq back(u') \preceq_V e_t$, which implies that (u,u') belongs to Δ_V. □

We prove Equation (22) in the next by applying (iii) and (iv). It states that

$$sector(V) = \text{2-scaling of } (\omega_V - \epsilon_V) \text{ about } V,$$

where ω_V denote the region bounded by the two special routes $\mathcal{L}_V$ and $\mathcal{R}_V$, and

$$\epsilon_V = \bigcup_{(u,u') \in \Delta_V, u \text{ is not ahead of } u'} u \oplus u'.$$

Proof. For convenience, we define $\frac{1}{2}sector(V)$ as the $\frac{1}{2}$-scaling of $sector(V)$ about V.
By (iii), we get that

$$\frac{1}{2}sector(V) = \bigcup_{u \text{ is ahead of } u', V \in \zeta(u,u')} u \oplus u'. \tag{41}$$

We need to prove that $\frac{1}{2}sector(V) = \omega_V - \epsilon_V$.

Consider the three regions $\frac{1}{2}sector(V), \omega_V$, and ϵ_V. First of all, we note that each of these regions is a union of several regions in $\{u \oplus u' \mid (u, u') \in \Delta_V\}$. The claims on ω_V and ϵ_V simply follow from the definitions. The claim on $\frac{1}{2}sector(V)$ follows from (41) together with fact (iv). Moreover, we know that the regions in $\{u \oplus u' \mid (u, u') \in \Delta_V\}$ are pairwise disjoint according to (ii). Therefore, to prove that $\frac{1}{2}sector(V) = \omega_V - \epsilon_V$, we only need to prove that

$$\text{for every } (u, u') \in \Delta_V, \text{ region } u \oplus u' \subseteq \frac{1}{2}sector(V) \text{ if and only if } u \oplus u' \subseteq \omega_V - \epsilon_V.$$

Let $\Delta'_V = \{(u, u') \in \Delta_V \mid u \text{ is ahead of } u'\}$. It further reduces to prove that

$$\text{for every } (u, u') \in \Delta'_V, \text{ region } \zeta(u, u') \text{ contains } V \text{ if and only if } u \oplus u' \subseteq \omega_V. \tag{42}$$

We prove (42) in the following.

First, let us consider the special case where $s = t$. In this case, $\Delta'_V = \{(v_s, v_{t+1})\}$ and $\mathcal{L}_V = \mathcal{R}_V = \omega_V = v_s \oplus v_{t+1}$, so we need to prove that $\zeta(v_s, v_{t+1})$ contains V.

Suppose to the opposite that V is not contained in $\zeta(v_s, v_{t+1}) = [Z^s_{s-1} \circlearrowleft Z^{s+1}_s]$. There are two possibilities: V lies in $[v_s \circlearrowleft Z^s_{s-1}]$, or V lies in $[Z^{s+1}_s \circlearrowleft v_{s+1}]$. Under the first possibility, UZ^+_{s-1} contains V, which contradicts the assumption of s; under the second possibility, UZ^-_{t+1} contains V, which contradicts the assumption of t; therefore V lies in $\zeta(v_s, v_{t+1})$.

Then, we assume that $s \neq t$. Consider any unit pair (u, u') in Δ'_V.

Case 1: u, u' are both edges.
By the definition of ω_V, the parallelogram region $u \oplus u'$ lies in ω_V if and only if $u \oplus u'$ is marked by '0'. So the following are equivalent: $u \oplus u'$ lies in ω_V; $Z^{u'}_u = V$; and $V \in \zeta(u, u')$.

Case 2: u, u' are an edge and a vertex. Assume that $(u, u') = (e_i, v_j)$.

Case 2.1: $j \neq t+1$. In this case, the following conditions are equivalent:
$V \in \zeta(e_i, v_j)$; $Z^{j-1}_i \leq_\rho V \leq_\rho Z^j_i$; region $e_i \oplus e_{j-1}$ is marked by '0/-' while $e_i \oplus e_j$ is marked by '0/+'; and region $e_i \oplus v_j$ is contained in ω_V.

Case 2.2: $j = t+1$. First, we note that Z^{t+1}_i is defined. The reason is as follows. We know u is ahead of u', i.e. e_i is ahead of v_{t+1}. So, $e_i \prec e_{t+1}$ and hence Z^{t+1}_i is defined. Moreover, we claim that $V \leq_\rho Z^{t+1}_i$, since otherwise UZ^-_{t+1} contains V, which contradicts the assumption of t. Since $V \leq_\rho Z^{t+1}_i$, we know that $V \in \zeta(e_i, v_{t+1})$ if and only if $Z^t_i \leq_\rho V$. Moreover, the following are equivalent: $Z^t_i \leq_\rho V$; $e_i \oplus e_t$ is marked by '0/-'; $e_i \oplus v_{t+1}$ is contained in $\mathcal{R}_V$; $e_i \oplus v_{t+1}$ is contained in ω_V.

Case 3: u, u' are both vertices. This case is similar to Case 2; we omit its trivial proof.

In each case, $V \in \zeta(u, u')$ if and only if $u \oplus u' \subseteq \omega_V$. □

F.3 Proof of the Sector-Continuity

Fact (v) *For each route, call its 2-scaling about V a* scaled-route. *Then, if we travel along a scaled-route, we will eventually get outside P and never return to P since then. (So there is at most one intersection between a scaled-route and ∂P.)*

Proof. By Fact (i), V is not contained in $[v_s \circlearrowleft v_{t+1}]$. So, the 2-scaling of $[v_s \circlearrowleft v_{t+1}]$ about V lies in the exterior of P. Because all routes terminate at $[v_s \circlearrowleft v_{t+1}]$, the scaled-routes must terminate on the 2-scaling of $[v_s \circlearrowleft v_{t+1}]$ about V. Together, we will eventually get outside P.

Consider a road $e_i \oplus v_j$ where $(e_i, v_j) \in \Delta_V$. Obviously, it lies on the right of $\overrightarrow{v_{t+1}v_i}$, whereas V lies on the left of $\overrightarrow{v_{t+1}v_i}$; therefore, the 2-scaling of $e_i \oplus v_j$ about V lies on the right of $\overrightarrow{v_{t+1}v_i}$.

On the other hand, since $e_i \prec e_t$, we do not return to P from outside P if we travel along any translation of e_i that lies on the right of $\overrightarrow{v_{t+1}v_i}$. In particular, we do not return to P from outside P when we travel along the scaled version of road $e_i \oplus v_j$. Symmetrically, for a road $v_i \oplus e_j$, we do not return to P from outside P if we travel along its scaled version. Finally, since the scaled-routes consists of the scaled versions of the roads, we obtain (v). □

Fact (vi) Let $\mathcal{L}_V^\star, \mathcal{R}_V^\star, \omega_V^\star$ denote the scaled version $\mathcal{L}_V, \mathcal{R}_V, \omega_V$. If the common starting point of $\mathcal{L}_V^\star, \mathcal{R}_V^\star$ lies in P, then $\omega_V^\star \cap \partial P = [\mathcal{L}_V^\star \cap \partial P \circlearrowright \mathcal{R}_V^\star \cap \partial P]$; otherwise $\omega_V^\star \cap \partial P$ is empty.

Proof. Let $S_V^\star$ denote the common starting point. When $S_V^\star$ lies outside P, by Fact (v), all the boundaries that bound $\omega_V^\star$ lie in the exterior of P, which implies that $\omega_V^\star \cap \partial P$ is empty.

When $S_V^\star$ lies in P, by Fact (v), the boundaries of $\omega_V^\star$ have exactly two intersections with ∂P. Therefore, $\omega_V^\star \cap \partial P$ either equals $[\mathcal{L}_V^\star \cap \partial P \circlearrowright \mathcal{R}_V^\star \cap \partial P]$, or equals $[\mathcal{R}_V^\star \cap \partial P \circlearrowright \mathcal{L}_V^\star \cap \partial P]$. We argue that it the former one, and the reason is as follows. When we travel along $\mathcal{L}_V^\star$, region $\omega_V^\star$ is always on our right side; this implies that $\omega_V^\star \cap \partial P \neq [\mathcal{R}_V^\star \cap \partial P \circlearrowright \mathcal{L}_V^\star \cap \partial P]$. □

Fact (vii) *$sector(V) \cap \partial P$ is a boundary-portion that has the same endpoints as $\omega_V^\star \cap \partial P$.*

Proof. For simplification, we assume that $e_s \neq e_t$; the proof for the case of $e_s = e_t$ is trivial.

Denote by $\epsilon_V^\star$ the scaled version of ϵ_V.

Denote by $\epsilon_V^{(1)}$ the region united by $\{u \oplus u' \mid (u, u') \in \Delta_V, u \text{ is not ahead of } u', u = v_s\}$, and $\epsilon_V^{(2)}$ the region united by $\{u \oplus u' \mid (u, u') \in \Delta_V, u \text{ is not ahead of } u', u' = v_{t+1}\}$. We claim:

1) $\epsilon_V = \epsilon_V^{(1)} \cup \epsilon_V^{(2)}$.

2) $\epsilon_V^{(1)} \subseteq \alpha$, where α denote the unique route that terminates at the midpoint of e_s.

3) $\epsilon_V^{(2)} \subseteq \beta$, where β denote the unique route that terminates at the midpoint of e_t

Proofs: By Fact (i), $[v_s \circlearrowright v_{t+1}]$ is a small portion. This implies that when $(u, u') \in \Delta_V$ and u is not ahead of u', either $u = v_s$ or $u' = v_{t+1}$. Therefore, we obtain 1). Claim 2) follows from the definitions of α and $\epsilon^{(1)}$. Claim 3) follows from the definitions of β and $\epsilon^{(2)}$.

Recall that $sector(V) = \omega_V^\star - \epsilon_V^\star$ (see Equation 22). In the next, we prove that $sector(V) \cap \partial P = (\omega_V^\star - \epsilon_V^\star) \cap \partial P$ is a boundary-portion whose endpoints are the same as $\omega_V^\star \cap \partial P$.

Case 1: $Z_s^t = V$ and so region $e_s \oplus e_t$ is marked by '0', as shown in Figure 45 (a).

By 1), 2) and 3), $\epsilon_V \subseteq \alpha \cup \beta$. Therefore, the closure of region $\omega_V - \epsilon_V$ equals ω_V. It follows that the closure of region $\omega_V^\star - \epsilon_V^\star$ equals $\omega_V^\star$. Therefore, $(\omega_V^\star - \epsilon_V^\star) \cap \partial P$ is a boundary-portion whose endpoints are the same as $\omega_V^\star \cap \partial P$.

Case 2: $Z_s^t <_\rho V$ and so region $e_s \oplus e_t$ is marked by '-', as shown in Figure 45 (b).

In this case, we argue that $\epsilon_V \subseteq \alpha$. The proof is as follows.

First, we claim that $e_s \prec e_{t+1}$. Suppose to the contrary that $e_{t+1} \prec e_s$, then $\mathsf{UZ}_s^+ = [v_{s+1} \circlearrowright Z_s^t]$ does not contain V, which contradicts the assumption of s.

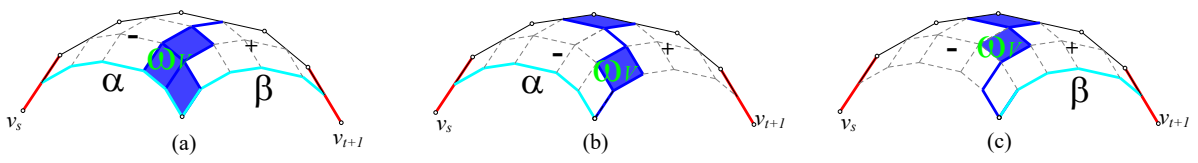

Figure 45: Illustration of the proof of (vii)

Since $e_s \prec e_{t+1}$, every unit in $[v_s \circlearrowleft v_{t-1}]$ beside v_s is ahead of v_{t+1}. (v_s may be ahead of or not ahead of v_{t+1}.) It follows that $\epsilon_V^{(2)} \subseteq \epsilon_V^{(1)}$.

Further by applying 1) and 2), we get $\epsilon_V = \epsilon_V^{(1)} \cup \epsilon_V^{(2)} = \epsilon_V^{(1)} \subseteq \alpha$.

Since $\epsilon_V \subseteq \alpha$, we know that $\omega_V \cap \epsilon_V$ contains nothing or a single point $\mathsf{M}(v_s, v_{t+1})$. Therefore, $\omega_V^\star - \epsilon_V^\star$ either equals $\omega_V^\star$, or equals $\omega_V^\star - S_V^\star$. Therefore, $(\omega_V^\star - \epsilon_V^\star) \cap \partial P$ is a boundary-portion whose endpoints are the same as $\omega_V^\star \cap \partial P$.

Case 3: $V <_\rho Z_s^t$ and so region $e_s \oplus e_t$ is marked by '+', as shown in Figure 45 (c).

This case is symmetric to Case 2 and we omit its proof.

□

F.4 Compute the endpoints of $sector(V) \cap P$

Here, we show the algorithm for computing intersection $\mathcal{L}_V^\star \cap \partial P$; the other intersection $\mathcal{R}_V^\star \cap \partial P$ can be computed symmetrically. By computing these two intersections, we compute the endpoints of $sector(V) \cap P$.

First, we introduce some notations and give an explicit definition for $\mathcal{L}_V$ (see (a) below). Recall the "smaller" order between the edges defined in Definition 4.8.

The terminal edge e_l. See Figure 46. We know that $\mathcal{L}_V$ terminates at the midpoint of some edge in $[v_s \circlearrowleft v_{t+1}]$; denote this particular edge by e_l.

***A*-type roads.** For any edge e_i in $[v_s \circlearrowleft v_l]$, let e_j denote the smallest edge in $[v_{l+1} \circlearrowleft v_{t+1}]$ such that region $e_i \oplus e_j$ is marked by '0/+' (or denote $e_j = e_{t+1}$ if no such edge exists); we denote $\eta_i = e_i \oplus v_j$ and call it a *A-type road*.

***B*-type roads.** For any edge e_i in $[v_{l+1} \circlearrowleft v_{t+1}]$, let e_j denote the smallest edge in $[v_s \circlearrowleft v_l]$ such that region $e_j \oplus e_i$ is marked by '0/+' (or denote $e_j = e_l$ if no such edge exists); we denote $\eta_i = v_j \oplus e_i$ and we call it a *B-type road*.

The following facts are obvious.

a) *$\mathcal{L}_V$ consists of all the A-type roads and all the B-type roads.*

b) *The order of the A-type roads on $\mathcal{L}_V$ is determined, which is equal to $\eta_s, \eta_{s+1}, \ldots, \eta_{l-1}$.*

c) *the order of the B-type roads on $\mathcal{L}_V$ is determined, which is equal to $\eta_t, \eta_{t-1}, \ldots, \eta_{l+1}$.*

Lemma F.2. *1. We can compute the subscripts s, t, l of edges e_s, e_t, e_l in $O(\log n)$ time.*

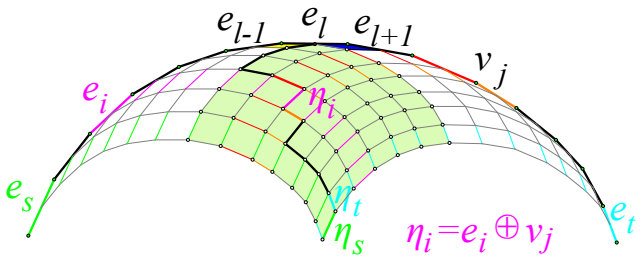

Figure 46: Illustration of the notations used in the algorithm for computing $\mathcal{L}_V^\star \cap \partial P$.

2. *Given an index i such that road η_i is defined (in other words, e_i lies in $[v_s \circlearrowleft v_{t+1}]$ and $e_i \neq e_l$), we can compute the endpoints of η_i in $O(\log n)$ time. In addition, let $\eta_i^\star$ denote the 2-scaling of η_i about V. We can distinguish the following in $O(\log n)$ time:*

   (A) $\eta_i^\star$ intersects ∂P;

   (B) $\eta_i^\star$ lies in the interior of P;

   (C) $\eta_i^\star$ lies in the exterior of P.

3. *Let $S_V^\star$ denote the starting point of $\mathcal{L}_V^\star$. We can compute $S_V^\star$ in $O(1)$ time. Moreover, if $S_V^\star$ lies in P, we can compute $\mathcal{L}_V^\star \cap \partial P$ in $O(\log^2 n)$ time.*

Proof. First, we show how to compute s; t can be computed symmetrically.

We state three arguments.

1) *For any edge e_i that is smaller than e_s, portion UZ_i^+ does not contain V.*

2) *For any edge e_i that is not smaller than e_s, portion UZ_i^+ contains V.*

3) *Given an edge e_i, we can determine whether UZ_i^+ contains V in $O(1)$ time.*

According these arguments, s can be computed in $O(\log n)$ time by a binary search. The proofs for these arguments are as follows: 1) directly follows from the definition of s_V, and 2) follows from the definition of UZ^+ and the bi-monotonicity of the Z-points. To determine whether UZ_i^+ contains V is to determine the relationship between Z_i^j and V, where j denotes the backward edge of δ_i; it can be determined in $O(1)$ time according to Lemma A.5.2.

Next, we show how to compute l. Recall that route $\mathcal{L}_V$ divides all the regions marked by '-' from those marked by '+/0', index l has following properties:

- *For edge e_i such that $e_s \leq_V e_i \leq_V e_{l-1}$, region $e_i \oplus e_{i+1}$ is marked by '-'.*
- *For edge e_i such that $e_{l+1} \leq_V e_i \leq_V e_{t-1}$, region $e_i \oplus e_{i+1}$ is marked by '+/0'.*

According to Lemma A.5.2, we can determine whether $e_i \oplus e_{i+1}$ is marked by '-', '0', or '+' in $O(1)$ time. Therefore, we can compute l in $O(\log n)$ time by a binary search.

Then, we show how to compute road η_i. Assume that $e_s \leq_V e_i \leq_V e_{l-1}$; otherwise $e_{l+1} \leq_V e_i \leq_V e_t$ and it is symmetric. By definition, it reduces to compute the vertex v_j such that $e_i \oplus e_{j-1}$ is marked by '-' while $e_i \oplus e_j$ is marked by '+/0'. By Lemma A.5.2, we can compute the mark in $O(1)$ time. Therefore, we can compute j in $O(\log n)$ time by a binary search.

When η_i is computed, we can compute $\eta_i^\star$. We can then distinguish the relationship between $\eta_i^\star$ and ∂P as follows. First, determine whether the endpoints of $\eta_i^\star$ lie in P, which can be determined in $O(\log n)$ time because P is convex. If both the endpoints lie in P, then $\eta_i^\star$ lies in P; if both of them lie outside P, then $\eta_i^\star$ lies outside P; otherwise, $\eta_i^\star$ intersects with ∂P. (The correctness of these claims follows from fact (v).)

Finally, let us show how to compute $\mathcal{L}_V^\star \cap \partial P$.

First of all, note that the starting point of $\mathcal{L}_V$ locates at $\mathsf{M}(v_s, v_{t+1})$. Therefore, $S_V^\star$ lies on the 2-scaling of point $\mathsf{M}(v_s, v_{t+1})$ about V, and thus it can be computed in $O(1)$ time.

Assume that $S_V^\star$ lies in P, so that $\mathcal{L}_V^\star$ has one intersection with ∂P.

We design two *subroutines*: one assumes that there is an A-type road whose 2-scaling (about V) intersects ∂P, and it finds this road if this assumption is true; the other is symmetric in that it assumes that there is a B-type road whose 2-scaling (about v) intersects ∂P. Because one of these two assumptions is true, one subroutine would success.

Each of these subroutine runs in $O(\log^2 n)$ time and the reason is as follows. According to (b), the A-type roads are in order on $\mathcal{L}_V$; so do the B-type roads. So, a binary search can be applied and in designing the subroutines, which costs $O(\log^2 n)$ time due to Claim 2. □

G Preprocess: Which sector does each vertex lie in and which units does $sector(V)$ intersect

In this appendix, we show how do we compute for each vertex V,

which sector does vertex V lie in

and

which units does region $sector(V)$ intersect,

provide that the endpoints of $sector(V) \cap \partial P$ are computed for each vertex V.

By the SECTOR-CONTINUITY , $sector(V) \cap \partial P$ is a boundary-portion of P. So, to compute the units that intersect $sector(V)$ reduces to compute the endpoints of $sector(V) \cap \partial P$. Since the endpoints of $sector(V) \cap \partial P$ are computed, we can compute the mentioned units efficiently.

A non-important note: If it happens that some endpoint of $sector(V) \cap \partial P$ is not contained in the sector, and simultaneously it lies on a vertex of P, then the vertex should not be included to the set of units that intersect $sector(V)$. (Notice that the endpoints of $sector(V) \cap \partial P$ may not be contained in $sector(V) \cap \partial P$, since $sector(V)$ is not always a closed set as we see in Appendix F.) Although not difficult to deal with, this would be somewhat trifling! In fact, we note that our algorithm still works even if we include this additional vertex to the set of units that intersect $sector(V)$, The reason for this is that the monotone property of ξ still holds by including this additional vertex, and so the major procedure still works in $O(n \log n)$ time.

In the following, we compute the sector containing V for each vertex V.

Recall that σP denotes the inner boundary of $f(\mathsf{T})$ and is defined in Subsection E.1. Recall that $\mathcal{L}_V^\star$ and $\mathcal{R}_V^\star$ are the two boundaries of $sector(V)$ defined in Subsection 4.3.

Outline. We use a sweeping algorithm. To design the algorithm, we introduce two groups of *event-points*. One group contains the points in $\{\mathcal{L}_V^\star \cap \partial P, \mathcal{R}_V^\star \cap \partial P\}$; and the other contains the intersections between σP and ∂P. Note that all the event-points lie in the boundary of P. Moreover, two tags are assigned to each event-point, which are called *future-tag* and *current-tag* respectively. The current-tag indicates the sector which contains the current event-point; the future-tag indicates the sector which contains the boundary-portion that starts at the current event-point and terminates at its (clockwise) next event-point. By sweeping around ∂P, we determine the sector containing each vertex by utilizing the tags of the event-points.

Definition G.1 (Event-points and their tags)**.** For ease of representation, the definition of the event-points consists of two process, an adding one and a removing one. The second process is designed to remove redundant event-points added in the first process.

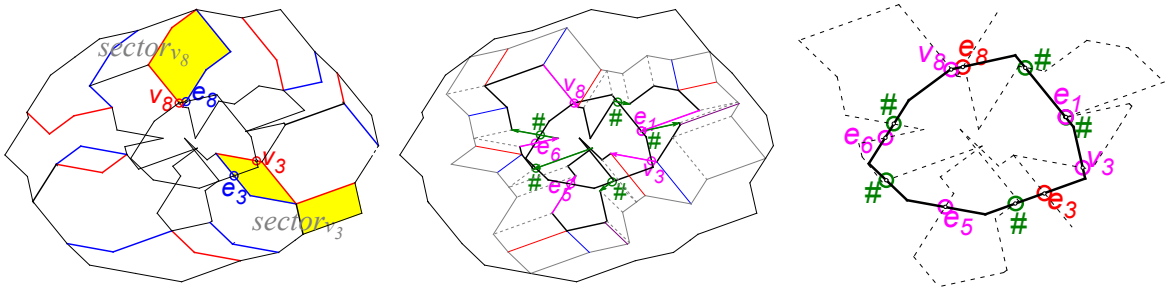

Figure 47: Illustration of the *event-points* and their *future-tags*. The left picture exhibits the event-points in Group 1 defined below; The middle exhibit the event-points in Group 2 defined below.

The *adding process* is as follows. (See Figure 47 for an illustration.)

Group 1: Consider any vertex V for which $sector(V)$ intersects with ∂P. We count $\mathcal{L}_V^\star \cap \partial P$ and $\mathcal{R}_V^\star \cap \partial P$ as two event-points, and define their tags as follows.

$$C(\mathcal{L}_V^\star \cap \partial P) = V, \quad F(\mathcal{L}_V^\star \cap \partial P) = V,$$
$$C(\mathcal{R}_V^\star \cap \partial P) = V, \quad F(\mathcal{R}_V^\star \cap \partial P) = forw(V).$$

Group 2: Consider any intersection K_i between σP and ∂P. We count it an event-point and define its tags as follows. Notice that σP is the concatenation of a few directional line segments. Assume that K_i comes from the directional line segment $\overrightarrow{AB}$ of σP. Note that one of A, B lies in P while the other lies outside P since $\overrightarrow{AB}$ intersects ∂P. Recall function g defined on σP in E.5. Denote

$$C(K_i) = \text{`\#'}, \qquad F(K_i) = \begin{cases} \text{`\#'}, & \text{when } A \in P, B \notin P; \\ \mathbf{u}(g(K_i)), & \text{when } A \notin P, B \in P. \end{cases}$$

For an event-point E, its *current-tag* and *future-tag* are defined by $C(E), F(E)$ respectively.

Note 1 The special symbol '#' is used to indicate the outside of $f(\mathsf{T})$.

When $C(E) =$ '#', no sector contains event-point E.

When $F(E) =$ '#', no sector contains the boundary-portion that starts from E to the clockwise next event-point of E.

Note 2 We define $C(K_i) =$ '#'. The reason for this is that the point K_i does not lie in $f(\mathsf{T})$ and thus does not lie in any sector, which is explained in Subsection E.5.

Removing process: If there are multiple event-points locating at the same position, we keep only one of them and remove the others according to the following priority.

- First, keep the event-point coming from $\{\sigma P \cap \partial P\}$;
- Second, keep the event-point coming from $\{\mathcal{R}_V^\star \cap \partial P\}$.

As a consequence of the Sector-monotonicity and Interleavity-of-f , we get the following corollary, which tells us the sector containing X for each point X on ∂P.

Corollary G.2. *Take any point X in ∂P. If X lies at some event-point E, it belongs to $sector(C(E))$. Otherwise, it belongs to $sector(F(E))$, where E is the closest event-point preceding X in clockwise order. Note that X belongs to no sector when we say it belongs to sector('#').*

Our algorithm works as follows.

1. Compute all of the event-points as well as their tags (corresponding to the adding process).
2. Sort the event-points in clockwise order and remove the redundant ones.
3. Use a sweeping algorithm to compute the closest event-point preceding each vertex and compute the sector containing each vertex by applying the Corollary G.2.

Next, we give details of the first step. Notice that the event-points from Group 1 can be computed efficiently since we have already computed $\mathcal{L}_V^\star \cap \partial P$ and $\mathcal{R}_V^\star \cap \partial P$ for each vertex V, we only need to compute the event-points in $\{\sigma P \cap \partial P\}$ as well as their future tags.

Lemma G.3. *The polygonal curve σP consists of $O(n)$ sides and can be computed in $O(n)$ time. Moreover, the intersections in $\sigma P \cap \partial P$ are of size $O(n)$ and can be computed in $O(n \log n)$ time. In addition, the future-tag of each of such intersection can be computed in $O(1)$ time.*

Proof. Recall the frontier-pair-list and the bottom borders of the frontier blocks defined in E.1. We state the following about the size of the bottom borders.

(i) the bottom borders of the blocks in the following set have in total $O(n)$ sides.

$$\{block(u, u') \mid (u, u') \in \text{frontier-pair-list, and } u, u' \text{ are both edges}\}.$$

(ii) the bottom borders of the blocks in the following set have $O(n)$ sides.

$$\{block(u, u') \mid (u, u') \in \text{frontier-pair-list, at least one of } u, u' \text{ is a vertex}\}.$$

Combining (i) and (ii), the bottom borders have in total $O(n)$ sides, i.e. σP is of size $O(n)$.

Proof of (i): Clearly, the frontier-pair-list contains $O(n)$ unit pairs, and the bottom border of $block(u, u')$ has at most two sides when u, u' are both edges; therefore, we obtain (i).

Proof of (ii): Let $((u_1, u'_1), \ldots, (u_m, u'_m))$ denote the sublist of the frontier-pair-list that contains all of the edge pairs. Denote $Z_i = Z_{u_i}^{u'_i}$ for short. See Figure 36. It can be observed that

(a) for any two neighboring edge pairs, e.g. (u_i, u'_i) and (u_{i+1}, u'_{i+1}), there is another unit pair (denoted by u, u') in the frontier-pair-list between (u_i, u'_i) and (u_{i+1}, u'_{i+1}), and the bottom border of $block(u, u')$ is exactly the reflection of $[Z_i \circlearrowright Z_{i+1}]$.

By the bi-monotonicity of the Z-points, $Z_1, \ldots, Z_m$ lie in clockwise order ∂P, which implies

(b) $\{[Z_1 \circlearrowright Z_2], \ldots, [Z_m \circlearrowright Z_1]\}$ is a partition of ∂P. (See Figure 42.)

Together, (a) and (b) imply (ii).

Next, we argue that the inner boundary σP can be computed in $O(n)$ time. To compute σP, we can first compute the frontier-pair-list by Algorithm 3, then compute $Z_1, \ldots, Z_m$ and generate each side in each bottom border of the frontier blocks. Note that we can compute $Z_1, \ldots Z_m$ in $O(n + m) = O(n)$ time by Lemma A.6 since these Z-points lie in clockwise order.

To compute the intersections between σP and ∂P, we can enumerate each side of σP and compute its intersection with ∂P. According to the common computational geometric result, by $O(n)$ time preprocessing, the intersection between a segment and the boundary of a fixed convex polygon P can be computed in $O(\log n)$ time. Thus, this takes $O(n \log n)$ time.

Finally, we argue that the future-tag of each intersection K_i can be computed in $O(1)$ time. Notice that computing the future-tag of K_i in $\sigma P \cap \partial P$ reduces to computing $\mathbf{u}(g(K_i))$. For any point X in σP, the unit $\mathbf{u}(g(X))$ can be regarded as a tag for point X. By the definition of g, this tag has the property the tags are identical for points on the same side of σP. In addition, we note that the tag of each side of σP can be easily computed when we compute σP. □

Clearly, the second sorting step runs in $O(n \log n)$ time, while the last sweeping step only costs $O(n)$ time. Overall, the preceding algorithm runs in $O(n \log n)$ time.

Remark: There is a purely linear time algorithm which computes the information "for each vertex V, which sector does V lie in and which units are intersected by $sector(V)$", provide that the endpoints of $sector(V) \cap \partial P$ are preprocessed for each vertex V. To design this linear time algorithm, the major difficulty lies in designing a linear time algorithm to compute all the intersections between σP and ∂P. Although, this purely linear time algorithm is much more delightful, we do not present it in this paper due to the lengthy of this paper.

H Preprocess: Which block does vertex V lie in

In this appendix, we present the details of the preprocessing procedure that computes "which block does vertex V lie in". This procedure is outlined in Subsection 4.4.

We assume that V lies in $f(\mathsf{T})$ and the sector containing V is computed. As discussed in the outline, there are two cases. We take care of the more difficult case $V \in \mathit{sector}(e_k)$ in Subsection H.2; and take care of the simpler case $V \in \mathit{sector}(v_k)$ in Subsection H.3.

H.1 Compute the two critical edges e_{p_V}, e_{q_V}

Recall

$$\nabla_V = \big\{(u,u') \mid u \text{ is a unit in } (\delta_i \circlearrowleft v_i), u' \text{ is a unit in } (v_i \circlearrowleft \delta_{i-1}), \text{ and } u \text{ is ahead of } u'\big\}.$$

Fact (vi) *If $\mathit{block}(u_1^*, u_2^*)$ contains V, the unit pair (u_1^*, u_2^*) belongs to ∇_V.*

Proof. Let $e_a = \mathit{forw}(u_1^*), e_{a'} = \mathit{back}(u_2^*)$. Recall $\mathsf{hp}_a^{a'}$ defined in Definition B.1.

Because $v_i \in \mathit{block}(u_1^*, u_2^*)$ and $\mathit{block}(u_1^*, u_2^*) \subset \chi_{u_1^*}^{u_2^*} = \chi_a^{a'} \subseteq \mathsf{hp}_a^{a'}$, we get $v_i \in \mathsf{hp}_a^{a'}$. Therefore, $v_i \in (v_a \circlearrowleft v_{a'+1})$. Since u_1^* is ahead of u_2^*, we have $e_a \preceq e_{a'}$. Together,

$$e_a \prec e_i \text{ and } e_{i-1} \prec e_{a'}.$$

Since $e_a \prec e_i$, edge e_a lies in $(\delta_i \circlearrowleft v_i)$, i.e. $\mathit{forw}(u_1^*)$ lies in $(\delta_i \circlearrowleft v_i)$. So,

$$u_1^* \text{ lies in } [\delta_i \circlearrowleft v_i). \tag{43}$$

Since $e_{i-1} \prec e_{a'}$, edge $e_{a'}$ lies in $(v_i \circlearrowleft \delta_{i-1})$, i.e. $\mathit{back}(u_2^*)$ lies in $(v_i \circlearrowleft \delta_{i-1})$. So,

$$u_2^* \text{ lies in } (v_i \circlearrowleft \delta_{i-1}]. \tag{44}$$

See Figure 20 (a). Because $e_{a'}$ lies in $(v_i \circlearrowleft \delta_{i-1})$, it also lies in $(v_i \circlearrowleft \delta_i)$. So, $e_{a'} \preceq \mathit{back}(\delta_i)$. Therefore, $\mathit{back}(\delta_i) \not\prec e_{a'}$, i.e. $\mathit{back}(\delta_i) \not\prec \mathit{back}(u_2^*)$. Therefore, δ_i is not ahead of u_2^*.

This argument implies that $u_1^* \neq \delta_i$ because u_1^* must be ahead of u_2^*. Symmetrically, $u_2^* \neq \delta_{i-1}$. Therefore, u_1^* lies in $(\delta_i \circlearrowleft v_i)$ and u_2^* lies in $(v_i \circlearrowleft \delta_{i-1})$. So, $(u_1^*, u_2^*) \in \nabla_V$. □

Before we prove the next two facts, we introduce some temporary notations.

For any boundary-portion ρ, let $\rho.s$ and $\rho.t$ denote its starting and terminal point.

See Figure 48 (a). For $1 < j \leq t$, let a_j and b_j respectively denote the edge pair in the upper right corner and in the lower left corner of α_j. For $1 \leq j < t$, let c_j and d_j respectively denote the edge pair in the upper right corner and in the lower left corner of β_j.

By the monotonicity of $\widehat{\chi}$ (Lemma 3.8), we have

$$\widehat{\chi}[\alpha_j] = (\widehat{\chi}[a_j].s \circlearrowleft \widehat{\chi}[b_j].t), \text{ for any } 1 < j \leq t. \tag{45}$$
$$\widehat{\chi}[\beta_j] = (\widehat{\chi}[c_j].s \circlearrowleft \widehat{\chi}[d_j].t), \text{ for any } 1 \leq j < t. \tag{46}$$

Fact (vii) *Denote $\alpha_{t+1} = \nabla_V$. Then, $\widehat{\chi}[\alpha_{j+1}] \cap \widehat{\chi}[\beta_j] = \varnothing$ for any $1 \leq j \leq t$.*

Proof. When $j = t$, set β_j is empty and the claim is obvious. Next, we assume that $j < t$.

We claim the following properties.

$$\widehat{\chi}[a_{j+1}].s, \widehat{\chi}[b_{j+1}].s, \widehat{\chi}[c_j].s, \widehat{\chi}[d_j].s \text{ lie in clockwise order around } \partial P. \tag{47}$$
$$\widehat{\chi}[a_{j+1}].t, \widehat{\chi}[b_{j+1}].t, \widehat{\chi}[c_j].t, \widehat{\chi}[d_j].t \text{ lie in clockwise order around } \partial P. \tag{48}$$
$$\widehat{\chi}[a_{j+1}] \text{ has no overlap with } \widehat{\chi}[d_j]. \tag{49}$$
$$\widehat{\chi}[b_{j+1}] \text{ has no overlap with } \widehat{\chi}[c_j]. \tag{50}$$

The first two properties follow from the monotonicity of $\widehat{\chi}$.

The last two properties are applications of the peculiarity of χ. The proof of (49) is as follows; the proof of (49) is similar and omitted. Notice that $a_{j+1} = (forw(\delta_i), e_i)$ and $d_j = (e_{i-1}, back(\delta_{i-1}))$. Clearly, edges $forw(\delta_i), e_i, e_{i-1}, back(\delta_{i-1})$ do not lie in a small portion. So, by applying the peculiar property of the bounding regions, $\chi^i_{forw(\delta_i)} \cap \chi_{i-1}^{back(\delta_{i-1})}$ lie in the interior of P. So, $\chi^i_{forw(\delta_i)} \cap \partial P$ has no overlap with $\chi_{i-1}^{back(\delta_{i-1})} \cap \partial P$. Therefore, we obtain (49).

Now, see Figure 48 (b). Combining the four properties above, we get

$$\widehat{\chi}[a_{j+1}].s, \widehat{\chi}[b_{j+1}].s, \widehat{\chi}[b_{j+1}].t, \widehat{\chi}[c_j].s, \widehat{\chi}[d_j].s, \widehat{\chi}[d_j].t \text{ lie in clockwise order around } \partial P.$$

In particular,

$$\widehat{\chi}[a_{j+1}].s, \widehat{\chi}[b_{j+1}].t, \widehat{\chi}[c_j].s, \widehat{\chi}[d_j].t \text{ lie in clockwise order around } \partial P.$$

Therefore, $(\widehat{\chi}[a_{j+1}].s \circlearrowleft \widehat{\chi}[b_{j+1}].t)$ is disjoint with $(\widehat{\chi}[c_j].s \circlearrowleft \widehat{\chi}[d_j].t)$.
This means that $\widehat{\chi}[\alpha_{j+1}]$ is disjoint with $\widehat{\chi}[\beta_j]$ further by (45) and (46). □

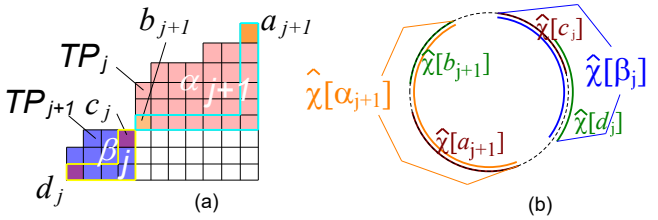

Figure 48: Proof of (vii).

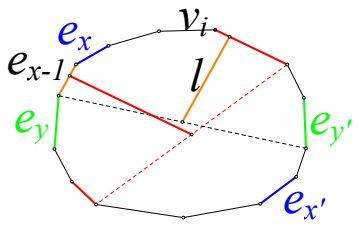

Figure 49: Proof of (viii).

Fact (viii) *There is a unique index in* $1..t$*, denoted by* j^**, such that* $v_i \notin \widehat{\chi}(\alpha_{j^*})$ *but* $v_i \in \widehat{\chi}(\alpha_{j^*+1})$*. We claim that* $(u_1^*, u_2^*) \notin \alpha_{j^*}$ *and* $(u_1^*, u_2^*) \notin \beta_{j^*}$ *and thus* $(u_1^*, u_2^*) \in \gamma_{j^*}$*. In addition, we can compute* j^* *by a binary search and thus compute* (e_p, e_q) *in* $O(\log n)$ *time.*

Proof. Since $block(u_1^*, u_2^*)$ contains v_i, we get

$$v_i \in block(u_1^*, u_2^*) \cap \partial P \subseteq \chi_{u_1^*}^{u_2^*} \cap \partial P \subseteq \widehat{\chi}_{u_1^*}^{u_2^*}.$$

Therefore, we obtain two simple facts: *(a) When* $(u_1^*, u_2^*) \in S$*, vertex* v_i *is contained in* $\widehat{\chi}[S]$*. (b) On the contrary, when* v_i *does not lie in* $\widehat{\chi}[S]$*, we can determine that* $(u_1^*, u_2^*) \notin S$*.*

We know $(u_1^*, u_2^*) \in \nabla_V$ by Fact (vi). So, further by (a), we get $v_i \in \widehat{\chi}[\nabla_V] = \widehat{\chi}[\alpha_{t+1}]$.
Moreover, since $\varnothing = \alpha_1 \subseteq \alpha_2 \subseteq \cdots \subseteq \alpha_{t+1}$, we have $\varnothing = \widehat{\chi}[\alpha_1] \subseteq \widehat{\chi}[\alpha_2] \subseteq \cdots \subseteq \widehat{\chi}[\alpha_{t+1}]$.
Together, we obtain the uniqueness of j^* stated in the fact.

By the definition of j^*, we have $v_i \in \widehat{\chi}[\alpha_{j^*+1}]$. This implies that $v_i \notin \widehat{\chi}[\beta_{j^*}]$ according to Fact (vii). It further implies that $(u_1^*, u_2^*) \notin \beta_{j^*}$ according to (b).
Also by the definition of j^*, we have $v_i \notin \widehat{\chi}[\alpha_{j^*}]$, and so $(u_1^*, u_2^*) \notin \alpha_{j^*}$.
However, $(u_1^*, u_2^*) \in \nabla_V = \alpha_{j^*} \cup \beta_{j^*} \cup \gamma_{j^*}$. Therefore, $(u_1^*, u_2^*) \in \gamma_{j^*}$.

To show that j^* can be computed in $O(\log n)$ time, we prove the following claim: *Given* $1 \le j \le t$*, in* $O(1)$ *time we can determine whether* V *lies in* $\widehat{\chi}[\alpha_j]$.
When $j = 1$, $\widehat{\chi}[\alpha_j] = \varnothing$ and thus we can determine that it does not contain v_i.
Now, assume that $j > 1$. Without loss of generalities, assume that $\mathsf{TP}_j = (e_x, e_{x'}), \mathsf{TP}_{j-1} = (e_y, e_{y'})$. Note that $b_j = (e_{x-1}, e_{y'})$. By (45), $\pi[\alpha_j]$ terminates at point $[b_j].t$, which according

to the definition equals the unique intersection between l and $[v_{x-1} \circlearrowright v_{y'+1}]$, where l denote $\mathsf{p}_{x-1}(\mathsf{M}(v_{x-1}, v_{y'+1}))$. See Figure 49 for an illustration. Therefore,

$v_i \in \widehat{\chi}[\alpha_j]$ if and only if v_i lies in the open half-plane bounded by l and containing e_{x-1}.

In $O(1)$ time we can compute l and then determine which side of l the vertex v_i lies on. Therefore, we can determine whether $v_i \in \widehat{\chi}[\alpha_j]$ in $O(1)$ time.

A note: we can compute TP_j and TP_{j-1} in $O(1)$ time. The reason for this is that except for the first and last element of TP, the other turning pairs are extremal pairs. We can obtain a list of extremal pairs beforehand, and use it to compute TP_j. □

H.2 Compute the block containing V when V lies in $sector(e_k)$

In this subsection, we assume that $V \in sector(e_k)$ where e_k is given.

Recall that (u, u') is *active* if u is ahead of u' and $\zeta(u, u')$ intersects e_k and

$$u \text{ lies in } [v_p \circlearrowright V) \text{ while } u' \text{ lies in } (V \circlearrowright v_{q+1}].$$

Fact (ii) *The target unit pair (u_1^*, u_2^*) is active.*

Proof of (ii). Assume $f^{-1}(V) = (X_1, X_2, X_3)$.
Since $V = f(X_1, X_2, X_3)$, it lies in $block(\mathbf{u}(X_3), \mathbf{u}(X_1))$ and $sector(\mathbf{u}(X_2))$.
However, we know that V lies in $block(u_1^*, u_2^*)$ and $sector(e_k)$.
Therefore, $(\mathbf{u}(X_1), \mathbf{u}(X_2), \mathbf{u}(X_3)) = (u_2^*, e_k, u_1^*)$.
Because $(X_1, X_2, X_3) \in \mathsf{T}$, point $X_2 \in \zeta(\mathbf{u}(X_3), \mathbf{u}(X_1))$. Therefore, $X_2 \in \zeta(u_1^*, u_2^*)$.
Because $\mathbf{u}(X_2) = e_k$, point $X_2 \in e_k$.
Together, $X_2 \in \zeta(u_1^*, u_2^*) \cap e_k$. So, $\zeta(u_1^*, u_2^*) \cap e_k \neq \varnothing$, which implies that (u_1^*, u_2^*) is active. □

The facts (iii)-(v) stated below are the full versions of (iii)-(v) stated in Subsection 4.4.

Fact (iii) *Assume that e_j is an active edge in $(v_p \circlearrowright V)$. Then,*

- *(a) The unit set $\{u \mid (e_j, u) \text{ is active}\}$ consists of consecutive units. Moreover, its first and its last unit (in clockwise order) can be computed in $O(\log n)$ time.*
- *(b) If (e_j, u) is active, then $cell(e_j, u)$ is a parallelogram with a pair of sides congruent to e_j. Moreover, this parallelogram can be computed in $O(1)$ time.*
- *(c) Assume $\{u \mid (e_j, u) \text{ is active}\} = \{u_s, \ldots, u_t\}$ (in clockwise order), then $cell(e_j, u_s)$, $\ldots, cell(e_j, u_t)$ are contiguous and lie monotonously in the opposite direction of e_k.*

Fact (iv) *The monotonicity between the layers.*

- *(a) The active edges in $(v_p \circlearrowright V)$ are consecutive. Moreover, the first and last such edges can be computed in $O(\log n)$ time. Symmetrically, the active edges in $(V \circlearrowright v_{q+1})$ are consecutive. The first and last such edges can be computed in $O(\log n)$ time.*
- *(b) All the layers lie in the closed half-plane bounded by ℓ_k and containing P.*
- *(c) All the A-type layers are disjoint and lie monotonously in the direction perpendicular to e_k. Symmetrically, all the B-type layers have the same monotonicity.*

Fact (v) *Given an active edge e_j, we can do the following tasks in $O(\log n)$ time:*

- *(a) Determine whether V lies in layer_j; if no, determine which side of layer_j it lies on.*
- *(b) Determine whether V lies in body_j; if so, find the cell in body_j that contains v_i.*

Moreover, given p, q, we can compute u_1^*, u_2^* in $O(\log^2 n)$ time.

For convenience, we introduce two temporary notations $b(j)$ and Π_j.

For any edge e_j in $(v_p \circlearrowleft v_i)$, we denote $b(j) = \begin{cases} q+1 & \text{if } e_j \prec e_{q+1}; \\ q & \text{otherwise,} \end{cases}$ and denote $b = b(j)$ when j is clear. Assume that $V = v_i$. Let Π_j denote the list of portions $(\zeta(e_j, u))$, where u takes over units from e_i to $e_{b(j)}$ in clockwise order. Formally,

$$\Pi_j = \big(\zeta(e_j, e_i), \zeta(e_j, v_{i+1}), \ldots, \zeta(e_j, v_b), \zeta(e_j, e_b)\big).$$

By the definition of $\zeta(e_j, u)$ and the bi-monotonicity of the Z-points, we get:

(I) $Z_j^i, Z_j^{i+1}, \ldots, Z_j^{b-1}, Z_j^b$ lie in clockwise order on $\rho = [v_{b+1} \circlearrowleft v_j]$.

(II) $\Pi_j = \Big(Z_j^i, [Z_j^i \circlearrowleft Z_j^{i+1}], \ldots, [Z_j^{b-1} \circlearrowleft Z_j^b], Z_j^b\Big)$.

Proof of (iii). (a): By (I) and (II), the elements in Π_j that intersect e_k are consecutive. So, $\{u \mid (e_j, u) \text{ is active}\}$ consists of consecutive units. In addition, computing the first unit reduces to computing index h such that $Z_j^{h-1} \leq_\rho v_k <_\rho Z_j^h$, which can be computed in $O(\log n)$ time by a binary search by applying Lemma A.5.2. The last unit can be computed similarly.

(b): Because (e_j, u) is active, $\zeta(e_j, u)$ intersects with e_k. By the definition,

$$\mathit{cell}(e_j, u) = f(\{(X_1, X_2, X_3) \mid X_1 = u, X_2 \in \zeta(e_j, u) \cap e_k, X_3 \in e_j\}).$$

Case 1: u is an edge, e.g., $u = e_{j'}$. In this case, $\mathit{cell}(e_j, e_{j'})$ is the 2-scaling of $e_j \oplus e_{j'}$ about $Z_j^{j'}$, which is a parallelogram with two sides congruent to e_j. In addition, since $\zeta(e_j, u) = Z_i^j$ and it intersects with e_k, point $Z_j^{j'}$ lies on e_k and hence can be computed in $O(1)$ time according to Lemma A.5.1. Therefore, $\mathit{cell}(e_j, e_{j'})$ can be computed in $O(1)$ time.

Case 2: u is a vertex, e.g. $u = v_{j'}$. First, we argue that $\zeta(e_j, v_{j'})$ is not a single point. Suppose to the opposite that $\zeta(e_j, v_{j'})$ is a single point. Then, its two endpoints $Z_j^{j'-1}, Z_j^{j'}$ must be identical, and must lie in e_k since $\zeta(e_j, v_{j'})$ intersects e_k. However, applying Lemma A.4.1, when $Z_j^{j'-1}, Z_j^{j'}$ lie on e_k, they lie on $\mathsf{M}(\mathsf{I}_{j,k}, \mathsf{I}_{j'-1,k})$, $\mathsf{M}(\mathsf{I}_{j,k}, \mathsf{I}_{j',k})$, respectively, and these two midpoints do not coincide because $\mathsf{I}_{j-1,k} \neq \mathsf{I}_{j',k}$. Contradictory.

Following this argument, $\zeta(e_j, v_{j'}) \cap e_k$ is a segment that is not a single point, which implies that $\mathit{cell}(e_j, v_{j'})$ is a parallelogram with a pair of sides congruent to e_j.

By applying Lemma A.5.1 and Lemma A.5.2, segment $\zeta(e_j, v_{j'}) \cap e_k$ can be computed in $O(1)$ time, and then $\mathit{cell}(e_j, v_{j'})$ can be computed in $O(1)$ time.

(c): Consider two incident units in $\{u \mid (e_j, u) \text{ is active}\}$, e.g., $v_{j'}$ and $e_{j'}$. (For two incident units $e_{j'}, v_{j'+1}$ in this set, the proof is similar.) Let us consider the projections of these cells along direction e_j onto ℓ_k, we shall prove that these projections are disjoint and are arranged in the opposite direction of e_k. See Figure 50 (1). Let M be the projection of $\mathsf{M}(v_{j+1}, v_{j'})$; and X the reflection of $Z_j^{j'}$ around M. Clearly, the projection of $\mathit{cell}(e_j, e_{j'})$ terminates at X while the projection of $\mathit{cell}(e_j, v_{j'})$ starts at X, thus they are disjoint and lie in the mentioned order. □

Proof of (iv). (a): Denote by μ_j the union of portions in Π_j. By (I) and (II), $\mu_j = [Z_j^i \circlearrowleft Z_j^{b(j)}]$. Further, due to the bi-monotonicity of the Z-points, the starting points of $\mu_p, \ldots, \mu_{i-1}$ lie in clockwise order around ∂P, and so do their terminal points. So, the portions in $\mu_p, \ldots, \mu_{i-1}$ that intersect e_k are consecutive. On the other hand, e_j is active if and only if μ_j intersects edge e_k. So, the active edges in $(v_p \circlearrowleft V)$ are consecutive.

Computing the first and last active edges in $(v_p \circlearrowleft V)$ reduces to computing the first and last portions in $\mu_p, \ldots, \mu_{i-1}$ that intersect with e_k. By Lemma A.5.2, in $O(1)$ time we can

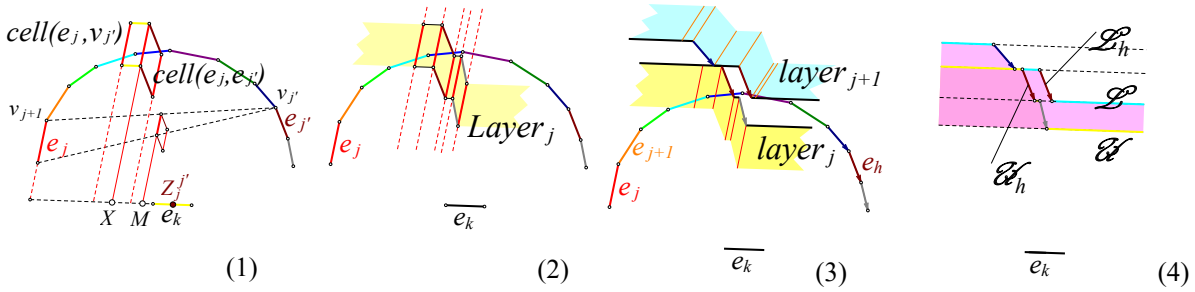

Figure 50: Illustration of the proof of the monotonicities of the cells and layers.

determine whether μ_j is contained in $[v_{b(j)+1} \circlearrowleft v_k]$ or in $[v_{k+1} \circlearrowleft v_j]$, or is intersecting with e_k. So, by a binary search, in $O(\log n)$ time we can find the mentioned two portions.

(b): Denote the half-plane by H. To prove that all layers lie in H, we only need to prove that all cells lie in H, which further reduces to prove that $sector(e_k) \subseteq H$. Let X be an arbitrary point in $sector(e_k)$. Then, there exists $(X_1, X_2, X_3) \in \mathsf{T}$ such that $X_2 \in e_k$ and $f(X_1, X_2, X_3) = X$. Because $X_1, X_3 \in \partial P$, their mid point (denoted by M) lies in H. Since X_2 lies on e_k, it lies on the boundary of H. Together, the 2-scaling of M about X_2, which is equal to X, lies in H.

(c): Assume that layer_j and layer_{j+1} are A-type layers. See in Figure 50 (3). We know that each layer has two boundaries; we refer to them as the *lower border* and the *upper border*, so that the lower one is closer to ℓ_k than the upper one. We shall prove that the upper border of layer_j (denoted by $\mathcal{U}$) lies between ℓ_k and the lower border of layer_{j+1} (denoted by $\mathcal{L}$).

To prove this argument, we make an auxiliary line parallels to ℓ_k at each vertex of the two borders; these auxiliary lines cut the plane to slices. It reduces to show that in each slice

1) the region under $\mathcal{U}$ is bounded by the region under $\mathcal{L}$.

As shown in Figure 50 (4), each slice is corresponding to some edge, e.g. the second slice is corresponding to e_h. We note that $\mathcal{U}_h$ and $\mathcal{L}_h$ are translations of e_h, where $\mathcal{U}_h, \mathcal{L}_h$ respectively denote the part of $\mathcal{U}$ that lie in this slice and the part of $\mathcal{L}$ that lie in this slice. Applying the monotonicity of cells within layer_h, we know 1) holds in the slice corresponding to e_h. □

Proof of (v). Assume that e_j lies in $(v_p \circlearrowleft V)$; otherwise it lies in $V \circlearrowleft v_{q+1}$ and is symmetric.

According to Fact (iii-b), the cells in $\{cell(e_j, u) \mid (e_j, u) \text{ is active}\}$ are parallelograms with a pair of sides parallel to e_j; the extended lines of those sides parallel to e_j divide the entire plane into several regions; and we refer to each such region as a *chop*. See Figure 50 (2). For convenience, we denote the chop that contains $cell(e_j, u)$ by $chop_u$.

Notice that 1) We can compute $chop_u$ in $O(1)$ time, since $cell(e_j, u)$ can be computed in $O(1)$ time by Fact (iii-b); 2) We can compute the first and the last unit in $\{u \mid (e_j, u) \text{ is active}\}$ in $O(\log n)$ time by Fact (iii-a); 3) The chops have the same monotonicity as the cells in $\{cell(e_j, u) \mid (e_j, u) \text{ is active}\}$ have. Altogether, we can use a binary search to find the chop that contains v_i, which costs $O(\log n)$ time. Moreover, we can solve the required tasks (a) and (b) easily in $O(1)$ time if the chop that contains V is computed.

To compute (u_1^*, u_2^*), we design two *subroutines*. One assumes that V is contained in a A-layer (i.e. it assumes that u_1^* is an edge), while the other assumes that V is contained in a B-layer (i.e. it assumes that u_2^* is an edge). The first subroutine works as follows; and the other subroutine works symmetrically. First, we compute the first and last active edges $e_g, e_{g'}$ in $(v_p \circlearrowleft V)$, which costs $O(\log n)$ time according to Fact (iv-a). Then, we compute the only A-layer in $\mathsf{layer}_g, \ldots, \mathsf{layer}_{g'}$ that contains v_i, which costs $O(\log^2 n)$ time according to (v-a). If

no such A-layer exists, we terminate the subroutine. Otherwise, we assume that layer_j contains V and we proceed as follows. We check whether body_j contains V and we compute the only cell in body_j that contains v_i (by (v-b)); If body_j does not contain v_i we also terminate; otherwise we find the cell containing V. This runs in $O(\log^2 n)$ time.

If u_1^* is an edge, the first subroutine obtains (u_1^*, u_2^*); if u_2^* is an edge, the second subroutine obtains (u_1^*, u_2^*); however, in a degenerated case, u_1^*, u_2^* can both be vertices, and the two subroutines both fail to find (u_1^*, u_2^*). (The reason that this case is degenerated is the following. When it occurs, there is a parallelogram inscribed on P with three anchored corners.)

To handle the degenerated case, we apply the following observation.

(I) *If $(v_j, v_{j'})$ is active and point X lies in cell$(v_j, v_{j'})$, then one of the following is true: (1) X lies on the boundary of cell$(v_j, e_{j'-1})$, (2) X lies on the boundary of cell$(e_j, v_{j'})$.*

It states that when (u_1^*, u_2^*) are both vertices, v_i lies on the boundary of some cell. By slightly modifying our two subroutines, we can find a cell that contains v_i or a cell whose boundary contains v_i. After find a cell whose boundary contains v_i, it is easy to find the cell that contains v_i in $O(1)$ time. Therefore, the degenerated case can be handled easily.

Proof of (I): Assume that $(v_j, v_{j'})$ is active and X lies on *cell*$(v_j, v_{j'})$. Denote $M = \mathsf{M}(v_j, v_{j'})$ and denote by X' the reflection of X around M. Because *cell*$(v_j, v_{j'})$ is the reflection of $\zeta(v_j, v_{j'}) \cap e_k$ around M, point X' lies in $\zeta(v_j, v_{j'}) \cap e_k$. Notice that $\zeta(v_j, v_{j'})$ is the concatenation of $\zeta(v_j, e_{j'-1})$ and $\zeta(e_j, v_{j'})$. Point X' either lies on $\zeta(v_j, e_{j'-1}) \cap e_k$ or lies on $\zeta(e_j, v_{j'}) \cap e_k$. In the former case, $(v_j, e_{j'-1})$ is active and the reflection of X' around M (which equals X) lies on the boundary of *cell*$(v_j, e_{j'-1})$; in the latter case, $(e_j, v_{j'})$ is active and X lies on the boundary of *cell*$(e_j, v_{j'})$. □

H.3 Compute the block containing V when V lies in *sector*(v_k)

Here, we consider the easier case where $V \in$ *sector*(v_k).

Let (X_1, X_2, X_3) denote the preimage of V under function f. Since V lies in *block*(u_1^*, u_2^*) and *sector*(v_k), we can get that $(\mathbf{u}(X_1), \mathbf{u}(X_2), \mathbf{u}(X_3)) = (u_2^*, v_k, u_1^*)$. So, u_1^*, v_k, u_2^* are the units containing X_3, X_2, X_1 respectively. On the other hand, according to (24), we know

$$[v_p \circlearrowleft V) \text{ contains } u_1^*; \text{ and } (V \circlearrowleft v_{q+1}] \text{ contains } u_2^*.$$

Therefore

$$X_1 \in (V \circlearrowleft v_{q+1}], X_2 \in v_k, X_3 \in [v_p \circlearrowleft V).$$

Also note that $VX_1X_2X_3$ is a parallelogram.

Lemma H.1. *There is a unique parallelogram $A_0A_1A_2A_3$ such that corners A_0, A_1, A_2, A_3 respectively lie on $V, (V \circlearrowleft v_{q+1}], v_k, [v_p \circlearrowleft V)$, and we can compute it in $O(\log^2 n)$ time.*

Proof. Suppose to the contrary that there exist two such parallelograms, denoted by VAv_kA' and VBv_kB'. Because their centers both locate at $\mathsf{M}(v_k, V)$, quadrant $ABA'B'$ is a parallelogram with all corners lying on curve $[v_p \circlearrowleft v_{q+1}]$. However, because $e_p \prec e_q$, $[v_p \circlearrowleft v_{q+1}]$ is a small portion, and so there could be no parallelogram with all corners lying on it according to Lemma 4.12.2, which is contradictory! To compute the parallelogram $A_0A_1A_2A_3$, we need to compute a pair of points A_3, A_1 on $[v_p \circlearrowleft V), (V \circlearrowleft v_{q+1}]$ so that their mid point lies on $\mathsf{M}(v_k, V)$. It is equivalent to compute the intersection between $[v_p \circlearrowleft V)$ and the reflection of $(V \circlearrowleft v_{q+1}]$ around $\mathsf{M}(v_k, V)$. We can compute it in $O(\log^2 n)$ time by a binary search. (Note: The case $V \in$ *sector*(v_k) can be regarded as a special case of the previous case where v_k is a sufficiently small edge, so we do not give all of the details for computing A_1, A_3, which are trivial.) □

According to the preceding lemma, after p, q are computed, we can compute (X_1, X_2, X_3) in $O(\log^2 n)$ time. Then, $(u_1^*, u_2^*) = (\mathbf{u}(X_3), \mathbf{u}(X_1))$ is obtained.

I Details of computing the LMAPs

To compute the LMAPs, we design the major procedure and the minor procedure. They are presented in Subsection 2.5 and Subsection 4.2 respectively. In this appendix we provide the proofs of lemmas that are omitted in these two subsections.

Proof of Lemma 2.13.2. Assume we know which block and which sector contains V, we show how to determine whether $V \in f(\mathsf{T})$ and compute $f^{-1}(V)$ in $O(1)$ time.

When no block (and no sector) contains V, we determine that $V \notin f(\mathsf{T})$. This is because otherwise $V \in f(\mathsf{T}) \cap \partial P$ and then V lies in a block and sector according to Lemma 2.13.1.

Now, assume that V is contained in $block(u, u')$ and $sector(w)$. We determine that $V \in f(\mathsf{T})$ since the blocks and sectors are subregions of $f(\mathsf{T})$. We compute $f^{-1}(V)$ as follows.

Denote $f^{-1}(V) = (X_1, X_2, X_3)$. Given V, u, u', w, we need to compute the positions of X_1, X_2, X_3 in $O(1)$ time. First, we state two arguments.

i. *Points X_1, X_2, X_3 lie on units u', w, u, respectively.*

ii. *Point X_2 lies in boundary-portion $\zeta(u, u')$.*

(i.) is proved in Lemma 2.13.1. (ii.) is because $(X_1, X_2, X_3) \in \mathsf{T}$ and due to (2).

Then, we discuss the following four cases.

Case 1: *u, u' are both edges*, e.g. $(u, u') = (e_i, e_j)$.

Because $\zeta(u, u')$ contains only one point Z_i^j, we get $X_2 = Z_i^j$ by (ii), which implies that Z_i^j lies in unit $\mathbf{u}(X_2) = w$. Since w is given, we can compute Z_i^j in $O(1)$ time by Lemma A.5.1.

When Z_i^j is computed, X_2 and $M = \mathsf{M}(V, X_2)$ can be computed in $O(1)$ time.

When M is computed, X_1, X_3 can be computed in $O(1)$ time as follows. X_1 is the intersection between e_j and the reflection of e_i around M; and X_3 is the intersection between e_i and the reflection of e_j around M.

Case 2: *u is a vertex and u' is an edge*, e.g. $(u, u') = (v_i, e_j)$.

Let s denote the 2-scaling of segment $v_i \oplus e_j$ about V, which is a line segment.

We first argue that segment s has at most one intersection with unit w. Applying Lemma A.3, $\zeta(v_i, e_j) = [Z_{i-1}^j \circlearrowleft Z_i^j] \subseteq [v_{j+1} \circlearrowleft \delta_j]$, whereas $X_2 \in \zeta(v_i, e_j)$; together, the unit containing X_2 (i.e. unit w) lies in $[v_{j+1} \circlearrowleft \delta_j]$. Because s is parallel to e_j, each unit in $[v_{j+1} \circlearrowleft \delta_j]$, including w, has at most one intersection with s.

Because $X_3 \in u$ and $X_1 \in u'$, we know $\mathsf{M}(X_1, X_3) = \mathsf{M}(V, X_2)$ lies on $v_i \oplus e_j$, so X_2 lies on segment s. Further, since $X_2 \in w$, point X_2 lies on both s and w.

In $O(1)$ time we can compute X_2 by computing the unique intersection of s, w.

In $O(1)$ time we can compute X_3 since X_3 lies on $u = v_i$.

Finally, X_1 can be computed since it lies on the reflection of X_3 around $\mathsf{M}(V, X_2)$.

Case 3: *u is an edge and u' is a vertex.* This case is symmetric to Case 2.

Case 4: *u, u' are both vertices*, e.g. $(u, u') = (v_i, v_j)$. Since $X_3 \in u = v_i$ and $X_1 \in u' = v_j$, they can be computed in $O(1)$ time. Further, since $V = f(X_1, X_2, X_3)$, point X_2 lies on the reflection of V around $\mathsf{M}(X_1, X_3)$ and thus can also be computed in $O(1)$ time.

□

Recall Lemma 2.13.3 and Lemma 2.13.4. They state that: For each vertex V, the union ξ_V is a boundary-portion. Moreover, $\xi_{v_1}, \ldots, \xi_{v_n}$ are disjoint, lie in clockwise, and can be computed in linear time when we know which units are intersected by $sector(V)$ for each vertex V.

Proof of Lemma 2.13.3 and Lemma 2.13.4. Let V denote an arbitrary vertex. Let $\mathbb{I}_V$ denote the set of units that intersects $sector(V)$. Denote

$$\mathbb{J}_V = \{u \mid V \text{ is ahead of } u\}, \quad \mathbb{G}_V = \{u \mid u \in \mathbb{I}_V, u \in \mathbb{J}_V\},$$

and recall that

$$\xi_V := \bigcup\nolimits_{u \in \mathbb{I}_V, V \text{ is ahead of } u} \zeta(V,u) = \bigcup\nolimits_{u \in \mathbb{G}_V} \zeta(V,u).$$

Clearly, $\mathbb{J}_V$ consists of consecutive units. According to the SECTOR-CONTINUITY , $\mathbb{I}_V$ consists of consecutive units. Therefore, their intersection $\mathbb{G}_V$ also consists of consecutive units.

Let $\acute{g}_V, \grave{g}_V$ denote the clockwise first and last units in set $\mathbb{G}_V$ when this set is nonempty, We claim that

$$\xi_V = \begin{cases} [Z_{back(V)}^{back(\acute{g}_V)} \circlearrowright Z_{forw(V)}^{forw(\grave{g}_V)}], & \text{when } \mathbb{G}_V \neq \varnothing; \\ \varnothing, & \text{when } \mathbb{G}_V = \varnothing. \end{cases} \tag{51}$$

Proof of (51): Assume $\mathbb{G}_V \neq \varnothing$, otherwise it is trivial. By definition of $\zeta(V,u)$ in (1),

$$\zeta(V,u) = [Z_{back(V)}^{back(u)} \circlearrowright Z_{forw(V)}^{forw(u)}] \text{ for any unit } u \text{ in } \mathbb{G}_V.$$

Based on this formula and according to the bi-monotonicity of the Z-points, $\bigcup_{u \in \mathbb{G}_V} \zeta(V,u)$ equals the boundary-portion, which starts at the starting point of $\zeta(V, \acute{g}_V)$ and terminates at the terminal point of $\zeta(V, \grave{g}_V)$, thus we obtain (51).

Equation (51) directly implies that ξ_V is a boundary-portion for each vertex V.

Next, we prove the monotone property of ξ. Let $V_1, \ldots, V_m$ denote all of the vertices in $\{V \mid \mathbb{G}_V \neq \varnothing\}$, where $V_1, \ldots, V_m$ lie in clockwise order. For $1 \leq j \leq m$, let $a_j = back(\acute{g}_{V_j})$ and $b_j = forw(\grave{g}_{V_j})$. By the SECTOR-MONOTONICITY , $a_1, b_1, \ldots, a_m, b_m$ lie in clockwise order around ∂P. (But the neighboring elements in this list could be identical.) Then, according to the bi-monotonicity of the Z-points, $Z_{back(V_1)}^{a_1}, Z_{forw(V_1)}^{b_1}, \ldots, Z_{back(V_m)}^{a_m}, Z_{forw(V_m)}^{b_m}$ lie in clockwise order around ∂P. Further, due to (51), $\xi_{V_1}, \ldots, \xi_{V_m}$ are disjoint and lie in clockwise order.

To compute ξ, we only need to compute the aforementioned Z-points. We can first compute $\mathbb{G}$ from $\mathbb{I}$ (note that array $\mathbb{I}$ is the preprocessed information), then compute a, b from $\mathbb{G}$, and then compute the Z-points all together by applying Lemma A.6. Each step is in linear time. □

Recall that Lemma 4.6 states some properties of κ^+ and κ^- that are quite similar to those of ξ. We prove the properties of κ^+ below; the properties of κ^- are symmetrically.

Proof of the properties of κ^+ stated in Lemma 4.6. By the definition of ζ given in (19), we get

$$\begin{aligned} \zeta(v_i, e_j) &= [Z_{i-1}^{back(\delta_{i-1})} \circlearrowright Z_i^j], \text{ for } e_j \in H_{v_i}; \\ \zeta(v_i, v_j) &= [Z_{i-1}^{back(\delta_{i-1})} \circlearrowright Z_i^j], \text{ for } v_j \in H_{v_i}. \end{aligned}$$

Applying these equations to (20) and applying the bi-monotonicity of Z-points, we get

$$\kappa_{v_i}^+ = \begin{cases} [Z_{i-1}^{back(\delta_{i-1})} \circlearrowright Z_i^{back(\delta_i)}], & \text{When } \delta_{i-1} \neq \delta_i; \\ \varnothing, & \text{When } \delta_{i-1} = \delta_i. \end{cases} \tag{52}$$

Due to (52), κ_V^+ is a boundary-portion for each vertex V.

By the bi-monotonicity of the Z-points, $Z_1^{back(\delta_1)}, \ldots, Z_n^{back(\delta_n)}$ lie in clockwise order around ∂P, which implies the monotone property of κ^+.

Computing κ^+ reduces to computing these Z-points. We can first compute δ and then apply Lemma A.6 to compute them, which costs $O(n)$ time. □

References

[1] P. K. Agarwal, N. Amenta, and M. Sharir. Largest placement of one convex polygon inside another. *Discrete & Comput. Geom.*, 19(1):95–104, 1998.

[2] A. Aggarwal, M. M. Klawe, S. Moran, P. Shor, and R. Wilber. Geometric applications of a matrix-searching algorithm. *Algorithmica*, 2(1-4):195–208, 1987.

[3] A. Aggarwal, B. Schieber, and T. Tokuyama. Finding a minimum-weight k-link path in graphs with the concave monge property and applications. *Discrete & Comput. Geom.*, 12(1):263–280, 1994.

[4] H. Alt, D. Hsu, and J. Snoeyink. Computing the largest inscribed isothetic rectangle. In *Proc. of CCCG95*, pages 67–72, 1994.

[5] G. Barequet. The on-line heilbronn's triangle problem. *Disc. Math.*, 283(1-3):7–14, 2004.

[6] C. Bertram-Kretzberg, Hofmeister T., and Lefmann H. An algorithm for heilbronn's problem. *SIAM J. Comput.*, 30(2):383–390, 2000.

[7] J. E. Boyce, D. P. Dobkin, R. L. (Scot) Drysdale, III, and L. J. Guibas. Finding extremal polygons. In *14th Symp. on TOC*, pages 282–289, 1982.

[8] S. Cabello, O. Cheong, and L. Schlipf. Finding largest rectangles in convex polygons. *EuroCG*, 2014.

[9] S. Cabello, J. Cibulka, J. Kynčl, M. Saumell, and P. Valtr. Peeling potatoes near-optimally in near-linear time. In *13th SOCG*, 2014.

[10] J. Chang and C. Yap. A polynomial solution for the potato-peeling problem. *Discrete & Comput. Geom.*, 1:155–182, 1986.

[11] B. Chazelle. The polygon containment problem. *Advan. in Comput. Research*, 1:1–33, 1983.

[12] K. Daniels, V. Milenkovic, and D. Roth. Finding the largest area axis-parallel rectangle in a polygon. *Comput. Geom.*, 7:125–148, 1997.

[13] C. H. Dowker. On minimum circumscribed polygons. *Bull. Amer. Math. Soc.*, 50:120–122, 1944.

[14] Y. Gordon, A. E. Litvak, M. Meyer, and A. Pajor. John's decomposition in the general case and applications. *J. Diff. Geom.*, 68(1):99–119, 2004.

[15] O. Hall-Holt, M. J. Katz, P. Kumar, J. S. B. Mitchell, and A. Sityon. Finding large sticks and potatoes in polygons. In *SODA*, pages 474–483, 2006.

[16] K. Jin and K. Matulef. Finding the maximum area parallelogram in a convex polygon. In *23rd CCCG*, 2011.

[17] D. Kirkpatrick and J. Snoeyink. Tentative prune-and-search for computing fixed-points with applications to geometric computation. *Fundam. Inf.*, 22(4):353–370, December 1995.

[18] C. Knauer, L. Schlipf, J. M. Schmidt, and H. R. Tiwary. Largest inscribed rectangles in convex polygons. *J. of Disc. Alg.*, 13:78–85, may 2012.

[19] M. Lassak. Approximation of convex bodies by centrally symmetric bodies. *Geom. Dedi.*, 72(1):63–68, 1998.

[20] H. Lefmann. Distributions of points in d dimensions and large k-point simplices. *Discrete & Comput. Geom.*, 40(3):401–413, 2008.

[21] H. Lefmann and N. Schmitt. A deterministic polynomial-time algorithm for heilbronn's problem in three dimensions. *SIAM J. Comput.*, 31(6):1926–1947, 2002.

[22] N. A. D. Pano, Y. Ke, and J. O'Rourke. Finding largest inscribed equilateral triangles and squares. In *Proc. Allerton Conf.*, pages 869–878, 1987.

[23] M. J. Post. A minimum spanning ellipse algorithm. In *22nd Symp. of FoCS*, pages 115–122, Oct 1981.

[24] E. Sas. über ein extremumeigenschaft der ellipsen. *Compositio Math*, 6:468–470, 1939.

[25] W. M. Schmidt. On a problem of heilbronn. *J. London Math. Soc.*, 4:545–550, 1971.

[26] M. Sharir and S. Toledo. Extremal polygon containment problems. *Comput. Geom. Theory Appl.*, 4(2):99–118, jun 1994.